CRITICAL EVALUATION OF STEREOPHOTOGRAMMETRIC METHODOLOGY WITH EMPHASIS ON CLOSE-RANGE APPLICATIONS
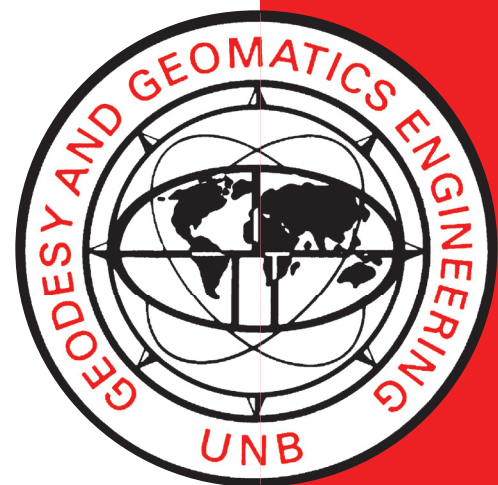
PETER TIAN-YUAN SHIH

May 1989

PREFACE

In order to make our extensive series of lecture notes more readily available, we have scanned the old master copies and produced electronic versions in Portable Document Format. The quality of the images varies depending on the quality of the originals. The images have not been converted to searchable text.

CRITICAL EVALUATION OF STEREOPHOTOGRAMMETRIC METHODOLOGY WITH EMPHASIS ON CLOSE-RANGE APPLICATIONS

Peter Tian-Yuan Shih

Department of Surveying Engineering
University of New Brunswick
P.O. Box 4400
Fredericton, N.B.
Canada
E3B 5A3

May 1989

PREFACE

This technical report is a reproduction of a Ph.D. dissertation submitted in partial fulfillment of the requirements of the degree of Doctor of Philosophy in the Department of Surveying Engineering, January 1989. Funding for the research undertaken was provided by the Natural Sciences and Engineering Research Council of Canada.

PREFACE

This technical report is a reproduction of a Ph.D. dissertation submitted in partial fulfillment of the requirements of the degree of Doctor of Philosophy in the Department of Surveying Engineering, January 1989. Funding for the research undertaken was provided by the Natural Sciences and Engineering Research Council of Canada.

ABSTRACT

This dissertation represents a critical evaluation of the photogrammetric methodology in terms of the functional model, stochastic model, numerical processing scheme, and operational system. This study then focuses on close-range applications.

For the functional model, the relationship between algebraic and physical form of the perspective transformation model is fully explored, and applications are provided for both the single photo case and multi-photo one. Different functional models are studied comparatively. As an extension of the basic functional models, the conventional approach with additional parameters is investigated from both functional and numerical perspectives, and other trend removal approaches are also evaluated. Finally, the recovery ability of "calibration" parameters in the conventional approach with additional parameters is studied with experiments.

Concerning the stochastic model and the numerical processing scheme, a weighted constraint model, and a parametric model with additional observations are compared with a combined model. The utilization of a variance-covariance-component-estimation technique (MINQUE) for covariance matrix estimation is evaluated. The application of Box-Jenkin's time series analysis technique, along with a general data processing scheme in the numerical realm are outlined.

Photogrammetry has been applied at close-range under different forms. A conceptualized model is developed in order to bring these together within a generalized photogrammetric family. Rasterstereography, one of the methods utilizing structured light, is found to be attractive in today's environment. An experiment with film-based rasterstereography is described. The feasibility of measuring image coordinates with an enlarger-digitizer approach is fully explored, and finally, the utilization of a home video camcorder for image acquisition is evaluated.

TABLE OF CONTENTS

LIST OF TABLES

LIST OF FIGURES

ACKNOWLEDGEMENT

CHAPTER 1

INTRODUCTION

The scope of this research is to explore extensively the functional model, the stochastic model, and the data processing system, with emphasis on close-range applications of photogrammetry.

The reasons why photogrammetric techniques are seriously considered over other techniques can be illustrated by one area of application: skeletal deformities and trunk shape. The major objective of this subject is to provide information for diagnosis and to trace the progress of skeletal deformities. The conventional and most direct method for this is using radiation, such as X-rays, for skeletal photographing. This is not a very good method, especially for mass-screen programs, and frequent use. Other "non-destructive" methods are preferred.

The trunk shape formed by skeletal elements and soft tissues, can be altered by both. The **non-destructive** methods use trunk shape measurements to diagnose skeletal deformities. In order to document and reproduce the evaluated status, various measuring methods are employed. Horst (1983) provided a simplified division :

1. plaster cast;
2. contour drawing;
3. contour measuring with surface contact :
   a) index methods;
   b) palpating methods;
   c) measurement of mobility;
4. contour measuring without surface contact :
   a) photogrammetry;
   b) stereo-photogrammetry.[1.1]

[1.1] Classification based on Horst (1983). The class "photogrammetry" refers to light sectioning, Morie topography, etc.; while "stereophotogrammetry" refers to narrow sense stereophotogrammetry.

The contact methods, such as plaster cast methods, measuring and drawing apparati, thoracography, tin ribbon method, formulator body contour tracer, and kyrtometer, etc. have been effectively used in the past and continue to be used at present. However, a non-contact method, which changes the trunk shape the least, is expected to be of greater value. Besides, photogrammetric methods

- provide the instaneous **freezing** ability in the time domain and

- serve as an excellent information **storage** medium.

Takasaki (1975) reported on the application of Moire Topography. Since then, Moire Topography is used in spinal deformity mass-screening, and pre-diagnosis programs. Moreland et.al. (1981), Drerup et.al. (1983) present a number of applications and further studies, concerning Moire Topography and other imaging methods, such as rasterstereography, line-sensing, etc.

This study does not intend to investigate the medical meaning or other physical interpretation of the measured shape, nor form models to relate the measured shape to any index; rather, the exploration of the photogrammetric technique itself for patternless medium sized objects is intended.

Under this task, various composite measuring components could be considered, for example, the various entity observations such as parallel lines, angles, distances, analytically modelled or approximated shapes on one hand; and multi-frame as well as multi-sensor images, both in the time- and spatial domains on the other. For the first aspect, a number of investigations have been reported; El-Hakim (1979) and Ethrog (1984) are two typical examples. For the second aspect, the combined use of conventional photogrammetric information and various electronic sensing devices, especially the linear array camera and the solid state matrix camera, are becoming very attractive. Hofmann et. al. (1984), Ebner & Mueller (1986), Kruck & Lohmann (1986) may serve as successful

2

examples. Within working group III/1 of the International Society for Photogrammetry and Remote Sensing, (Accuracy Aspects of Combined Point Determination), navigation data (such as the Global Positioning System) are included along with the two solid state camera types stated above (Ebner et. al, 1986). However, for most close-range applications, navigation data are unlikely to be effective for the present time. Although the combined application of acoustic devices and, touch sensors, force sensors, etc., along with vision sensors (e.g. a solid-state imaging system) has been utilized in Bio-Engineering, as well as in Robotics, the metric aspect of vision sensors has not been explored as yet.

However, no matter how sophisticated a system is going to be, a basic strategy for data processing is essential and should be established, including both functional and stochastical parts. Above all, the specific aspects of photogrammetry should be addressed. Then, a general scheme can be formed, with photogrammetry as the root. The reason for this lies in the large amount information usually acquired by photogrammetric means, as compared to other approaches.

The presentation scheme of this research can be outlined as:

• Functional models
• Stochastic models and numerical processing scheme
• Operational systems
     -- the conceptualized general model
     -- the processing system for non-metric imagery
     -- the processing system for digital cameras

Under the functional model, the basic perspective transformation models are evaluated, and also their refinement in terms of additional parameters. It is believed that each variant has its own usage, its own advantages and disadvantages. A detailed understanding would be helpful for setting up a general strategy for selecting the most

suitable model for a particular purposed system, and also provide much insight into the phenomena with which we are already familiar. The recovery ability of calibration parameters in a bundle block adjustment with additional parameters should also be examined.

Concerning the stochastic model and numerical processing scheme, upon which the performance of the optimization process depends, the basic methodology used for the adjustment, such as the parametric model with additional observations, weighted constraints, and combined models, are discussed. The applications of a variance-covariance-components-estimation method: MINQUE, the application of Box-Jenkin's time series analysis technique, as well as the numerical processing scheme are also studied.

In the operational system aspect, the general model for various methodologies is conceptualized first. Basic concepts, stereographic interpretation, accuracy factors, as well as advantages and disadvantages are analyzed. Based on the consideration of the current environment, rasterstereography is thought to be attractive.

Concerning the instrumentation aspect within system evaluation, data-processing systems, particularly for close-range photogrammetry with non-metric cameras, are studied. An alternative method for extracting image coordinates from imagery using a photographic enlarger and a cartographic digitizer are analyzed. This was done bearing in mind a general methodology which could be utilized in any laboratory equipped with a micro computer. An economical photogrammetric information processing unit has been proposed and developed. Finally, the applications of digital cameras are investigated.

The objective of this study is to develop a generalized concept for designing a measuring system, particularly for close-range applications. This system ideally should:

1. be operable in a non-photogrammetric environment by a non-photogrammetrist;

2. be as integrated as possible;

4

3. have software which does not require in depth knowledge for operation and maintenance;

4. be adaptive (self-adjusting in the time sequence);

5. operate with maximum accuracy as provided by the physical limitations of the system;

6. be time-effective, cost-effective, and have high fidelity for down-stream data processing.

Within this study, the evaluation and refinement of present methodology, as well as the mathematical model for data handling, are emphasized. In order to reach the objectives, the functional and stochastic models for analytical photogrammetry are explored first, followed by the system investigation and experiments.

CHAPTER 2

FUNCTIONAL MODELS

There are many types of projections which could be applied in photogrammetry. The perspective transformation has a very important place, mainly because of the nature of today's generally used imaging devices. Practically, one particular perspective model, the collinearity equation model, is generally applied. Then, the model is extended by additional parameters to compensate for various systematic errors, which cause a deviation of the real situation from the ideal central perspective transformation.

Overviewing the existing models, a simplified classification may be drawn:

• Point based methods

    • Unit: Photo

        * Image pyramid model

        * Direct Linear Transformation model

        * Collinearity equation model

    • Unit: Stereo model

        * Coplanarity model

        * RDLT model

        (* Collinearity equation model)

• Methods relying on entities

Since all entities can be included in point based models by either expanding the observation space or form constraints in the parameter space, this study concentrates on general point based models. However, the significance of the entity methods should not be overlooked. Most of them are designed independent of the origin of the object coordinate system; therefore, they are ideal for shape/form evaluations, and particularly useful in

close-range cases. Besides, some of them provide a closed form solution. In Table 2.1, some of them are listed.

TABLE 2.1 Methods Relying on Entities

Publication	Remarks
Williamson& Brill(1987)	• graphic analysis • 2 point perspective • 3-D known shape • x_0, y_0, c, ω, ϕ, κ, scaled X_c, Y_c, Z_c
Brill& Williamson (1987)	• graphic analysis • 3-D known shape • x_0, y_0, c, ω, ϕ, κ, scaled X_c, Y_c, Z_c
Brown (1971)	• parallel and perpendicular lines (plumb lines) • x_0, y_0, radial and other distortions
Ethrog (1984)	• parallel and perpendicular lines • x_0, y_0, c, ω, ϕ, κ, radial and other distortions • closed form
Haralick & Chu (1984)	• circle or other analytically formed shape • x_0, y_0, c, ω, ϕ, κ, (space resection) • iterative method
Masry (1981)	• straight- or curved lines with object coordinates • x_0, y_0, c, ω, ϕ, κ (space resection) • iterative method
Rawiel (1980)	• well distributed corner points • x_0, y_0, c, ω, ϕ, κ, radial and other distortions • closed form
Wunderlich (1982) (1984)	• 4 points in a plane and not lying in a line • rectification without knowing the object coordinates • closed form
Novak (1986)	• 4 points in a plane; • closed form, multi photo • close relationship with Killian (1984) method

The general perspective model is extensively investigated and then compared with other functional models both photo- and stereo model based.

2.1 GENERAL PERSPECTIVE TRANSFORMATION

An arbitrary 3-D coordinate system (X, Y, Z), can be perspectively transformed into any other arbitrary coordinate system (x,y,z) through a finite series of rotations:

$$\begin{vmatrix} X & Y & Z & 1 \end{vmatrix} \begin{vmatrix} L_1 & L_5 & R_1 & L_9 \\ L_2 & L_6 & R_2 & L_{10} \\ L_3 & L_7 & R_3 & L_{11} \\ L_4 & L_8 & R_4 & 1 \end{vmatrix} = \lambda \begin{vmatrix} x & y & z & 1 \end{vmatrix}$$

...(Eq. 2-1)

where L_9, L_{10}, L_{11} contain the information for λ, the perspective scale; L_4, L_8, R_4 represent translations; and the left-upper 3 by 3 matrix contains the concatenated rotations (Keefe, et al., 1986). With (X, Y, Z) representing the object space, and (x, y, z) the image space, z can be set as 0, assuming the image space to be an ideal plane. Therefore, $R_1 = R_2 = R_3 = R_4 = 0$, which reduces the perspective transformation to:

$$x = (L_1 X + L_2 Y + L_3 Z + L_4)/\lambda$$
$$y = (L_5 X + L_6 Y + L_7 Z + L_8)/\lambda$$
$$\lambda = (L_9 X + L_{10} Y + L_{11} Z + 1)$$

...(Eq. 2-2 a,b,c)

This is the general form of 3-D to 2-D projective transformation[2.1] , often written as:

$$x = \frac{a X + b Y + c Z + d}{m X + n Y + p Z + 1}$$

$$y = \frac{e X + f Y + g Z + h}{m X + n Y + p Z + 1}$$

...(Eq. 2-3 a,b)

where, the (x,y), (X,Y,Z) are the image and object space coordinates respectively and (a, b, ...) are transformation coefficients.

This model is commonly known as the DLT (Direct Linear Transformation) model (Abdel-Aziz & Karara, 1971), and has been widely applied, especially in close-range photogrammetry. While DLT was initially developed as a single photo approach, it actually represents a general model.

[2.1] 'Projective transformation' is a more general term. 'Perspective transformation' is one of the projective transformations with central perspective geometry, such as the gnomonic projection in the map projection theory (McDonnell, 1979).

In the following sections a physical interpretation for all eleven parameters is presented together with a way to extract these eleven physical parameters from the DLT values.

2.1.1 Mathematical Model with Physical Interpretation

Concerning the physical interpretation of the 11 parameters, the derivations given by Bopp & Krauss (1977), van Wijk & Ziemann (1976), and the original paper by Abdel-Aziz & Karara (1971) are slightly different. However, none provides directly 11 physical parameters from the DLT parameters. Hadem (1981) and Okamoto (1981) indicated that these 11 DLT parameters are equivalent to 6 exterior orientation parameters and 5 interior orientation parameters.

Following the original derivation by Abdel-Aziz & Karara (1971), and taking the perspective centre as the origin, (Eq. 2-4) can be formed.

$$
\overset{\text{ideal}}{\begin{vmatrix} x - x_0 \\ y - y_0 \\ -c \end{vmatrix}} = \overset{\text{measured}}{\begin{vmatrix} \lambda_x(x - x_0) \\ \lambda_y(y - y_0) \\ -c \end{vmatrix}}
$$

...(Eq. 2-4)

Therefore, with the well-known collinearity equation, the transformation becomes :

$$
\begin{vmatrix} \lambda_x & 0 & -\lambda_x x_0 \\ 0 & \lambda_y & -\lambda_y y_0 \\ 0 & 0 & -c \end{vmatrix} \begin{vmatrix} x \\ y \\ 1 \end{vmatrix} = \lambda M \begin{vmatrix} X - X_c \\ Y - Y_c \\ Z - Z_c \end{vmatrix} = \lambda M \begin{vmatrix} 1 & 0 & 0 & -X_c \\ 0 & 1 & 0 & -Y_c \\ 0 & 0 & 1 & -Z_c \end{vmatrix} \begin{vmatrix} X \\ Y \\ Z \\ 1 \end{vmatrix}
$$

...(Eq. 2-5)

$$
\begin{vmatrix} x \\ y \\ 1 \end{vmatrix} = \lambda \begin{vmatrix} \lambda_x & 0 & -\lambda_x x_0 \\ 0 & \lambda_y & -\lambda_y y_0 \\ 0 & 0 & -c \end{vmatrix} \begin{vmatrix} m_{11} & m_{12} & m_{13} \\ m_{21} & m_{22} & m_{23} \\ m_{31} & m_{32} & m_{33} \end{vmatrix} \begin{vmatrix} 1 & 0 & 0 & -X_c \\ 0 & 1 & 0 & -Y_c \\ 0 & 0 & 1 & -Z_c \end{vmatrix} \begin{vmatrix} X \\ Y \\ Z \\ 1 \end{vmatrix}
$$

$$
= (\lambda/K) \begin{vmatrix} \lambda_y(c) & 0 & -\lambda_x\lambda_y x_0 \\ 0 & \lambda_x(c) & -\lambda_x\lambda_y y_0 \\ 0 & 0 & -\lambda_x\lambda_y \end{vmatrix} M \begin{vmatrix} 1 & 0 & 0 & -X_c \\ 0 & 1 & 0 & -Y_c \\ 0 & 0 & 1 & -Z_c \end{vmatrix} \begin{vmatrix} X \\ Y \\ Z \\ 1 \end{vmatrix}
$$

...(Eq. 2-6)

9

where:

$$K = -\det \begin{vmatrix} \lambda_x & 0 & -\lambda_x x_0 \\ 0 & \lambda_y & -\lambda_y y_0 \\ 0 & 0 & -c \end{vmatrix} \quad,$$

or

$$\begin{vmatrix} x \\ y \\ 1 \end{vmatrix} = (\lambda/K) \begin{vmatrix} \lambda_y(c\ m_{11}-\lambda_x x_0 m_{31}), & \lambda_y(c\ m_{12} - \lambda_x x_0 m_{32}), & \lambda_y(c\ m_{13} - \lambda_x x_0 m_{33}), & A \\ \lambda_x(c\ m_{21}-\lambda_y y_0 m_{31}), & \lambda_x(c\ m_{22} - \lambda_y y_0 m_{32}), & \lambda_x(c\ m_{23} - \lambda_y y_0 m_{33}), & B \\ -\lambda_x\lambda_y m_{31}, & -\lambda_x\lambda_y m_{32}, & -\lambda_x\lambda_y m_{33}, & C \end{vmatrix} \begin{vmatrix} X \\ Y \\ Z \\ 1 \end{vmatrix}$$

where A: $-\lambda_y(c(m_{11}X_c + m_{12}Y_c + m_{13}Z_c) - \lambda_x x_0(m_{31}X_c + m_{32}Y_c + m_{33}Z_c))$

B: $-\lambda_x(c(m_{21}X_c + m_{22}Y_c + m_{23}Z_c) - \lambda_y y_0(m_{31}X_c + m_{32}Y_c + m_{33}Z_c))$

C: $\lambda_x\lambda_y(m_{31}X_c + m_{32}Y_c + m_{33}Z_c) = \lambda_x\lambda_y C_0$

...(Eq. 2-7)

This is expressed as :

$$\begin{vmatrix} x \\ y \\ 1 \end{vmatrix} = (\lambda/K)C \begin{vmatrix} b_{11} & b_{12} & b_{13} & b_{14} \\ b_{21} & b_{22} & b_{23} & b_{24} \\ b_{31} & b_{32} & b_{33} & 1 \end{vmatrix} \begin{vmatrix} X \\ Y \\ Z \\ 1 \end{vmatrix}$$

...(Eq. 2-8)

and can be further presented in the conventional DLT form:

$$x = \frac{b_{11}X + b_{12}Y + b_{13}Z + b_{14}}{b_{31}X + b_{32}Y + b_{33}Z + 1}$$

$$y = \frac{b_{21}X + b_{22}Y + b_{23}Z + b_{24}}{b_{31}X + b_{32}Y + b_{33}Z + 1}$$

...(Eq. 2-9)

Now the orthogonality condition of the rotation matrix is applied:

1. $m_{31}^2 + m_{32}^2 + m_{33}^2 = 1$
   $b_{31}^2 + b_{32}^2 + b_{33}^2 = \lambda_x^2\lambda_y^2 C^{-2} = C_0^{-2}$

2. $m_{11}m_{31} + m_{12}m_{32} + m_{13}m_{33} = 0$
   $b_{11}b_{31} + b_{12}b_{32} + b_{13}b_{33} = x_0 C_0^{-2};$

3. $m_{21}m_{31} + m_{22}m_{32} + m_{23}m_{33} = 0$
   $b_{21}b_{31} + b_{22}b_{32} + b_{23}b_{33} = y_0 C_0^{-2};$

4. $m_{11}^2 + m_{12}^2 + m_{13}^2 = 1$
   $b_{11}^2 + b_{12}^2 + b_{13}^2 = c^2 \lambda_x^{-2} C_0^{-2} + x_0^2 C_0^{-2}$

5. $m_{21}^2 + m_{22}^2 + m_{23}^2 = 1$

$$b_{21}^2 + b_{22}^2 + b_{23}^2 = c^2\lambda_y^{-2}C_o^{-2} + y_0^2C_o^{-2}$$

6. $m_{11}m_{21} + m_{12}m_{22} + m_{13}m_{23} = 0$
   $b_{11}b_{21} + b_{12}b_{22} + b_{13}b_{23} = x_0y_0C_o^{-2}$

Although there are 6 parameters : C_o, x_0, y_0, c, λ_x, λ_y, among these 6 equations, only C_o, x_0, y_0, $c/\lambda_x(=c_x)$, $c/\lambda_y(=c_y)$, are independent and could be solved with the first 5 equations. For this reason, Bopp & Krauss(1977) utilized condition 6 as one of their constraints without providing a physical interpretation.

Using conditions 1 to 5, and the corresponding DLT parameters, we obtain:

$m'_{31} = -C_ob_{31}$; $m'_{21} = (C_ob_{21} + y_0m'_{31})/c_y$; $m'_{11} = (C_ob_{11} + x_0m'_{31})/c_x$;
$m'_{32} = -C_ob_{32}$; $m'_{22} = (C_ob_{22} + y_0m'_{32})/c_y$; $m'_{12} = (C_ob_{12} + x_0m'_{32})/c_x$;
$m'_{33} = -C_ob_{33}$; $m'_{23} = (C_ob_{23} + y_0m'_{33})/c_y$; $m'_{13} = (C_ob_{13} + x_0m'_{33})/c_x$.

$$...(Eq. \ 2-10)$$

Applying the Q-R orthogonalization procedure (Bjerhammar, 1973), results in:

$$M = \begin{vmatrix} 1 & 0 & 0 \\ d & 1 & 0 \\ 0 & 0 & 1 \end{vmatrix} \begin{vmatrix} m'_{11} & m'_{12} & m'_{11} \\ a & b & c \\ m'_{31} & m'_{32} & m'_{33} \end{vmatrix}$$

where : $d = (m'_{11} m'_{21} + m'_{12} m'_{22} + m'_{13} m'_{23})$
          $a = m'_{21} - d \, m'_{11}$; $b = m'_{22} - d \, m'_{12}$; $c = m'_{23} - d \, m'_{13}$

$$...(Eq. \ 2-11)$$

It should be noted that M' is a matrix formed without condition 6. Now, we can modify the image space transformation to:

$$\begin{vmatrix} \text{ideal} & & & & & & & \text{measured} \\ x \\ y \\ -c \end{vmatrix} = \begin{vmatrix} 1 & 0 & 0 \\ -d & 1 & 0 \\ 0 & 0 & 1 \end{vmatrix} \begin{vmatrix} \lambda_x & 0 & -\lambda_x x_0 \\ 0 & \lambda_y & -\lambda_y y_0 \\ 0 & 0 & -c \end{vmatrix} \begin{vmatrix} x \\ y \\ 1 \end{vmatrix}$$

$$...(Eq. \ 2-12)$$

The 11 independent physical parameters, corresponding to the 11 DLT parameters are now : x_0, y_0, ω, ϕ, κ, X_c, Y_c, Z_c, c_x, c_y, and d, where d is the shear factor (see section 2.1.2).

2.1.2 Transfer from DLT Parameters to Physical Ones

According to Abdel-Aziz & Karara (1971), the direct linear transformation is composed of two individual transformations, from the comparator to the image, and from the image to the object space.

When analyzing these, the author found that the first one expresses a shear model, while the second one encompasses the collinearity equation. It should be noted that this model is different from the affine distortion model applied by Moniwa (1977):

$$
\begin{vmatrix} x \\ y \end{vmatrix}_{ideal} = \begin{vmatrix} \lambda'_x(x-x_0) \\ \lambda'_y(y-y_0) - \lambda'_x(x-x_0)d \end{vmatrix}_{measured} = \begin{vmatrix} \lambda_x(x-x_0)\cos\beta \\ \lambda_y(y-y_0) + \lambda_x(x-x_0)\sin\beta \end{vmatrix}_{measured}
$$

where:

$\lambda_x, \lambda_y, \lambda'_x, \lambda'_y$: the scale along the x, y coordinate axis;

$d = \tan\beta'$;

β, β': the non-orthogonality of the coordinate system.

...(Eq. 2-13)
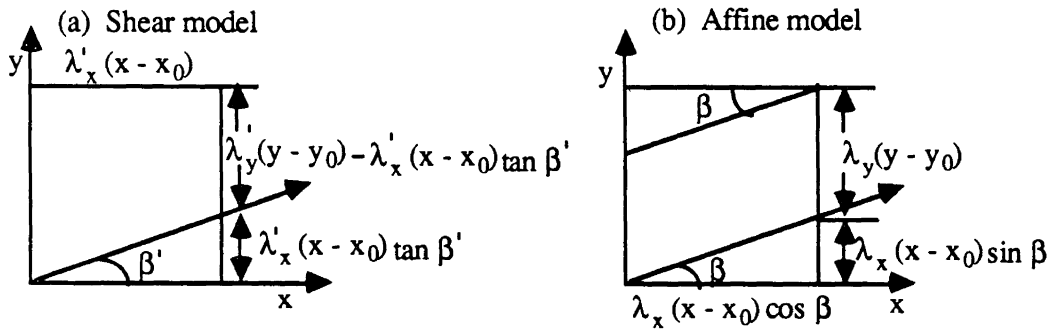
Figure 2.1: Shear and Affine model Interpretation

Following the procedures used in section 2.2.1, the DLT model could be derived and exactly interpreted by implementing the shear model. However, it can be shown that the affine model which is generally used, is equivalent to the shear model:

$$
\begin{vmatrix} x \\ y \end{vmatrix}_{assumed} = \begin{vmatrix} \lambda'_x{}^{-1}x \\ \lambda'_x{}^{-1}y \end{vmatrix} = \begin{vmatrix} (x-x_0) \\ \lambda'_y\lambda'_x{}^{-1}(y-y_0) - (x-x_0)\tan\beta' \end{vmatrix}_{measured} = \begin{vmatrix} (x-x_0) \\ a'(y-y_0) + b'(x-x_0) \end{vmatrix}_{measured}
$$

...(Eq. 2-14)

12

Affine model

$$
\begin{vmatrix} x \\ y \end{vmatrix} = \begin{vmatrix} x\lambda_x^{-1}\cos\beta \\ y\lambda_x^{-1}\cos\beta \end{vmatrix} = \begin{vmatrix} (x-x_0) \\ \lambda_y\lambda_x^{-1}(1/\cos\beta)(y-y_0)+(x-x_0)\tan\beta \end{vmatrix} = \begin{vmatrix} (x-x_0) \\ a(y-y_0)+b(x-x_0) \end{vmatrix}
$$

...(Eq. 2-15)

This indicates that we can derive the exact physical interpretation for the DLT model either by extending the Bopp& Krauss (1977) approach or by reducing the dependent parameters in the original Abdel-Aziz & Karara (1971) formulation.

For the shear model, we have : $a'=\lambda'_y\lambda'^{-1}_x$; $b'=\tan\beta'$ (see Figure 2.1). If $\lambda'_x=1$, then $\lambda'_y=a'$, and $\beta'=\tan^{-1}b'$. For the affine model, we have: $a=\lambda_y\lambda_x^{-1}(1/\cos\beta)$; $b=\tan\beta$ (see Figure 2.1). If $\lambda_x=1$, then $\beta=\tan^{-1}b$, and $\lambda_y=a.\cos\beta$.

According to the author's derivation, the DLT equations contain the following parameters :

$$
\begin{aligned}
b_{11} &= (1/C)(x_0 m_{31} - c m_{11}) \\
b_{12} &= (1/C)(x_0 m_{32} - c m_{12}) \\
b_{13} &= (1/C)(x_0 m_{33} - c m_{13}) \\
b_{14} &= -(b_{11}X_c + b_{12}Y_c + b_{13}Z_c) \\[6pt]
b_{21} &= (1/C)(y_0 m_{31} - (c/a)m_{21} + b(c/a)m_{11}) \\
b_{22} &= (1/C)(y_0 m_{32} - (c/a)m_{22} + b(c/a)m_{12}) \\
b_{23} &= (1/C)(y_0 m_{33} - (c/a)m_{23} + b(c/a)m_{13}) \\
b_{24} &= -(b_{21}X_c + b_{22}Y_c + b_{23}Z_c) \\[6pt]
b_{31} &= -(1/C)m_{31} \\
b_{32} &= -(1/C)m_{32} \\
b_{33} &= -(1/C)m_{33} \\
C &= -(m_{31}X_c + m_{32}Y_c + m_{33}Z_c)
\end{aligned}
$$

...(Eq. 2-16)

Now 11 physical parameters can be found by applying the orthogonality conditions:

1. Station parameters (X_c, Y_c, Z_c):

$$
\begin{vmatrix} X_c \\ Y_c \\ Z_c \end{vmatrix} = \begin{vmatrix} -b_{11} & -b_{12} & -b_{13} \\ -b_{21} & -b_{22} & -b_{23} \\ -b_{31} & -b_{32} & -b_{33} \end{vmatrix}^{-1} \begin{vmatrix} b_{14} \\ b_{24} \\ 1 \end{vmatrix}
$$

...(Eq. 2-17)

2. Interior orientation and comparator parameters (x_0, y_0, c, a, b)

$$
\begin{aligned}
x_0 &= C^2(b_{11}b_{31} + b_{21}b_{32} + b_{13}b_{33}) \\
y_0 &= C^2(b_{21}b_{31} + b_{22}b_{32} + b_{23}b_{33}) \\
c^2 &= C^2(b_{11}^2 + b_{12}^2 + b_{13}^2) - x_0^2 \\
y_0^2 + c^2a^{-2} + b^2c^2a^{-2} &= C^2(b_{21}^2 + b_{22}^2 + b_{23}^2) \\
x_0y_0 - bc^2a^{-1} &= C^2(b_{11}b_{21} + b_{12}b_{22} + b_{13}b_{23})
\end{aligned}
$$

...(Eq. 2-18)

From the last two equations, a and b can be solved, while $C^{-2} = (b_{31}^2 + b_{32}^2 + b_{33}^2)$

3. The rotation matrix (as a function of ω, ϕ, κ)

$$
\begin{aligned}
m_{31} &= -Cb_{31}; & m_{11} &= (x_0m_{31} - Cb_{11})c^{-1}; & m_{21} &= (y_0m_{31} + bca^{-1}m_{11} - Cb_{21})ca^{-1}; \\
m_{32} &= -Cb_{32}; & m_{12} &= (x_0m_{32} - Cb_{12})c^{-1}; & m_{22} &= (y_0m_{32} + bca^{-1}m_{12} - Cb_{22})ca^{-1}; \\
m_{33} &= -Cb_{33}; & m_{13} &= (x_0m_{33} - Cb_{13})c^{-1}; & m_{23} &= (y_0m_{33} + bca^{-1}m_{13} - Cb_{23})ca^{-1}.
\end{aligned}
$$

...(Eq. 2-19)

The rotation matrix can be decomposed into the actual rotations, following standard procedures.

2-1-3   Verification of the Developed Interpretation Model

In order to show the fidelity of the presented model, several numerical tests were performed. Test data are listed in Table 2-2a , with each set containing 27 points. True camera parameter values for simulated data, and approximate values for real data , are listed in Table 2-2b.

TABLE 2-2a
Project Parameters of the Test Data

Data Set	Scale	Object relief:Object Distance	Object dimensional ratio	Resolution		Remarks
1	1:100	2:5	1 :1 :1	1	µm	Simulated
2a	1:5000	0.02:5	1:1:0.2	0.01	µm	Simulated
2b				1	µm	
3	1:11	0.37:5.84	1:1 :0.1	10	µm	Real data

TABLE 2-2b
Camera Parameters for the Test Data Sets

Data Set	x_0	y_0	c_x	c_y	d	ω	ϕ	κ	X_C	Y_C	Z_C
1	0.	0.	50.	50.	0.	2.2	1.1	26.5	0.1	0.2	5.0
2	0.	0.	1.	1.	0.	-11.	11.	45.	1.0	1.0	5.0
3	-5025.54	5023.50	53.92	53.94	0.	8.0	-2.3	-90.	5034.56	4956.35	5597.05

The standard deviations of the image coordinates were used as accuracy indicators. After the parameters were calculated, the ground coordinates were transformed back to image space, and then the difference between the original observation and the transformed one was used to compute the standard deviation. The following three sets of parameters were studied:

Approach a: the 11 DLT parameters;
Approach b: the 9 parameters of the Bopp & Krauss (1977) model (but without the 2 constraints);
Approach c: the 11 physical parameters as derived in this thesis from the 11 DLT parameters.

The standard deviation of the image residuals are given in Table 2.3.

TABLE 2.3

Standard deviations of image residuals in μm

Test data	Approaches		
	a	b	c
1	0.464	0.472	0.464
2a	0.446	3.52	0.446
2b	0.594	6.01	0.594
3	17.5	19.4	17.5

The physical parameters obtained from DLT were also compared with the combined model of collinearity equations and shear distortion parameters with the results listed in Table 2.4.

TABLE 2.4
The estimated parameters

	data	σ	X_c	Y_c	Z_c	ω	ϕ	κ
DLT	1	0.464	0.09997	0.19999	5.0000	-2.287	1.145	26.565
Collinearity		0.464	0.09997	0.19999	5.0000	-2.287	1.145	26.565
DLT	2a	0.446	1.22227	0.70031	5.0302	-11.327	11.351	45.003
Collinearity		0.632	0.65676	0.43202	2.5490	-5.591	5.687	44.148
DLT	2b	0.594	1.24651	0.70590	6.2459	-14.079	13.990	45.646
Collinearity		1.17	0.38995	0.24402	1.6756	-3.653	3.734	44.031
DLT	3	17.5	5034.04	4954.13	5606.28	8.197	-2.398	-89.293
Collinearity		17.6	5034.56	4956.35	5597.05	8.014	-2.359	-90.909

Table 2.4 continue

	data	x_0	y_0	c_x	c_y	d
DLT	1	0.00101	0.00180	50.000	49.999	-0.183×10^{-5}
Collinearity		0.00101	0.00180	50.000	49.999	-0.183×10^{-5}
DLT	2a	0.00075	-0.0596	1.0059	1.0031	-0.0186
Collinearity		0.0814	-0.0316	0.503	0.505	0.0106
DLT	2b	0.1483	-0.0705	1.1910	1.2180	-0.0216
Collinearity		0.0582	-0.0214	0.3220	0.3281	-0.0071
DLT	3	-5025.40	5023.51	54.822	54.830	0.1048×10^{-2}
Collinearity		-5025.49	5023.51	53.929	53.948	0.8589×10^{-3}

These results indicate that the presented physical model describes the DLT model and, provided that the numerical condition is good, the DLT will give exactly the same results as the collinearity equations with proper additional parameters. However, for the real data (data set 3), the results are slightly different, due to the different numerical structure, and the different levels of round off errors. In a very poorly defined case (data 2b), the collinearity equation model essentially fails, due to fatal correlations between parameters. However, in the DLT model, the correlation has been restructured into a better condition, and better results were achieved (closer to the true value), even though the determinacy remains much lower. The correlation is illustrated for this particular data set in Table 2.5a,b,c.

TABLE 2.5a
Correlation coefficients for data set 2b
from 11 para. collinearity equation. (Condition number: 0.36×10^8)

	x_0	y_0	c_x	c_y	d	ω	ϕ	κ	X_c	Y_c	Z_c
x_0	1.										
y_0	-0.02	1.									
c_x	0.08	-0.30	1.								
c_y	0.05	-0.30	1.	1.							
d	-0.	0.98	-0.16	-0.16	1.						
ω	-0.05	0.30	-1.	-1.	0.16	1.					
ϕ	0.05	-0.30	1.	1.	-0.17	-0.99	1.				
κ	0.08	-0.23	0.76	0.76	-0.05	-0.78	0.75	1.			
X_c	0.66	-0.72	0.50	0.48	-0.67	-0.47	0.48	0.39	1.		
Y_c	0.69	0.57	0.30	0.28	0.63	-0.28	0.28	0.24	0.15	1.	
Z_c	0.02	-0.30	1.	1.	-0.16	-1.	1.	0.76	0.46	0.26	1.

TABLE 2.5b
Correlation coefficients for data set 2b
of DLT parameters   (Condition number: 0.64×10^5)

	b_{11}	b_{12}	b_{13}	b_{14}	b_{21}	b_{22}	b_{23}	b_{24}	b_{31}	b_{32}	b_{33}
b_{11}	1.										
b_{12}	0.01	1.									
b_{13}	0.	0.	1.								
b_{14}	0.01	0.01	-0.	1.							
b_{21}	-0.	-0.	-0.	-0.01	1.						
b_{22}	0.	0.	0.	0.01	-0.	1.					
b_{23}	0.	-0.	-0.	0.	-0.	-0.	1.				
b_{24}	0.01	-0.	-0.	-0.	-0.07	-0.07	-0.	1.			
b_{31}	0.06	0.07	0.	0.45	0.01	0.04	-0.	-0.44	1.		
b_{32}	0.07	0.06	0.	0.44	-0.03	-0.01	0.	0.45	0.02	1.	
b_{33}	0.	0.	0.06	-0.	-0.	0.	-0.	0.	0.	0.	1.

TABLE 2.5c
Correlation coefficients for data set 2b
of physical parameters from DLT

	x_0	y_0	c_x	c_y	d	ω	ϕ	κ	X_c	Y_c	Z_c
x_0	1.										
y_0	0.63	1.									
c_x	-0.91	-0.26	1.								
c_y	-0.94	-0.32	1.	1.							
d	0.79	0.26	-0.85	-0.86	1.						
ω	-0.94	-0.33	1.	1.	-0.85	1.					
ϕ	-0.63	-0.18	0.65	0.65	-0.55	0.66	1.				
κ	-0.01	-0.76	-0.38	-0.32	0.21	-0.32	-0.25	1.			
X_c	-0.47	0.29	0.73	0.70	-0.85	0.70	0.46	-0.64	1.		
Y_c	-0.22	0.45	0.51	0.46	-0.09	0.47	0.31	-0.83	0.38	1.	
Z_c	-0.92	-0.28	1.	1.	-0.85	1.	0.65	-0.36	0.72	0.50	1.

Using the same data sets, but introducing artificial shear distortions, the compensation ability of the DLT model is shown. The artificial distortion is generated by assigning a non-orthogonality angle (β) and a y scale (λ_y), then calculating the corresponding a and b values,

$$\begin{vmatrix} x \\ y \end{vmatrix}^{\text{pseudo obs.}} = \begin{vmatrix} x \\ (1/a)y + (-b/a)x \end{vmatrix}^{\text{original obs.}}$$

...(Eq. 20)

The results are given in Table 2.6.

TABLE 2.6
The recovery ability of interior orientation and comparator
parameters (shear introduced)

data	introduced		recovered			recovered	
			shear model results			affine model results	
	λ_y	β	c_x	c_y	d	a	b
1	0.98	0.1	50.000	51.020	0.10033	0.98000	-0.10033
2b			1.201	1.254	0.07631	0.95789	-0.07631
3			54.731	55.856	0.09939	0.97985	-0.09939
1	0.98	0.0	50.000	51.020	0.00000	0.98000	0.00000
2b			1.186	1.237	-0.02154	0.95847	0.02154
3			54.830	55.956	-0.00105	0.97987	0.00105
1	1.00	0.1	50.000	49.999	0.10033	1.00000	-0.10033
2b			1.206	1.234	0.07620	0.97721	-0.07620
3			54.725	54.734	0.09939	0.99984	-0.09939

By introducing affine distortion artificially to the previously used data sets in the same way, the recovering ability of DLT model is tested (see Table 2.7). It should be noted that $d = -\tan\beta$, $b = +\tan\beta$ in the shear model, and because the same values for λ_y and β are introduced, the a, b, values differ between shear model and affine model.

TABLE 2.7
The recovery ability (affine introduced)

data	introduced		recovered values			σ (mm)
	λ_y	β	c	a	b	
1	0.98	0.1	50.000	0.98492	0.10033	0.473×10^{-3}
2b	(a=0.98492)		1.174	0.96367	0.11957	0.609×10^{-3}
3	(b=0.10033)		54.929	0.98480	0.10149	17.5×10^{-3}
1	0.98	0.0	50.000	0.98000	0.00000	0.468×10^{-3}
2b	(a=0.98)		1.186	0.95847	0.02167	0.602×10^{-3}
3	(b=0.0)		54.830	0.97987	0.00105	17.7×10^{-3}
1	1.00	0.1	50.000	1.00502	0.10033	0.468×10^{-3}
2b	(a=1.00502)		1.179	0.98311	0.11964	0.602×10^{-3}
3	(b=0.10033)		54.917	1.00489	0.10148	17.4×10^{-3}

2.1.4   1-D DLT Model

For the sake of completeness, as well as for practical application of linear array sensors in industry, a 1-D DLT model is derived.

Assuming: y=0; $Y_c = 0$; $Y = 0$; the collinearity equation is reduced to:

$$x - x_0 = -c \; \frac{m_{11}(X-X_c) + m_{12}(Z-Z_c)}{m_{21}(X-X_c) + m_{22}(Z-Z_c)}$$

Other assumptions could have been made by cutting the 3-D space along any profile, however, this one provides a good formulation.

The above equation can be reduced to the DLT form as:

$$x = \frac{a_1 X + b_1 Z + c_1}{a_2 X + b_2 Z + 1}$$

...(Eq. 2-21)

where :

$$
\begin{aligned}
a_1 &= (x_0 m_{21} - c\, m_{11})/C \\
b_1 &= (x_0 m_{23} - c\, m_{12})/C \\
c_1 &= -\{(x_0 m_{21} - c\, m_{11})X_c + (x_0 m_{22} - c\, m_{12})Z_c\}/C \\
a_2 &= m_{21}/C \\
b_2 &= m_{22}/C \\
1 &= C/C = -(m_{21}X_c + m_{22}Z_c)/C
\end{aligned}
$$

The five corresponding physical parameters of the five 1-D DLT equation are:

1. Station parameters (X_c, Z_c)

$$
\begin{vmatrix} X_c \\ Z_c \end{vmatrix} = -C \begin{vmatrix} (x_0 m_{21} - c\, m_{12}) & (x_0 m_{22} - c\, m_{12}) \\ m_{21} & m_{22} \end{vmatrix}^{-1} \begin{vmatrix} c_1 \\ 1 \end{vmatrix}
$$

with $C = (a_2{}^2 + b_2{}^2)^{-1}$

...(Eq. 2-22)

2. Interior orientaion (x_0, c)
$$x_0 = C^2(a_1 a_2 + b_1 b_2)$$
$$c^2 = C^2(a_1{}^2 + b_1{}^2) - x_0{}^2$$

...(Eq. 2-23)

3. Rotation matrix (as function of ϕ)
$$m_{21} = a_2 C$$
$$m_{22} = b_2 C$$
$$m_{11} = (x_0 m_{21} - a_1 C)/c$$
$$m_{12} = (x_0 m_{22} - b_1 C)/c$$

...(Eq. 2-24)

The same can be realized from the 3-D to 2-D DLT model, considering that the non-orthogonality and scale variation do not exist for 1-D image space, and in a plane only one rotation element is present. With the elimination of Y_c and y_0, there are 5 parameters remaining from the 11 physical parameters.

19

2.1.5   2-D Object Space DLT

The 2-D to 2-D projective transformation, which has been known as analytical rectification, has the following form:

$$x = \frac{a_1 X + b_1 Y + c_1}{a_3 X + b_3 Y + 1}$$

$$y = \frac{a_2 X + b_2 Y + c_2}{a_3 X + b_3 Y + 1}$$

$$...(Eq.\ 2\text{-}25)$$

Conventionally, these equations are interpreted by the rectifier geometry as stated in textbooks, e.g. Moffitt & Mikhail (1980). However, another way of thinking, coming from the collinearity equations may be instructive as well. It can be shown that any 8 of the 11 DLT equivalent physical parameters can be chosen for interpretation, although there are numerical conditions caused by critical configuration which limit some combinations. Obtaining initial values from a 2-D to 2-D projective transformation and then transforming to physical parameter space, provides a good complementary method to Rampal (1979).

Assuming that $a = 1$, $b = x_0 = y_0 = 0$, and C^2 is never equal to zero, because of the nature of the rotation matrix, we have:

$$
\begin{aligned}
b_{11}b_{31} + b_{12}b_{32} + b_{13}b_{33} &= 0 \\
b_{21}b_{31} + b_{22}b_{32} + b_{23}b_{33} &= 0 \\
C^2(b_{11}{}^2 + b_{12}{}^2 + b_{13}{}^2) &= c^2 \\
C^2(b_{21}{}^2 + b_{22}{}^2 + b_{23}{}^2) &= c^2 \\
b_{11}b_{21} + b_{12}b_{22} + b_{13}b_{23} &= 0
\end{aligned}
$$

$$...(Eq.\ 2\text{-}26)$$

From these equations, we can solve for b_{23}, b_{13}, b_{33}, and then, the collinearity parameters can be obtained by utilizing the DLT-to-physical parameter routine.

$$
\begin{aligned}
b_{23}{}^2 &= -K \pm (K^2 + 4(b_{11}b_{21} + b_{12}b_{22}))^{0.5} \\
&\quad\text{where } K = b_{21}{}^2 + b_{22}{}^2 - b_{11}{}^2 - b_{12}{}^2 \\
b_{13} &= (b_{11}b_{12} + b_{12}b_{22})/b_{23} \\
b_{33} &= (b_{21}b_{31} + b_{22}b_{32})/b_{23}
\end{aligned}
$$

$$...(Eq.\ 2\text{-}27)$$

20

The algebraic sign of b_{13}, b_{23}, b_{33} is not defined, which means that the camera station can appear on either side of the object. This is understandable because a horizontal plane object cannot define a three-dimensional datum. However, if there is a slight deviation from the object plane, then the sign can be defined from the relief displacements. Although three points uniquely define a plane, this dual solution problem does not happen in an iterative space resection approach with collinearity equations, because the initial values have already specified the side.

Based on these relations, the 2-D to 2-D perspective transformation can be utilized for space resection, then transformed from the algebraic space into the physical space. This approach requires a nearly plane object. When the 3 dimensionality increases, biases from relief displacements will adversely influence the solution. Therefore, this approach is a good supplement to the DLT approach with respect to the initial value problem. When the object has sufficient depth differences, the full DLT approach should be used. When the object is flat, then the 2-D DLT is sufficient.

In order to make it work, the coordinate component in one dimension of the object space should be constant or zero. For simplicity's sake, Z was selected, i.e., all points have Z=0. This could be achieved for a flat object simply by applying a similarity transformation with 2 rotations (ω and ϕ) and 1 translation (z). An inverse transformation will have to be carried out after the space resection. A detailed report is given in Shih & Faig (1988). Numerical examples for utilizing this scheme for initial values are also provided there.

2.1.6 General Potential Applications

The DLT model has been widely applied with close-range applications, especially for non-metric camera imagery. In real-time photogrammetry, it also has been shown that it is extremely suitable for digital sensors (Burner, et. al.,1985). Functionally the affine/shear distortion represents the most significant additional parameter set to most of the

digital sensors. In addition, extensive tests by the author proved that DLT is a good computational algorithm. These tests were published by Faig & Shih (1987).

Practically, the derivation given in this thesis does not affect the applications much, because in most cases, the 3-D coordinates of the station are required, which are not affected by the deviation of the Abdel-Aziz & Karara (1971) formulation from the exact physical model. In cases where space intersection is also needed, the 11 DLT parameters should be applied directly. However, if a calibration is planned, the author's model provides a complete solution, and an alternative to the conventional collinearity equations.

One potential application might be in the DLT block, which is a simultaneous block adjustment with the DLT model as its functional model. For the single photo resection case, the DLT model projects 11 corresponding physical parameters from the physical parameter space to another parameter space, where the parameters are less correlated than in the original parameter space. Therefore, better numerical conditions for the entire system can be expected. The comments, that the DLT model cannot take any a-priori information of parameters, can now be overcome by introducing additional observation equations using the relations provided in section.2.1.2. Although the practicality of doing this may require further investigation, mainly because of the non-linearity of these equations, the DLT model provides a valid alternative to the collinearity equations.
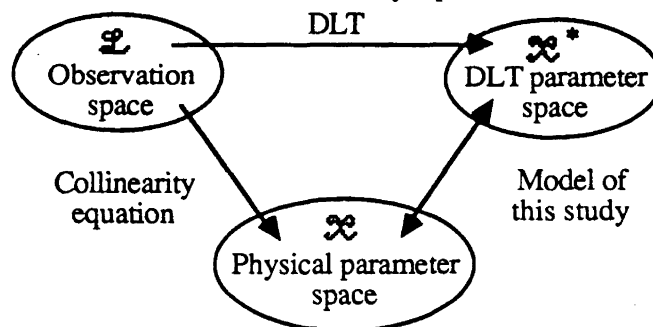
Figure 2.2: The Illustration of Space Transformation

The DLT block could be applied without knowing the model presented in this study, if the weighted constraints for unknown parameters are not considered. However, the transformation tool developed here will provide a better interpretation of the resulting

22

parameters. It should be noted though, that the covariance matrix for the estimated physical parameters can only be approximated after this transformation, because the transformation from the 11 DLT parameter space to the 11 physical parameter space represents non-linear mapping, and the covariance law is only valid for linear mapping or locally linear mapping. In the DLT case, only the first order factor could be conveyed if the second moment in the physical parameter space only is calculated. Even if the higher order moments were computed, the covariance law would still provide only an approximation, although a better one.

2.2 COMPARATIVE STUDY OF FUNCTIONAL MODELS (Unit: PHOTO)

As stated at the beginning of this chapter, the functional models could be classified into two categories by judging the dependence on entities, and further divided by the computational unit used. In this section, the most generally used functional models in computational photogrammetry: the collinearity equations, the DLT formulation, and the image pyramid model, were compared for space resection in terms of: correlation between parameters, dependency on initial values, condition numbers of the numerical system, variance of the residuals and of the estimated values, as well as the number of iterations required. Through all computations, the computational strategy suggested by Faig & Shih (1986) is applied.

These three models use the photograph as the unit and generally require the datum definition, either by observations or constraints. In essence, the space resection makes use of image coordinates and heavily weighted or fixed object coordinates to determine the positional and rotation elements of the photograph or camera. The basic space resection of a single photo can be extended to include the interior orientation parameters, or reduced to include positional or rotation elements only. Therefore, a space resection may have 3 parameters (e.g.,X_c,Y_c,Z_c), 6 parameters (e.g., $X_c,Y_c,Z_c,\omega,\phi,\kappa$), or more.

A block adjustment essentially is space resection combined with space intersection. This can be done in two stages, or simultaneously. The DLT approach is a two stage method, where resection and intersection represent two distinctly different phases. The methods devised in Shmutter & Perelmuter (1979) and Hadem (1981) are iterative approaches, where a refined intersection is followed by another resection-intersection. The methods such as used in UNBASC-2 (Moniwa, 1977), GEBAT-V (El-Hakim, 1979), PTBV(Armenakis, 1987), are simultaneous block adjustments.

Besides its important role in block adjustment, space resection by itself is an important procedure when applying vision sensors for robotic positioning.

Extensive studies on the algorithms of space resection have been conducted in the past. For instance, Rapp (1966) compared the image pyramid method with the collinearity equations. Although the collinearity equations were preferred, the results of his study indicate that parameters of smaller variance were achieved by the image pyramid method. Boge (1965) investigated the inter-dependency of number of iterations, initial values, and the station parameters. He concluded that the number of iterations required for a solution appears to be related to the angular orientation of the photograph, and although a rough initial approximation for rotation elements reduced the required number of iterations, further refinement had little effect. Concerning the initial values, Bolt & Atkinson (1984) made a concise statement : "to ensure successful convergence, *the rotations had to be approximated to within 1 radian of their true value."*

It is realized that, in the digital sensor era, the speed of the selected algorithm becomes essential, however, for a general purpose vision system, the generality of the adopted algorithm is equivalently important. While a rigidly specified algorithm will probably gain on speed, but sacrifice flexibility, a generalized algorithm risks inefficiency of computation.

For a single photo space resection, the image pyramid method has only three unknowns, while collinearity equations have six. On the other hand, when higher accuracy

is desired, more factors have to be taken into account. The DLT model not only provides 11 parameters which cover the exterior and interior orientations, as well as affine correction, but is also *independent of initial values.*

In order to limit the range of this investigation, it is restricted to the fundamental types of these three functional models. Thus, to provide cross comparison, the image pyramid method is compared with collinearity equations excluding interior orientation parameters, while the DLT model is compared with collinearity equations including the corresponding five interior orientation parameters.

2.2.1   The Functional Models

2.2.1.1   The Collinearity Equation Model

This model is well-known and conventionally used. However, it suffers from the problems of dependency on parameter approximations and slow processing of the trigonometric terms in its rotation matrix. The latter problem has been tackled by utilizing the Rodrigues matrix (Schut, 1959; Pope, 1970), with Schut's formulation being recommended for its better performance (ASP, 1980). However, there are certain limitations for its application. Within the scope of this study, the conventional trigonometric rotation matrix is used.

2.2.1.2   The Image Pyramid Model

The concept of this model is based on the relationship between the image pyramid, formed by three image points plus the perspective centre, and the object pyramid formed by the corresponding object points and the perspective centre. In this model, the observation equations are formed for pairs of points. Therefore, the number of the independent conditions for n properly distributed points, is equal to the number of sides of the non-overlapping triangulated surfaces, which is (2n-3) (Wang, 1979).

There are two major methods in this category: Church's method and Rampal's method.

Church, based on the image pyramid model, developed the well known Church method (ASP, 1980) around 50 years ago. This model is an equivalent model to the collinearity equation model with a reduced parameter set. Only the positional elements are included. However, this is also a non-linear model.

Considerable effort has been devoted to methods that avoid the requirement for initial values. Such approaches are termed closed solution. Rampal (1979) formulated an approach, which is in closed form. It is based on the image pyramid model and utilizes the distance relations. However, one condition is assumed: the **object plane** is near **parallel** to the **image plane**.

Hadem (1981) generalized Rampal's approach, but with different constraints: either one distance between an object point and the perspective centre is approximately known, or numerical analysis techniques are used.

Church's method utilizes the space angle formed in image space by the perspective centre plus two points, and in object space by the corresponding points. Three points form a pyramid which uniquely defines the perspective centre. The functional model can be expressed either in terms of angles, or their cosine values. The latter are used more generally and are applied in this study.

This method is classified as approximate because :
1. The correlation between station parameters and rotation elements is ignored;
2. The method is optimized by minimizing a functional value instead of the residuals of the observations;
3. The difficulty in rigorously forming the design matrix, i.e., (2n - 3) independent equations, is avoided by either using n equations or n(n-1)/2 equations which include some dependent equations.

When addressing the first point, it should be noted that for the image pyramid method, the station coordinates are actually independent of the rotation elements. The image pyramid method should thus provide a better solution than others, if there are no biases such as interior orientation parameters, lens distortion etc., because there are no redundant parameters.

This functional model is neither efficient nor sufficient when the rotation elements are also required. However, the estimated parameters could be carried into a second stage with their covariance matrix for a collinearity equation model to retain the rigor (Chen,Y., 1985). However, it should be noted that this weighted constraint scheme is only applicable when different observations are used in these two stages. This approach requires increased computational effort. There might be one advantage, that the initial value problem may not be so severe, although it is based on knowledge of station coordinates within a certain range to get the image pyramid method started.

The second point can be avoided by introducing the second design matrix into a combined adjustment model. Once again, the cost is increased computational effort, because the second design matrix for this model is not diagonal.

The draw-back of introducing the second design matrix is apparent. Because its profile is always the same as the number of points, it does not improve when the n equation approach is used. The shape of the normal equation coefficient matrix is diagonally banded with one element in the far corner. Although it is structured and sparse, a special technique is required for better handling.

As to the third point, the n equation method generally is taking the pairs in sequence, i.e., (1,2), (2,3), ... , (k,k+1), ... (n,1) (see Figure 2.3), while the n(n-1)/2 equation method is using all combinations. As a matter of fact, rigorously forming (2n-3) independent equations can be accomplished by taking (1,2),(1,3), ..., (1,n), and (2,3),(3,4), ...,(n-1,n). Although the numerical condition associated with this simple

scheme requires further investigation, it provides an alternative to the triangulation of the image plane with certain optimal conditions.
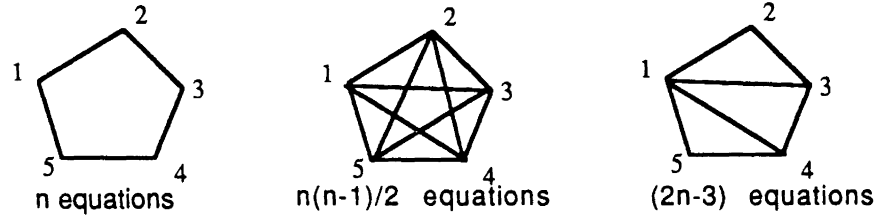
Figure 2.3: n, n(n-1)/2, (2n-3) approaches

As a summary, the following approaches are available:

1. n equations;
2. n(n-1)/2 equations;
3. (2n-3) equations with simple scheme;
4. (2n-3) equations with triangulation scheme.

The influence on accuracy is insignificant when the second condition is not satisfied. The numerical condition may be the selecting standard. Shmutter & Perelmuter (1979) recommended the n(n-1)/2 equation approach for better convergence speed.

If only the scheme of forming observation equations is considered among the first two, the n(n-1)/2 approach implies wrong weights for the observations, whereas the n equation approach ignores some conditions. Judged by the computational effort, the n equation approach is preferred. However, Shmutter & Perelmuter (1979) have pointed out that by using the n(n-1)/2 method, all combinations are used, and then, the frequency of each measured point is equivalent. This seemingly provides a double negative compensation in the weighting scheme.

2.2.1.3 The DLT Model

Concerning the form of the observation equations, Wong (1976) provides two different ways. One is stated as iterative, the other as direct. The direct method describes the same situation as the Church method. The residual of the condition equation is used as the optimization object. In the iterative method, the residual of the observation (image

28

coordinate) is used. The difference between these lies in the weight, because both of them are linear in their (pseudo) observation space. In order to clarify this, the observation equations are given here. For both DLT and the collinearity equations, they could be written as:

$$x = m/q;$$
$$y = n/q.$$

...(Eq. 2-28)

Including the residual terms (v_x, v_y), this leads to the following for the direct method:

$$(x)q - m = v_x;$$
$$(y)q - n = v_y.$$

...(Eq. 2-29)

and for the iterative method :

$$(x + v_x')q - m = 0;$$
$$(y + v_y')q - n = 0.$$

...(Eq. 2-30)

Actually, it is found that the lack of the second design matrix in the DLT model is essentially the same as for the conventional collinearity equations.

Because the second design matrix in this case could be formed as a diagonal one, the computational work does not increase much as long as a diagonal weight matrix is used. Numerically, the initial approximations are not required in either case, and practical tests show that only one iteration is sufficient in most cases for the iterative method. The one with a correct weighting scheme does provide better accuracy in terms of standard deviations of the image residuals throughout all experiments. Certainly, it falls under the assumption that all image coordinate observations are weighted as they should be, i.e., equal accuracy for all observations in the tests of this study.

2.2.2   Concepts of Equivalent Model and Simplified Model

Two linear models are said to be equivalent when the location and dispersion of the common estimates are equivalent. Baksalary & Kala (1981) and Baksalary (1984) investigated the equivalence between a Gauss-Markoff Model and its augmentation by

nuisance parameters. Based on these works, Lindlohr & Wells (1985) and Schaffrin & Grafarend (1986) illustrated the equivalence relation in GPS data processing applications. The author decided to apply this concept to the comparison of the functional models.

Generally, to reduce the number of parameters in a mathematical model, there are two ways: **nuisance parameter elimination** or **parameter simplification**. The first one leads to an equivalent model to the original one. The second approach may result in very close estimates, where the differences are insignificant in some cases, but still cannot be classified as mathematically equivalent model.

Church's model is an equivalent model to the collinearity equation model with exterior orientation (6 parameters) only. Compared with the collinearity equation model with interior orientation parameters or the DLT model, both the 6 parameter collinearity equation and Church's model are simplified models. It should be noted that, although the models are equivalent, the numerical conditions are not necessarily the same, in fact most often they are not.

2.2.3   The Geometrical Configuration

Geometric configuration refers to the dimensional measure of the object and its relations to the camera station. Five cases were studied. All test data were generated by computer simulation. At first, each individual factor was tested under different conditions, and each test was investigated by its condition number, the standard deviations of the image residuals, and the closeness to the true station parameters. The image residuals were calculated by projecting the object points to the image using the estimated parameters. In Church's method, the true values of the rotation elements were used.

The details of the generated data and part of the test results concerning the systems' numerical conditions are described as follows:

2.2.3.1 Ratio Between Object Distance and Camera Constant (Z_c/f)

This factor usually is referred to as scale, and indicates the resolution in this idealized case. The tests were performed for nine cases, with different ratios, ranging from 10 to 156 250. Each case was analyzed for two resolutions, firstly, 1 μm and secondly, as far as the double precision on the IBM 3090 computer can provide.

Analyzing the test results, it is found that improved resolution has no influence on numerical conditions in terms of the system condition number and iterations required, provided that the image points can be differentiated. This is true for all three functional models. The accuracy and the significant digits of the estimated parameters improved with the increased resolution, a result well known to surveyors.

It is of interest that the numerical condition does become worse for collinearity when the Z_c/f ratio becomes larger, because of an increase in the ($Z - Z_c$) term, while there is no significant change for the DLT model. The condition number becomes larger, although at a slower rate, for the Church method as well, caused by the decreasing value of the vertex angle of the image pyramid.

Studying the correlation matrix, the correlations between X_c and ϕ, Y_c and ω, are increasing along with the Z_c/f ratio in the collinearity equation model, while in Church's method, the X_c and Y_c correlation increased. In the DLT model, the correlations remain the same throughout.

2.2.3.2 The Terrain Relief (Z_C/dZ)

The terrain relief which plays an important role in single image photogrammetry, is also of importance in the multi-image case with either on-the-job or self-calibration. This factor usually is represented by the ratio between the object distance (sensor to object) and the dimension deviation of object points in the direction of the imaging axis (the relief), i.e., Z_c/dZ.

The test data is generated by keeping the scale of the image constant. That is, with the increase of Z_C, and dZ fixed, the principal distance is numerically enlongated.

The numerical condition of the DLT model is not affected by Z_C/dZ as reported in Faig & Shih (1986). The Z_C/dZ factor is more effective in the 9 parameter collinearity equation model with basic interior orientation, than the one using only 6 parameters and fixed interior orientation. This is known to be caused by the correlation between Z_C and the camera constant. However, the major part lies in the collinearity equation itself. It should be noted that the data generated in this case represents a change of viewing angle. For a fixed image scale, an increase of Z_C/dZ is equivalent to a decrease of the viewing angle.

Looking at the correlation matrices, the correlation between X_C and f, Y_C and ω -- for 6 parameters, Z_C and f, y_o and ω, x_o and f -- for 9 parameters, as well as X_C and Y_C in the Church method, are increasing with the ratio of Z_C/dZ.

2.2.3.3   Dimensional X/Y/Z Ratio of Object

Faig & Shih (1986) reported that the dimensional ratio of the imaged object has a major influence on the numerical condition of the DLT model. For the other two functional models, the following was obtained:

1. The collinearity equations with 6 parameters apparently are not affected by the dimensional ratio.

2. For the 9 parameter collinearity equations, the condition number gets larger when the dimensional ratio gets larger. This is caused by the inclusion of interior orientation parameters, in the same way as for the DLT model. It is interesting to note, that for changes in the X and Y dimensional ratios, DLT is better by a factor of 2, and for Z by a factor of 3, the reshaping effect of DLT, which reduces the correlations in the DLT model.

3. The 11 parameter collinearity case indicates slightly larger condition numbers than the corresponding 9 parameter results. This means that the affine factors are not as highly correlated to other parameters as the basic interior orientation parameters.

4. Church's method is affected through the change of the cosine value. The X dimensional ratio has the same effect as the Y dimensional ratio, while the Z dimensional ratio has no effect. Concerning the correlation, the largest correlation is always between X_C and Y_C.

In the past, the terrain relief was indicated by the Z_C/dZ ratio, which is correct when the focal length of the imaging device is fixed. That is, for larger Z_C , the coverage is larger, but the dimension along the imaging axis is unchanged. In this case, Z_C/dZ is equivalent to the three dimensional ratio of object. It may thus be justified to conclude that the three dimensional ratio of the object is a more suitable indicator for expressing the relief.

2.2.3.4   The Translation

The normal case with translation of the perspective centre in X direction was tested. The resulting effect is a shift of the image point cluster sideways. For the 6 parameter collinearity case, the increasing condition number is caused by the increase of $(X - X_C)$. In Church's method, it remains almost the same, and for the DLT model, there is no influence.

2.2.3.5   The Rotations

Three cases were studied:

1. rotate the object and the camera station with respect to the origin of the object coordinate system.

2. rotate the object around its centre of gravity, and keep the camera station fixed;

33

3. rotate the camera station around the origin of the object coordinate system, and keep the object fixed.

Each case contains 9 tests with different combinations of rotation angles under permutation.

The first case essentially does not change the geometrical configuration. The second one remains the normal case. Because the object used is a cube, it is justified that the numerical condition does not vary much. The last one changes the geometrical configuration as well as the rotation angles. Through all simulations, the condition numbers for all three models do not change significantly.

2.2.4 The Initial Values

For a non-linear least squares adjustment, Pope (1974) theoretically explored two methods. The one most frequently used in surveying currently is termed the **Newton-Gauss** method. In this method, we form normal equations from approximated linear equations, then solve exactly, and start the iteration all over. The collinearity equation model and the image pyramid method are both non-linear models with respect to the station parameters. Therefore, initial approximations for the estimated parameters are required. This aspect could be investigated by the condition numbers of the formed system. It is known that the numerical condition of a system is affected by its geometrical configuration, the parameter formulation, and the approximate values used in the non-linear case. Therefore, when fixing the geometrical configuration within a specified mathematical model, the condition number of the normal equation system can be studied for the influence of initial values.

The initial values not only affect the numerical condition, but also play an important role in the convergence of the computation. This is caused by ignoring the higher order terms in the Taylor series expansion and cannot be readily revealed by the condition numbers. Besides the problem of possible divergence, possible multi-local minima as well as the convergence speed, complicate the situation. The first aspect has been solved in

Haralick & Chu (1984) for their entity type model of a parameterized curve. They used the **generating multiple random initial guesses method**. However, its application would be difficult, if it is not impossible, for the point mode collinearity equations or for Church's method. The key point is the known existence of multi-local minima. Therefore, this study intends to confirm the general instructions which could be utilized for evaluating the a-priori goodness of initial values. By doing so, a proper scheme for solving a space resection may be selected.

Concerning the convergence criteria, several different concepts and different methods are currently in use (Mikhail & Ackermann, 1976; Owolabi, 1988; Torlegard, 1981). In this study, Wang's (1979) recommendation of 1 to 10 milli-gon for rotation elements for an image coordinate accuracy close to 5 μm, is followed. 0.0001 radians is used for rotation, and 0.001 m is used for translation parameters.

For the 6 parameter collinearity equation and the image pyramid method, the interior orientation is assumed to be error-free. Although this may not be true, it simplifies the tests.

The tests on the initial values revealed the following:

When the true value was specified as the initial approximation, most of the tests only required one iteration, and only a few with bad resolution required two.

When the X_C, Y_C, Z_C were initialized with values of 10 000.0, 10 000.0, 12 345.0 away from the true value, together with true values for rotations, most of them required three iterations, some four. The condition number at the first iteration was huge, however it dropped very quickly when converging. When the rotations also differ from the true values by 0.1 and 0.2 radians, the number of iterations required increased to five, with a few requiring four. When the rotations were off by 0.5 radians, the required iterations ranged from five to nine. More significantly, some tests converged eventually to another local minimum.

When the translation parameters start with the true values, but the rotations are off by 1 radian, one third of the tests did not converge at 30 iterations. Some others converged to a local minimum.

Cases of only one rotation being initialized wrongly by 1 radian, along with other elements with small permutations, also have been tested. All converged in six or seven iterations.

It is not intended to completely test all possibilities. However, at this stage, it might be concluded that:

1. the magnitude of the rotations does not influence the convergence in all tested cases;

2. the translation parameters are only necessary to be approximated in the range that the condition number of the first iteration will not exceed the computing device afforded;

3. the 1 radian reference is helpful, however, if all rotation elements are off by 1 radian the convergence cannot be secured;

4. for Church's method, the requirement of initial values for station coordinates is much tighter.

2.2.5   Other Aspects used for Comparison

1. Correlation between Parameters

The correlation between parameters has a significant influence on the numerical stability of the system, and is reflected in the condition number. However, it is not the only factor influencing the condition number because the trend of the correlation does not always fit the trend of the condition number.

Comparing DLT with 9 and 11 parameter collinearity, the lower correlation among the DLT parameters is again confirmed in all cases.

2. Computational Effort

The required CPU time for the computations was counted for a single call of each algorithm. The input and output, as well as other optional computations were not included.

An inversion routine with a Cholesky decomposition method was used for all of them. The results are listed in Table 2-8. The major factor is the size of the matrix inversion. The difference between DLT and 11 parameter collinearity is understood as caused by the trigonometric terms involved in the design matrix formation. It should be kept in mind, that most frequently the collinearity approach requires three iterations, while DLT requires one for the direct method, and two for the iterative method.

TABLE 2.8
Single Run CPU Time for Space Resection on IBM 3090 Computer
unit: 10^{-4} sec

Routine	6 para. Collinearity	11 para. Collinearity	Church	DLT
cpu time	218	543	92	510

3. Accuracy of Estimated Parameters

Church's method used in this study is using the differences of cosine values as observations. Therefore, the Q matrix is not directly comparable with the one from the collinearity approach. After multiplying Q with the corresponding a-posteriori variance, they become comparable. It should be noted that there is no Gaussian random error introduced in all tests, therefore the variance calculated is caused by the resolution of simulated observations and by round-off errors. Generally the Church method provides competitive results, but does not provide a smaller covariance matrix. This finding is well supported by the equivalent model concept. Church's method is an equivalent model to the 6 basic parameter collinearity equation, while it is a simplified model compared with the collinearity equations with interior orientation parameters.

4. Algorithmetic Characteristics

This study revealed that the three functional models have the following algorithmetic characteristics:

- image pyramid model
   -- Church method: not in a closed form;
   -- Rampal's method: closed form; the image plane should be near parallel to the object plane;

37

-- Hadem's method: closed form; with an additional distance constraint,or applying numerical analysis techniques;

• collinearity equations: not a closed form;

• DLT
-- 3D-2D DLT: closed form; requires 3 dimensionally distributed control points;
-- 2D-2D DLT: closed form; control points should be on a plane;

Because different constraints are required, for each closed form solution, these solutions provide a useful group of alternatives for different practical cases.

For the case where the station translation parameters are well approximated a-priori, the Church method could be used for an initial stage computation, then one should proceed to the collinearity equations for the rotation elements. However, the Church method requires a much better initial estimation of station coordinates than the collinearity equations. The requirement of closeness on rotation parameters for the collinearity equations is not very high either. When other parameters can be closely approximated initially, then one of the rotation angles can be initially off by as much as 1 radian. The major influence of the deviation of initial values of station coordinates is the increased condition number in the first few iterations, but it reduces very fast, provided the rotation elements are known better.

5. Potential Applications

The DLT model is justified as a very good computation algorithm. The numerical stability of the system generally only relies on the object dimensional ratio. For a pre-designed environment, e.g., factory, farm yard, or other environment where robot vision may be used, the panels of field control points could well be designed close to a cube. This will strengthen the numerical condition. One may comment on the big parameter set, which is an **over-parameterization**, and does deteriorate the numerical condition of the system. However, it is a price we pay for easier handling of the data. The justification is "we need it or not". The numerical condition would not become better if the parameters were necessary, but it is "paid for" in this case. In many other cases, a significance test is

needed. But here, the significance is beyond what a statistical tool can provide. If we have sufficient observations, the most sophisticated model, as far as these studies revealed, will provide the most benefits. *Sophistication does not cost, it pays.*

2.3 COMPARATIVE STUDY OF FUNCTIONAL MODELS (Unit:MODEL)

In analytical photogrammetry, the **model** (more precisely, **stereo-model**), is very important. Stereo perception can be achieved in a "model". The model contains 3-D object information in general, and therefore most map compilation work is done with it. Although a model could represent a triplet, quadruplet, etc., it usually indicates the stereo-pair which has been restituted by the procedure of relative orientation. When the relative orientation is generalized to include more than one pair, then a multi-photo model can be formed.

Here, three functional models can be identified:

- Collinearity equations;
- Coplanarity equation;
- RDLT (Direct Linear Transformation of Relative Orientation).

In this section the first two classic models will be conceptually outlined, while the RDLT model will be explored in more detail. A closed form algorithm as developed by Novak (1986), based on the concepts of Wunderlich (1982), and of Killian (1984), is also investigated.

Since the reliability and numerical stability of relative orientation under different control patterns have been extensively studied by others, e.g., Rostom (1981), it will not be repeated here.

2.3.1 Collinearity and Coplanarity Equations

Relative orientation means the orientation procedure which recovers the relative relationship within the stereo-pair. In brief, for 2 photos in a stereo-pair, there are 6 degrees of freedom from each. After removing the 7 elements for datum definition, 5

39

elements remain. Because of the geometry of a stereo-pair which commonly has the two camera axes nearly parallel to each other, some dependence exists between the parameters. Therefore, not any combination of 5 elements out of these 12 can be chosen. When realized with coplanarity conditions, the base vector and the corresponding image vectors should form a plane. Three rotations between these two image vectors and 2 of the 3 base components form the parameter set.

Both models are non-linear, and iterative procedures have to be applied. The initial values once again constrain the universality.

Concerning the application, the coplanarity equation was implemented in the early stages of development of UNBASC-2, a self-calibration bundle block adjustment program. However, it has been concluded that the coplanarity equation can be substituted by collinearity equations in a block adjustment (Moniwa, 1977). Conceptually, the coplanarity condition is defined through different geometric interpretation by the collinearity equations or the coplanarity equation. In the collinearity equations, it is defined by stating that two vectors from different images of the same point intersect at the same point. Since two intersecting lines define a unique plane, this also states exactly the coplanarity equation. In the coplanarity equation, the coplanarity is stated by the volume formed by the base vector and the two corresponding image vectors, which equals zero. Therefore, it is justified to say that the coplanarity condition is embedded in the collinearity equations when a stereo-pair exists. Although Okamoto (1981) utilized the coplanarity condition along with collinearity equations, where 22 perspective transformation parameters of two overlapping photographs are solved by using 7 equations based on the coplanarity condition of corresponding rays and 15 equations based on 8 measured distances or 5 object space control points on each photograph, calibration and theoretical interest were of major concern.

2.3.2 RDLT Model

Khlebnikova (1983) introduced a closed form solution for relative orientation, and reported successful implementation. Chang (1986) provided a somewhat similar formulation, tested it on a Zeiss Planicomp C-100, and named it RDLT (Direct Linear Transformation of Relative Orientation). Because this model is not commonly used by photogrammetrists, it is investigated and detailed in this subsection.

2.3.2.1 The Formulation

Starting with the coplanarity equation, the base vector (B_X, B_Y, B_Z), and the two corresponding image vectors (U, V, W) and (U', V', W') form the condition:

$$\begin{vmatrix} B_X & B_Y & B_Z \\ U & V & W \\ U' & V' & W' \end{vmatrix} = 0$$

...(Eq. 2-31)

where,

$$\begin{vmatrix} U \\ V \\ W \end{vmatrix} = \begin{vmatrix} x_i - x_o + dx \\ y_i - y_o + dy \\ -f \end{vmatrix} = \begin{vmatrix} x \\ y \\ -f \end{vmatrix}$$

$$\begin{vmatrix} U' \\ V' \\ W' \end{vmatrix} = \begin{vmatrix} x_i' - x_o' + dx' \\ y_i' - y_o' + dy' \\ -f' \end{vmatrix} = \begin{vmatrix} m_{11} & m_{12} & m_{13} \\ m_{21} & m_{22} & m_{23} \\ m_{31} & m_{32} & m_{33} \end{vmatrix} \begin{vmatrix} x' \\ y' \\ -f' \end{vmatrix} = M \begin{vmatrix} x' \\ y' \\ -f' \end{vmatrix}$$

and R is an orthogonal matrix.

Expanding the above equation, the following can be obtained:

$$L_1 y\ x' + L_2 y\ y' - L_3 y\ f' + L_4 f\ x' + L_5 f\ y' - L_6 f\ f' + L_7 x\ x' + L_8 x\ y' - L_9 x\ f' = 0$$

...(Eq. 2-31)

where:

$L_1 = B_X m_{31} - B_Z m_{11};$	$L_2 = B_X m_{32} - B_Z m_{12};$	$L_3 = B_X m_{33} - B_Z m_{13};$
$L_4 = B_Y m_{11} - B_X m_{21};$	$L_5 = B_Y m_{12} - B_X m_{22};$	$L_6 = B_Y m_{13} - B_X m_{23};$
$L_7 = B_Z m_{21} - B_Y m_{31};$	$L_8 = B_Z m_{22} - B_Y m_{32};$	$L_9 = B_Z m_{23} - B_Y m_{33}.$

Since this equation is homogeneous, one parameter can be removed. For the majority of cases, where B_X is much larger than the other two components, L_5 is selected.

$$L_1' y\ x' + L_2' y\ y' - L^3' y\ f' + L_4' f\ x' - L_6' f\ f' + L_7' x\ x' + L_8' x\ y' - L_9' x\ f' - f\ y' = 0$$

...(Eq. 2-32)

41

where, $L_i' = L_i/L_5$

When the misclosure of this equation is subjected to optimization, this model is linear. A direct solution for these 8 parameters can be achieved without knowing any approximate values.

2.3.2.2   Physical Interpretation of Algebraic Parameters

Five relative orientation parameters can be obtained from these 8 algebraic parameters. Utilizing the 6 conditions of the orthogonal matrix, we can form 6 equations.

$$
\begin{array}{rcll}
L_1'^2 + L_2'^2 + L_3'^2 &=& (B_X^2 + B_Z^2)/L_5^2 & (1)\\
L_4'^2 + L_5'^2 + L_6'^2 &=& (B_Y^2 + B_X^2)/L_5^2 & (2)\\
L_7'^2 + L_8'^2 + L_9'^2 &=& (B_Z^2 + B_Y^2)/L_5^2 & (3)\\
L_1 L_4 + L_2 L_5 + L_3 L_6 &=& B_Y B_Z & (4)\\
L_1 L_7 + L_2 L_8 + L_3 L_9 &=& B_X B_Y & (5)\\
L_4 L_7 + L_5 L_8 + L_6 L_9 &=& B_X B_Z & (6)
\end{array}
$$

...(Eq. 2-33)

With given B_X, solving the first 3 equations one can obtain:

$$L_5^2 = 2B_X^2/((1)+(2)-(3)) ; \quad B_Y^2 = ((2)+(3)-(1)).L_5^2/2 ; \quad B_Z^2 = ((1)+(3)-(2)).L_5^2/2.$$

...(Eq. 2-34)

where, (1), (2), (3) denote the appropriate left hand side of the corresponding equations.

From the definition of the algebraic parameters, the elements of the rotation matrix can be obtained.

$$
\begin{vmatrix}
-B_Z & 0 & B_X \\
B_Y & -B_X & 0 \\
0 & B_Z & -B_Y
\end{vmatrix}
\begin{vmatrix}
m_{11} & m_{12} & m_{13} \\
m_{21} & m_{22} & m_{23} \\
m_{31} & m_{32} & m_{33}
\end{vmatrix}
=
\begin{vmatrix}
L_1 & L_2 & L_3 \\
L_4 & L_5 & L_6 \\
L_7 & L_8 & L_9
\end{vmatrix}
$$

...(Eq. 2-35)

Since the first matrix on the left hand side has a zero determinant, i.e., only 6 out of 9 equations are independent, 3 other equations are required in order to solve the 9 parameters of the rotation matrix. Utilizing the orthogonality condition, i.e., an element of

42

an orthogonal matrix of unit determinant is equivalent to the determinant of its cofactor matrix, the following three equations are obtained.

$$m_{11} = \begin{vmatrix} m_{22} & m_{23} \\ m_{32} & m_{33} \end{vmatrix}; \quad m_{22} = \begin{vmatrix} -m_{21} & m_{23} \\ m_{31} & m_{33} \end{vmatrix}; \quad m_{13} = \begin{vmatrix} m_{21} & m_{22} \\ m_{31} & m_{32} \end{vmatrix}.$$

...(Eq. 2-36)

Taking the first 6 equations of the parameter definition; and the above 3 orthogonality condition equations, the solution is formed as follows:

$$\begin{vmatrix} d & -b & a \\ b & d & -c \\ -a & c & d \end{vmatrix} \begin{vmatrix} m_{11} \\ m_{12} \\ m_{13} \end{vmatrix} = \begin{vmatrix} L_6 L_2 - L_3 L_5 \\ -L_6 L_1 - L_3 L_4 \\ L_5 L_1 - L_2 L_4 \end{vmatrix}$$

...(Eq. 2-37)

where:

$d = B_X^2;$
$a = L_5 B_Z + L_2 B_Y;$
$b = L_3 B_Y + L_6 B_Z;$
$c = L_4 B_Z + L_1 B_Y.$

and:

$m_{21} = (B_Y m_{11} - L_4)/B_X; \quad m_{31} = (B_Z m_{11} + L_1)/B_X;$
$m_{22} = (B_Y m_{12} - L_5)/B_X; \quad m_{32} = (B_Z m_{12} + L_2)/B_X;$
$m_{23} = (B_Y m_{13} - L_6)/B_X; \quad m_{33} = (B_Z m_{13} + L_3)/B_X.$

The equivalent physical parameters for these 8 algebraic parameters in the RDLT model can be formed with conventional 5 elements and 3 extra parameters defined from the rotation matrix when removing three orthogonality conditions. However, by doing this, the advantage of the closed form will disappear.

If the residuals of the image coordinates were used as the optimization object, the formulation would be relatively complicated. Meanwhile, the covariance matrix of the estimated physical parameters from RDLT will still be an approximation due to the linear characteristics of the covariance law. The normal process is to generate the initial values by RDLT and then follow by a collinearity or coplanarity equation solution.

43

The problem of sign determination for B_Y, B_Z can be solved by using equations (4), (5), (6) for a sign check. An APL test program was written for experiments in this research and the excellent performance of RDLT was once again confirmed.

2.3.3 Novak's (1986) algorithm

As stated in Novak (1986), when there are four points which lie in the same plane and appear on both photos, the relative orientation can be performed, provided the interior orientation is known. This approach should not be considered as a functional model, instead, it is considered as a special algorithm for orientation. The procedures are as follows:

1. Transform all measured image coordinates to the principal points, and normalize them by the principal distance.

2. Perform a 2-D to 2-D perspective transformation from image 1 to image 2 using these four point pairs. The resulting 8 parameters, catenated with the integer 1, form a 3x3 matrix A.

3. Compute the eigen-values and eigen-vectors of B, where B is the inner product of A, i.e., $B=AA^T$.

4. Define a right handed coordinate system with these eigen-vectors. Classify the eigen-vectors by referring to their values. The direction of the corresponding largest eigen-value is referred to as the X axis.

5. Calculate the sine and cosine values of angle ω, by utilizing the eigen-values.

6. Perform an eigen-value transformation on the shifted and normalized image coordinates, followed by a rotation with the angle ω. By assuming the plane lies in the X-Y plane, the model coordinates are obtained.

The algorithm does not require any initial values, and no iterations are required. However, the decision on which root should be selected imposes a problem. Three methods for solving this have been configured by Novak (1986).

In the case that there are three photos, and the principal point coordinates were known, the principal distance can be calibrated. In Novak (1986), Ethrog (1984)'s algorithm is suggested for a full calibration for principal point coordinates and principal distance.

2.3.4   Comparative Findings

RDLT has the significance in providing a closed form solution for relative orientation. This would be very helpful when a quick solution for a general case is required. Since RDLT does not rely on any entity, and a simultaneous adjustment by including all observations can be easily implemented, it may be justified to say that it has some advantages over Novak's (1986) approach. However, for RDLT the number of image point pairs should be no less than 8.

Compared with the coplanarity equation, the collinearity equations can easier be expanded for including additional parameters, and also can easier be generalized from the basic stereo-pair to a multi-photo case. Therefore, they are generally preferred over the coplanarity equation.

CHAPTER 3

THE EXTENSION OF THE FUNCTIONAL MODEL

Both the DLT and collinearity models can be extended with additional parameters. Functionally, the 3 (or 5 for DLT) basic interior orientation parameters and 6 exterior orientation parameters per frame are well defined. However, due to the imperfections in metric cameras and the poor geometric quality of non-metric cameras, remaining systematic errors have been found. This has resulted in the refined functional model: bundle adjustment with additional parameters (APs).

For nearly 20 years, this approach has been very effective. However, despite its success, some questions remain:

1. Which is the *best* additional parameters model (base function)? Many different APs models have been developed, tested, and pronounced to be the best.

2. What is a rigorous way to form the additional parameter set? How can remaining systematic errors be evaluated to form the best working parameter set and how can one select the *best set*?

   How can the APs be utilized along with a proper weighting scheme in order to achieve a better numerical condition?

3. Should the parameters be block-invariant, group-invariant, or photo-variant? What is the relationship between these parameters in different time realizations if only one image sensing system is used? How do these parameters change with time?

For the first question, the answer is "No single parameter set was found to be superior to the others" (Kilpelae, 1980a). But, is there a general rule behind this conclusion?

For the second question, the statistical testing, e.g., the Student test, gives a good answer. The selection scheme designed to eliminate highly correlated parameters and

insignificant parameters was used by many authors, e.g., Jacobsen (1982a,b). However, Bouloucos & Molenaar (1987) have stated that "the simple tests used to date are not sufficient". More elaborate testing procedures have been proposed, such as in Molenaar (1978a), Bouloucos (1986). Further investigation may be helpful as indicated by the change in the method used in investigations presented in the literature. Concerning the weighting, it is well-known that either the weighted or functional constraint can strengthen the numerical condition, but questions remain on how to form the relationship.

As stated in Ackermann (1984), the refinement can be done through either the functional model or the stochastic model, or both. With respect to the basic functional model, such as collinearity equations with exterior orientation as parameters only, the application of additional parameters is a method used to refine the functional model, while collocation would be one method to refine the stochastic model. Several studies on the application of the collocation technique to photogrammetric block adjustment have been made, e.g. Rampal (1976), El-Hakim (1979). Ebner (1975), Foerstner & Schroth (1982), applied the covariance analysis technique, while Kruck & Lohmann (1986) applied a variance-component-estimation method to improve the weighting scheme. Schroth (1984) applied Box-Jenkin's time series analysis technique to examine the behavior of additional parameters, and found the AR(1), auto-regressive process of order one, would be suitable.

In this chapter, the mathematical models of additional parameters are analyzed in the argument domain. The fidelity to the known physical characteristics of the photographic imaging system, e.g., radial distortion, decentering distortion, etc., the correlation between additional parameters, their significance as well as the optimization scheme are studied. Results are presented in sections 3.1, 3.2, 3.3 correspondingly. The recovery ability of this approach is investigated in section 3.4. Compared with the conventional additional parameter approach, an entirely different solution scheme, the Finite Element Approach will be verified in section 3.5. The unifying theory for analytical photogrammetry, namely the potential theory (Okamoto, 1986), and several concluding remarks are presented in 3.6.

47

The application of collocation, Box-Jenkin's time series analysis technique, variance-covariance-component-estimation technique, are referred to as extensions in the stochastical model, and will be discussed in chapter 4 along with the numerical processing scheme.

3.1 THE FIDELITY OF THE FUNCTIONAL MODEL

In the search for a higher fidelity of the functional model for photo-triangulation, Additional Parameters (APs) play an essential role. This has been extensively studied during the last two decades. In addition to many individual studies, a group study was held by the International Society for Photogrammetry (working group III/3) under the coordination of E. Kilpelae during 1976-1980. In that study, many models of APs were *empirically* investigated.

More recently, H. Ziemann and S.F. El-Hakim from the National Research Council of Canada compared component calibration, system calibration and self-calibration with real data from metric aerial cameras. Various APs models were reviewed as well (Ziemann & El-Hakim, 1986). It was found, that the physical characteristics of the lens system play an important role in the fidelity of APs models, and that "several of the investigated models lack in effectiveness in regard to the correction of non-linear image deformation or rotational-symmetrical lens distortion. The effect of decentering distortion corrections proved to be rather small", i.e., the magnitude of radial distortion plays the dominant role.

At about the same time, a Japanese group (Murai, Matsuka and Okuda, 1984a,b) compared 9 APs models with real data from several non-metric cameras, and also with data from a terrestrial metric camera. They concluded that :

> those physical models which take into account the lens distortion, such as Murai's model, Brown's model and Kilpelae's model, showed best accuracy, while those polynomial models such as Ebner's model, Gruen's

model, Mauelshagen's model, and Schut's model showed lower accuracy. (Murai, et al., 1984a,b).

It becomes very interesting then to investigate the functional nature of those APs models. Within this study, the fit of 8 APs models to the known physical characteristics, such as radial distortion, decentering distortion, and affinity, is investigated for single frames with real data from calibration values as well as with fictitious data.

3.1.1   The Nature of Lens and Film: Known Physical Characteristics

Based on theoretical and empirical investigations, mathematical models were developed for the major distortions in a lens system namely radial- and decentering distortions. However, it is more difficult to find an accurate formulation for film deformation. With dense object space control or dense image space control (reseau), a high order polynomial might be used. However, in most cases, an affinity model is the most practical one (Moniwa, 1977).

Radial Distortion

Ziemann & El-Hakim (1983) have shown that radial distortion can be nearly perfectly represented by odd-power polynomials. A 7 term equation was recommended, based on the experiences with a collimator bank camera calibration system, namely

$$dr = K_0 r + K_1 r^3 + K_2 r^5 + K_3 r^7 + K_4 r^9 + K_5 r^{11} + K_6 r^{13}$$

...(Eq. 3-1)

where r ... radial distance in (mm), dr ... radial distortion in (μm).

The components in the x/y directions are:

$$dr_x = dr(x/r) = x\{K_0 + K_1 r^2 + K_2 r^4 + ...\}$$
$$dr_y = dr(y/r) = y\{K_0 + K_1 r^2 + K_2 r^4 + ...\}$$

...(Eq. 3-2)

Because of the direct dependency between camera constant and the linear coefficient of the radial lens distortion polynomial, singularity problems arise. The equations introduced for

self-calibration (e.g. UNBASC-2, see Moniwa (1977)), where the camera constant is included as one of the unknowns, thus omit the K_0- term:

$$dr_x = x\{K_1r^2 +K_2r^4 +K_3r^6\}$$
$$dr_y = y\{K_1r^2 +K_2r^4 +K_3r^6\}$$

...(Eq. 3-3)

Concerning the parameterization, there are generally two schemes for radial distortion in physical model: the *Gaussian* distortion function, and the *balanced* radial distortion function. The balanced radial distortion function is based on a calibrated principal distance, such that positive and negative distortion values within the format are balanced. Rather than being to achieve perfect balance, a specific radial distance r_o is singled out (usually somewhere in the middle of the format, depending on the lens used), where the distortion is forced to zero, which then uniquely determines this calibrated principal distance associated with the remaining distortion curve.

Physically, the balanced radial distortion is just a cosmetic process (Fryer, 1986), with the effect that numerically the corrections applied to the image coordinates are smaller.

Decentering Distortion

Brown (1966) presented an extension of the Conrady model, which is now commomly known as the Brown-Conrady model. Since then, this model has been used extensively for decentering distortion. Sometimes it is expressed in terms of its radial-tangential components, but more often in the following form:

$$dx = \{P_1(r^2 +2x^2) +2P^2xy\}\{1 +P_3r^2 +P_4r^4+...\}$$
$$dy = \{2P_1xy +P_2(r^2 +2y^2)\}\{1 +P_3r^2 +P_4r^4+...\}$$

...(Eq. 3-4)

Film Deformation

Under film deformation, usually several distortions are covered, not just physical changes in the film, such as shrinkage, but also external influences, such as unflatness during exposure and systematic errors in the image coordinate measuring device. Therefore, it is very difficult to predict accurately this influence for practical applications.

According to Moniwa (1977), the simplest mathematical model is based on the affinity equation.

$$\begin{array}{c} \text{ideal} \\ \begin{vmatrix} x & -x_o \\ y & -y_o \end{vmatrix} \end{array} = \begin{vmatrix} 1 & \sin\beta \\ 0 & \cos\beta \end{vmatrix} \begin{vmatrix} \lambda_x & 0 \\ 0 & \lambda_y \end{vmatrix} \begin{array}{c} \text{measured} \\ \begin{vmatrix} x-x_o \\ y-y_o \end{vmatrix} \end{array}$$

...(Eq. 3-5)

This leads to:

$$dx = (\lambda_x-1)(x-x_o) + (\lambda_y \sin\beta)(y-y_o)$$
$$dy = (\lambda_y \cos\beta -1)(y-y_o)$$

...(Eq. 3-6)

and with $\lambda_x = 1$ to:

$$dx = A(y-y_o)$$
$$dy = B(y-y_o)$$

...(Eq. 3-7)

There are other models which are usually more complicated.

3.1.2   Type of Models: Physical, Algebraic and Hybrid

According to the formulation of APs models, there are generally two ways, namely *reduction* and *generalization* (Voon, 1986). The resulting models can be categorized into physical, algebraic and hybrid.

Physical models are formulated according to physical characteristics, such as the one implemented in UNBASC-2 (Moniwa, 1977). The advantage is, that all parameters can easily be interpreted, while the disadvantages as pointed out by El-Hakim (1979) are:

1. the existence of high correlations between these parameters;

2. irregular distortion characteristics which can be considered as a combination of several unpredictable components, may not be efficiently detected.

On the other hand, a group of *algebraic* models were formed based on geometrical considerations only (usually with orthogonal or near orthogonal components), as reported,for instance, by Ebner (1976), Gruen (1978), Schut (1979). Their advantages are

51

the opposite of the shortcomings of the physical models, namely low correlations, and the capability to compensate for unpredicated (or unspecified) errors. The spherical-harmonics function model, which was fully investigated and developed by El-Hakim (1979), could be taken as a prime example of an attempt to use a general model for all possible distortions. The ability to compensate for known distortions provides a means for evaluating their fidelity.

The group of *hybrid* models is supported by both algebraic and physical aspects. An example was introduced by Ziemann & El-Hakim (1986), which uses a spherical-harmonics function together with an even-order polynomial for radial distortion. This is similar to Brown's model (Brown, 1976); which uses an odd-power polynomial for radial distortion as well as 12 parameters for film deformation. However, since his model was designed based on physical characteristics, it is sometimes classified as a physical model, (Murai et.al, 1984a,b) or called "extended physical model" (Kilpelae, 1980a).

In the author's view, model classification does not have a great significance. However, it is worthwhile to know the basic considerations for the formulation of these models.

3.1.3   Fitting to Known Physical Characteristics

In order to study the behavior of various APs models, eight additional parameter sets, as listed in Table 3.1 are selected for numerical tests. The studies on APs models include several parts:

1. Fitting to known physical characteristics;

2. Correlation between APs;

3. Significance of parameters and selection scheme;

The latter two items are treated in the subsection 3-2. Here, results of fitting to known characteristics are reported.

TABLE 3.1

APs Models included in this study[3.1]

Model #1	Brown's model (Brown, 1976)
	$dx = a_1x + a_2y + a_3xy + a_4y^2 + a_5x^2y + a_6xy^2 + a_7x^2y^2 + (x/c)[a_{13}(x^2 - y^2)$ $+ a_{14}x^2y^2 + a15(x^4 - y^4)] + x[a_{16}(x^2 + y^2) + a_{17}(x^2 + y^2)^2 + a_{18}(x^2 + y^2)^3]$ $+ a_{19} + a_{21}(x/c)$ $dy = a_8xy + a_9x^2 + a_{10}x^2y + a_{11}xy^2 + a_{12}x^2y^2 + (x/c)[a_{13}(x^2 - y^2) + a_{14}x^2y^2$ $+ a_{15}(x^4 - y^4)] + y[a_{16}(x^2 + y^2) + a_{17}(x^2 + y^2)^2 + a_{18}(x^2 + y^2)^3] + a_{20} + a_{21}(y/c)$
Model #2	4th order spherical harmonics model (extended from El-Hakim's model, 1979)
	$dx = q(x/r)$ $dy = a_1y + a_2x + q(y/r)$ $\quad$ q is the spherical harmonics function of the 4th order $q = a_3x + a_4y + a_5r^2 + a_6(x^2 - y^2) + a_7(2xy) + a_8r^2x + a_9r^2y + a_{10}(x^2 - 3y^2x)$ $\quad + a_{11}(3x^2y - y^2) + a_{12}r^4 + a_{13}r^3x + a_{14}r^3y + a_{15}r^3(x^2 - y^2) + a_{16}r^2(2xy)$ $\quad + a_{17}r(x^3 - 3xy^2) + a_{18}r(3x^2y - y^3) + a_{19}(x^4 + y^3 - 6x^2y^2) + a_{20}(4x^3y - 4xy^3)$
Model #2a	3rd order spherical harmonics function model
	Contains the first 11 parameters of Model #2.
Model #3	Gruen's model (Gruen, 1978)
	$dx = a_1y + a_2xy + a_3xy^2 + a_4x^2y + a_5y^2 + a_6x^2y^2$ $dy = b_1y + b_2xy + b_3xy^2 + b_4x^2y + b_5x^2 + b_6x^2y^2$
Model #4	Schut's model (Schut, 1979)
	$dx = a_3xy + a_5y^2 + a_7x^2y + a_9xy^2 + a_{11}x^2y^2 + a_{13}x^3$ $dy = a_1y + a_2x + a_4x^2 + a_6xy + a_8x^2y + a_{10}xy^2 + a_{12}x^2y^2 + a_{14}y^3$
Model #5	Kilpelae's model (Kilpelae, 1980b)
	$dx = a_1x + a_2y + a_3xr^2(1 - r_o/r) + a_4xr^4(1 - r_o/r) + a_5xr^6(1 - r_o/r) + a_6(2xy)$ $\quad + a_7(r^2 + 2x^2)$ $dy = -a_1y + a_2x + a_3yr^2(1 - r_o/r) + a4yr^4(1 - r_o/r) + a_5yr^6(1 - r_o/r) + a_6(r^2 + 2y^2)$ $\quad + a_7(2xy)$ r_o : a specified constant; in this study r_o was set to zero.
Model #6	Mauelshagen's model (Kilpelae, 1980)
	$dx = a_3xy + a_5y^2 + a_7x^3 + a_9x^2y + a_{11}xy^2 + a_{13}y^3$ $dy = a_1y + a_2x + a_4x^2 + a_6xy + a_8x^3 + a_{10}x^2y + a_{12}xy^2 + a_{14}y^3$
Model #7	Murai, Matsuoka, & Okuda's model (Murai, et.al. 1984)
	$dx = x\{ a_1r^2 + a_2r^4 + a_3r^6 \} + a_4x + a_5y + a_6xy + a_7y^2$ $dy = y\{ a_1r^2 + a_2r^4 + a_3r^6 \} + a_8xy + a_9x^2$
Model #8	Ziemann & El-Hakim model (modified El-Hakim 79 model)
	$dx = x[a_6r + a_7r^3 + a_8r^5] + a_9(x/r)(x^2 - y^2) + a_{10}(x/r)(2xy) + a_{11}x^2r + a_{12}rxy$ $\quad + a_{13}(x/r)(x^3 - 3xy^2) + a_{14}(x/r)(3x^2y - y^3)$ $dy = a_1x + a_2y + a_3(x^2/r) + a_4(xy/r) + a_5(y^2/r) + y[a_6r + a_7r^3 + a_8r^5]$ $\quad + a_9(y/r)(x^2 - y^2) + a_{10}(y/r)(2xy) + a_{11}rxy + a_{12}y^2r + a_{13}(y/r)(x^3 - 3xy^2)$ $\quad + a_{14}(y/r)(3x^2y - y^3)$

[3.1] Not all mathematical models relate to the same physical situation.

a) Radial distortion

The following radial distortions were used as reference: 12 sets of odd-power polynomials from Ziemann & El-Hakim (1983) which represent laboratory calibration values for aerial cameras (case a,b ...m), plus 3 sets for non-metric cameras from the output of UNBASC-2 for a calibrated test body (case n, o, p). The fitting of each APs model to these was computed with 81 regularly distributed points (9x9 matrix).

The tests can be classified into two groups. The first group does not include the term K_0 into the generation of radial distortion, because usually the APs models are designed for higher order components while the K_0 term is taken care of by the camera constant. In the second group, the K_0 term is included. The maximum radial distortion is defined such that it is the same as for the given calibration data. The results, present in Table 3.2 provide the standard deviations of the image residuals in (μm) after fitting the APs models (model 1, 2 ... to 8) to the different distortion curves (case a,b ...to p).

Several observations can be made:

1. General quality of fit

The results can be graded according to model type as physical, spherical harmonic and purely polynomial. The Ziemann & El-Hakim model, which jointly uses an even-power polynomial and a spherical harmonics function, gives the best results in some cases, but not always.

In the case of surface fitting to a high order odd polynomial (e.g., 13th order in this test, K_1, K_2, K_3, K_4, K_5, K_6) , it appears that sometimes the even-order polynomial is better than the odd-order one, especially if only 3 coefficients were used.

Generally, the spherical harmonics models provide better results than those using pure polynomials. This agrees with Murai, et al.'s (1984a,b) statements, where his test results show a standard deviation of 9.7 μm for the 3rd order

54

spherical harmonics function, compared to 5.6 µm for Brown's model, and 36.5µm for Gruen's model. However, in the study of this dissertation, the 3rd order spherical harmonic function (model #2a) behaves mostly like conventional polynomial models (model #3, 4, 6). For the cases of c, n, o, p, it provides the worst fit. It should, however, be noted that the cases n, o, p, do not provide an ideal standard for evaluating the fit to known physical phenomena, because in these cases, the 7 term radial distortion function is truncated to 3 terms in the original coefficient determination. The results of this study also indicate that the 4th order spherical harmonics function is significantly better than the 3rd order in most cases.

2. Ziemann & El-Hakim 86 v.s. 4th order spherical harmonics function

It is remarkable that in some cases, (case g and h of group 1; case h, l, m of group 2), the 4th order spherical harmonics function is slightly better than Ziemann & El-Hakim 86. A possible reason is that in those cases, the fitting of a 3 parameter even-order polynomial to a 7 parameter odd-order polynomial is not sufficient, while the 4th order spherical harmonics function model is slightly better than the 3rd order one. However, the correlations in the 9x9 symmetrically distributed image pattern case are much worse for the 4th order spherical harmonics function model than the 3rd order one. This means that the 4th order model should be utilized along with a rejection scheme for highly correlated parameters.

3. Group 1 v.s. Group 2

The placement of the models in both groups is generally similar. However, group 2 can be viewed as having fixed basic interior orientation parameters, then the linear component of radial distortion is compensated by the APs.

TABLE 3.2
Standard deviations in μm of image residuals when fitting of APs models to various radial distortion curves

group 1

Model	a	c	d	e	f	g	h	i	j	k	l	m	n	o	p
0	36.80	96.80	11.40	15.50	35.80	13.50	1.89	8.90	18.20	5.14	14.70	5.14	0.24	6.07	0.94
1	0.46	4.38	1.09	0.51	2.56	0.40	0.66	0.20	4.00	0.65	0.15	0.19	0.00	0.00	0.00
2	1.81	33.50	2.20	1.63	5.43	0.92	0.78	1.18	5.33	1.48	1.53	0.86	0.09	1.23	0.25
2a	7.21	64.34	3.21	1.93	6.34	2.36	1.28	2.31	7.65	1.87	4.83	2.38	0.21	3.99	0.69
3	17.70	53.10	5.55	6.58	15.10	6.37	1.43	4.58	11.30	2.66	7.88	3.11	0.17	3.05	0.53
4	8.89	47.50	3.45	2.06	7.94	3.08	1.14	2.61	7.56	1.92	4.82	2.13	0.16	2.55	0.47
5	0.49	5.08	1.20	0.59	2.96	0.42	0.76	0.23	4.64	0.73	0.17	0.22	0.00	0.00	0.00
6	8.89	47.50	3.45	2.06	7.94	3.08	1.14	2.61	7.56	1.92	4.82	2.13	0.16	2.55	0.47
7	0.49	5.07	1.20	0.58	2.95	0.42	0.76	0.23	4.62	0.73	0.17	0.22	0.00	0.00	0.00
8	0.73	10.70	0.28	0.48	1.59	0.93	0.84	0.18	4.39	0.26	1.11	0.71	0.01	0.12	0.03

group 2

Model	a	c	d	e	f	g	h	i	j	k	l	m
0	6.23	86.60	1.62	4.95	6.53	2.79	1.29	2.14	8.14	1.54	2.92	1.82
1	3.30	5.77	0.58	2.02	2.72	1.61	0.75	0.73	5.20	0.39	1.44	0.61
2	4.95	32.50	1.54	2.91	4.04	1.84	0.83	1.83	6.42	1.22	1.79	0.90
2a	5.47	66.59	1.61	4.69	6.25	2.00	1.20	2.01	7.76	1.33	2.75	1.71
3	5.83	53.60	1.62	4.26	5.36	2.27	1.16	2.08	7.98	1.34	2.59	1.55
4	5.21	49.30	1.58	3.50	5.12	1.89	1.05	1.95	7.26	1.30	`2.38	1.38
5	3.62	6.66	0.59	2.25	2.85	1.76	0.85	0.78	5.99	0.43	1.56	0.68
6	5.21	49.30	1.58	3.50	5.12	1.89	1.05	1.95	7.26	1.30	2.38	1.38
7	3.59	6.63	0.59	2.23	2.84	1.75	0.85	0.78	5.96	0.43	1.55	0.68
8	2.59	11.40	0.79	1.17	3.09	1.53	0.88	0.43	4.85	0.41	1.82	0.91

Note: model 0 is the bundle adjustment without APs, used as reference.
group 1: K_0 term included in noise generation
group 2: K_0 term not included in noise generation

b) Decentering distortion

Two sets of decentering distortion curves were adapted from Brown (1966), which represent the stellar calibration results of 2 SSL phototheodolites. Three sets for Cannon-A1 non-metric camera photos, which came from the output of UNBASC-2, and one fictitious data set were used as well (see Table 2).

It is notable that through 4 test samples, the accuracy improvement ratio for each APs model is almost the same. Since Kilpelae's model (5) implicitly includes the compensation parameters for decentering distortion, it provides the best fit. Among others, the spherical harmonics function- and related models showed consistently better results. Since the overall magnitude of decentering distortion is relatively small, the improvement in the sense of overall accuracy is trivial; however, with respect to the maximum distortion along the edge, this might still be significant.

TABLE 3.3
Fitting to Decentering Distortion Curves (residual in $nm^{3.2}$)

	SSL001	SL002	A1-16	A1-17	A1-18	Fic.
0	33	11	20	84	14	3610
1	16	5	10	42	7	1800
2	10	3	6	27	4	1140
3	16	5	10	42	7	1800
4	16	5	10	42	7	1800
5	0	0	0	0	0	0
6	21	7	12	53	9	2260
7	21	7	12	53	9	2260
8	9	1	5	23	4	1010

c) Film deformation

Three sets of non-metric camera data, which were obtained from UNBASC-2, together with one fictious data set were used (see Table 3.4).

Based on the results, Gruen's model appeared to be superior to the others. However, grading with respect to overall accuracy among other models was difficult. In

---

3.2 The unit of (nm) would be something too small to be considered, however, for a numerical simulatiion, the goodness of fitting still can be compared, and this also reflects the size of decentering distortion.

most cases, models 5 and 7 were found to be worse than the others. The reason is quite apparent from their formulation. On the other hand, the spherical harmonics function related models generally gave reasonable results. It is suspected that in the sense of *local fit,* the spherical harmonics function is even more meaningful and effective.

TABLE 3.4
Affine Distortion, (residuals in nm)

	A1-16	A1-17	A1-20	Fic.
0	18	88	9.7	1890
1	2	13	0.5	289
2	8	6	6.6	189
3	0	0	0.0	0
4	8	5	6.	172
5	8	9	6.5	243
6	4	3	3.2	91
7	2	15	0.5	314
8	9	6	6.8	193

3.2 NUMERICAL CONSIDERATIONS

The feasibility of additional parameter sets is investigated from the numerical aspect, in terms of the correlation between additional parameters and the significance of each individual parameter.

3.2.1 Correlations Between APs

The correlation between the parameters in each model was analyzed. It was found that:

1. The correlation changes with the pattern (distribution) of image points. The difference between symmetric (in x and in y), and non-symmetric patterns is quite significant.

2. With identical patterns, but a different number of points, e.g., 9x9; 7x7; 5x5, the values of the correlation coefficients changed only slightly, while the distribution of high-correlation and low-correlation remained the same.

When the pattern changes from symmetric to non-symmetric, the structure of the correlation matrix changes. As an example, the correlation matrices for Kilpelae's model are listed for 3 cases in Table 3.5.

TABLE 3.5
Correlation matrices for Kilpelae's model

Case 1 : 9x9 symmetric

	a_1	a_2	a_3	a_4	a_5	a_6	a_7
a_1	1.						
a_2	0.	1.					
a_3	0.	0.	1.				
a_4	0.	0.	-0.98	1.			
a_5	0.	0.	0.95	-0.99	1.		
a_6	0.	0.	0.	0.	0.	1.	
a_7	0.	0.	0.	0.	0.	0.	1.

Case 2 : 7x7 with origin on (5,6)

	a_1	a_2	a_3	a_4	a_5	a_6	a_7
a_1	1.						
a_2	-0.26	1.					
a_3	-0.42	0.58	1.				
a_4	0.15	-0.25	-0.83	1.			
a_5	0.	0.16	0.75	-0.98	1.		
a_6	-0.70	0.68	0.68	0.21	0.11	1.	
a_7	-0.15	0.85	0.63	-0.28	-0.20	0.68	1.

Case 1 : 7x7 symmetric

	a_1	a_2	a_3	a_4	a_5	a_6	a_7
a_1	1.						
a_2	0.	1.					
a_3	0.	0.	1.				
a_4	0.	0.	-0.98	1.			
a_5	0.	0.	0.95	-0.99	1.		
a_6	0.	0.	0.	0.	0.	1.	
a_7	0.	0.	0.	0.	0.	0.	1.

3. For symmetric patterns (with respect to both axes), and a non-symmetric pattern, (9x9) pattern with the origin at (3,2) (Figure 3.1), the maximum correlation for these models is given in Table 3.6.

origin: (0,0)   origin: (3,2)
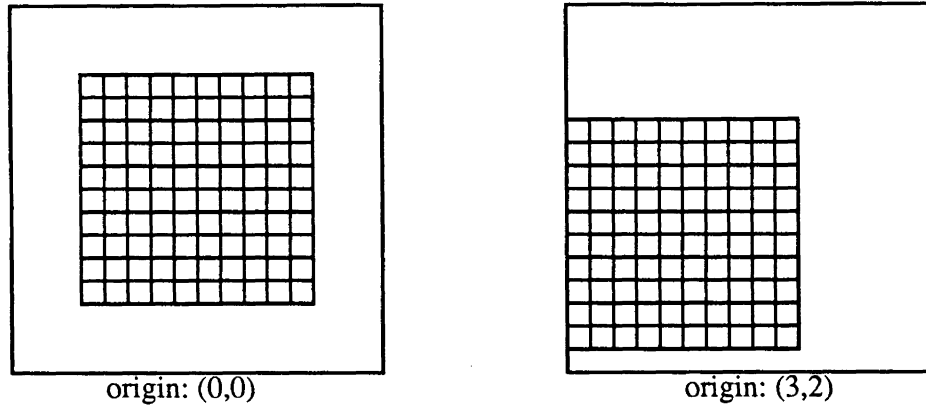
Figure 3.1 Tested Image pattern

TABLE 3.6
Maximum Correlation Magnitudes

Case Model	1	2	2a	3	4	5	6	7	8
symmetric	0.95	0.99	0.92	0.75	0.84	0.98	0.84	0.98	0.98
non-sym.	0.96	0.98	0.79	0.96	0.96	0.97	0.98	0.98	0.90

The same parameters in different models did not necessarily have the same correlation coefficients, as shown for the group of physical models. As in real cases, the correlations are affected by the characteristics of other parts of the coefficient matrix of the normal equation system, which can be mathematically proven.

3.2.2   Significance of the Parameters and Selection Scheme

Many authors have warned against the risk of over-parameterization, e.g. Kilpelae (1980a). Because of this, statistical testing is generally implemented for the selection of significant parameters. Most commonly, a 1-D Student's test is applied, testing the ratio of absolute value/standard deviation for each parameter (Kupfer & Mauelshagen, 1982). Since the correlation is not considered in the 1-D Student's test, some authors have applied a generalized Student's test, such as the Hotelling test, along with the 1-D Student's test (Ackermann, 1980a; Jacobsen, 1982a).

TABLE 3.7
The Significant Parameters of APs

	Radial distortion						Decentering distortion			
	camera a		camera k		camera p		SSL001		SSl002	
	i	$x_i/q_{ii}^{1/2}$	i	$x_i/q_{ii}^{1/2}$	i	$x_i/q_{ii}^{1/2}$	i	$x_i/q_{ii}^{1/2}$	i	$x_i/q_{ii}^{1/2}$
1 (Brown)	1	11.20	14	1.27	18	1.19	7	0.11		
	6	6.73	16	8.04			8	0.11		none
	10	6.13	17	9.80						
	13	7.30	18	9.95						
	14	5.40								
	15	5.04								
	16	8.33								
	17	19.60								
	18	22.40								
2 (El-Hakim 1979)	1	5.19	5	4.99	5	2.16				
	5	2.84	12	4.62	12	2.68	none		none	
	6	1.53	19	4.75						
	12	14.00								
	19	20.50								
3 (Gruen)	3	12.60	3	4.06	3	4.91	6	0.11		
	7	8.36	7	3.68	10	3.84	8	0.11		none
	10	2.02								
4 (Schut)	1	10.10	1	4.25	1	2.23	6	0.11		
	8	2.02	9	1.75	8	3.84	11	0.11		none
	9	2.18	13	1.69	9	3.21				
	13	16.20	14	2.70	14	2.14				
	14	17.10								
5 (Kilpelae)	3	22.40	3	11.70	5	1.36	7	0.28	6	0.10
	4	29.40	4	11.70						
	5	32.40	5	11.80						
6 (Mauelsha gen)	1	10.10	1	4.25	1	2.23	1	10.10		
	7	16.20	7	1.69	10	3.84	5	0.19		none
	10	2.02	11	1.75	11	3.21	6	0.11		
	11	2.18	14	2.70	14	2.14				
	14	17.10								
7 (Murai,et al)	1	11.20	1	11.00	3	1.34	7	0.19		
	2	28.00	2	11.40			8	0.11		none
	3	31.40	3	11.60						
	4	3.85								
8 (Ziemann & El-Hakim)	2	1.61	6	11.30	2	1.61	11	0.23		
	6	32.70	7	11.40	7	1.24				none
	7	41.50	8	1.40	8	2.37				
	8	43.10								

The significant APs differ from block to block in practical situations, since the image/object point distribution, geometrical configuration of camera stations, and quality of the camera, are all different. Differences may exist from photo to photo as well, since the condition of each photo might be different. Thus, the significant APs which are of concern here are those significant to certain physical characteristics. It should be noted that

even with a certain specified distortion, different distortion curves may result in different significant APs. The significant APs for radial distortion and decentering distortion are listed in Table 3.7 where an absolute Student's test value of 1 was used as rejection criterion for radial distortion, and of 0.1 for decentering distortion.

3.3 THE OPTIMIZING SCHEME

The tests presented in the previous two sections are first summarized, then an optimizing scheme for bundle block adjustment with APs is discussed.

3.3.1 The Fidelity

This study investigated the fit of different APs models onto known physical characteristics. It was found that grading in terms of overall accuracy in the fitting of radial distortion had the same trend as reported by Murai et. al. (1984), where the fidelity of APs models was investigated by fully controlled non-metric cameras and a metric camera close-range image. This also generally agrees with results reported by Ziemann & El-Hakim (1986), where aerial photographs with dense ground control and 60% overlap in both directions were used.

It has been shown again that the radial distortion is the major distortion in most cases, while decentering distortion is relatively unimportant. Therefore, the effectiveness on compensation of radial distortion will determine the fidelity of a specified APs models.

3.3.2 The Correlation and Numerical Condition

As mentioned before, the correlation between APs will be affected by other parts of the first coefficient matrix of the normal equations, which means that the object point distribution and the geometrical configuration of camera stations also play important roles. The pattern of image points will have a significant effect as well. There is no particular additional parameter set which should be expected to have generally lower correlation. It is suggested that for each real case, the APs models should be tested at their design stage.

3.3.3 The Optimization

Reviewing the bundle block adjustment programs currently available in UNB, the mode and type of "calibration" parameters can be summarized as shown in Table 3.8. This illustrates the different arrangements made from different points of view.

TABLE 3.8
The Mode & Type of Calibration Parameters

	(x_0, y_0, c)	APs model	APs mode
UNBASC2	photo-var.	physical model	photo-variant
GEBAT	block-inv.	spherical harmonics	block-invariant
GEBAT-V	photo-var.	spherical harmonics	photo-variant
NRC-BUNDLE	N/A	polynomial model	block-invariant
PTBV	photo-var.	physical model	photo-variant
ROBUD	either	8 alternatives	either

UNBASC-2 is a self-calibration program designed for both aerial and close-range photography, using metric or non-metric cameras (Moniwa,1977). However, the photo-variant arrangement is designed for non-metric cameras mainly, and deals with the most general case. Except for the ground coordinates of the object points, no other weights are allowed for unknown parameters. The parameters included in each iteration are specified at the input stage. When the parameter is ON, zero weight is issued for this parameter, while when the parameter is OFF, the coefficients from partial derivatives for this parameter are excluded from the design matrix. The underlaying concept requires that the self-calibration should be used with good geometric configuration only; therefore the option for introducing weighted constraints to basic interior orientation parameters (x_0, y_0, c) and APs is not provided. Besides, compared with weighted constraints, this approach saves computational time by trimming down the dimensions of unknown parameters.

GEBAT is designed for aerial photography as its major application. Weighted constraints for all parameters, including projective parameters and APs, can be provided. GEBAT-V is the photo-variant version for non-metric cameras; and in addition, provides a data-snooping scheme (El-Hakim, 1979).

NRC-BUNDLE is designed for aerial photography. The interior orientation parameters are introduced as constants. The concept behind is to account for all deviations from the basic collinearity equation by APs. Since the APs are supposed to take care of all distortions introduced by interior orientation, film distortion, etc., the generalization scheme is utilized; therefore, a polynomial basis is implemented. Besides, the APs are introduced to the adjustment at only the last iteration (Schut, 1978).

PTBV has similar features as UNBASC-2, but it also computes the rigorous covariance matrix for each object point, and is designed to be linked with a sequential monitoring scheme for deformations (Armenakis, 1987). Weighted constraints for all parameters are allowed.

ROBUD is a general purposed self-calibration program. The current version provides 8 APs sets. Options for either photo-variant or block-variant operation are provided. Any parameter can be weighted. Up to 20 different schemes for gross-error detection are provided, including various robust estimators and data snooping. Although the statistical tests for significance, correlation, are not implemented in the current version, the correlation and covariance matrix for each parameter group can be included in the output and studied off-line (Owolabi, 1989)[3.3]. Programs which implement more than one set of APs, can also be found elsewhere, e.g., Kilpelae (1980b).

It can be observed then, that the program can be quite sophisticated and elaborate if this is justified at the programming stage. The software engineering concept may be better implemented if a operational package is designed.

Based on the analyses performed in this study, a picture of the best APs model might be drawn:

[3.3] It should be noted that ROBUD is an experimental package designed for extensive studies on systematic errors and the gross error detection schemes.

1. Basic Components

    The basic components are the known physical characteristics of the operating system, and the general model for image deformation. Models based on physical understanding is preferred than others.

2. Photo-variant

    The photo-variant concept (Moniwa, 1977) should be generalized so that each photo could have its own set of significant APs. Jacobsen (1984) imposes an objection to the photo-variant approach by warning that we may just fit the observation to the control, thereby actually distorting the real nature. This problem is fundamental for almost all trend analysis by regression with a selected base function. Therefore, Jacobsen's (1984) statement should be interpretated as a call for modelling the additional parameters with physical understanding, and a proper selecting scheme. For the non-metric camera and multi-camera cases, the photo-variant approach is justified.

3. High correlation rejection

    Highly correlated parameters, among APs and also between APs and interior and exterior orientation parameters, should be rejected. The Hannover group used 0.85 as a rejection standard (Jacobsen, 1982b); while Gruen (1980) suggested 0.90.

4. Significance test

    The significance test is essential in the selection of a proper group of parameters. Both the 1-D Student test and the Hotteling test should be used. A 99.9% level was used in the Stuttgart approach (Kilpelae, 1980a). In order to avoid a divergency problem, an initial run without APs is necessary for the generation of approximate values and also for systematic error detection and the significance test.

5. Weighting of APs

    The weights are supposed to be determined such that the effect of an additional parameter is of the desired magnitude in a desired position on the image. 5 μm was

used by the Helsinki group, while 3 μm was used by the Aalborg group (Kilpelae, 1980a). This should be determined based on the knowledge of the image acquisition system. This concept is theoretically logical, and practically helpful in handling ill-conditioning. Since the weight for each additional parameter is usually hard to be individually obtained, counting the entire distortion budget on each image point serves a more logical reasoning. However, the current way of introducing it is not rigorous. One can set :

$$K f(x,y) = a$$

...(Eq. 3-8)

where:
K: the value of the investigated additional parameters;
a: the desired value of effect on the specified position;
(x,y): the image coordinates;
f: the function which relates the AP and its effect.

Assuming the value of the AP to be its standard deviation, the weight is calculated (Heikkila & Inkila,1978).

Such a scheme implies the question of whether the effects of different additional parameters should be weighted separately. However, the most theoretically appealing solution, which introduces a linear constraint (an inequality), requires the quadratic programming technique.

6. Weighting of interior orientation parameters

In most cases, the interior orientation elements can be either obtained from the manufacturer or else observed. For the metric camera case, this is particularly true. Therefore, introducing these values either via weighted constraints or additional observations with proper weights, would be justified. However, this issue is even more complicated than it looks. Two concepts may serve as the general rules:

• all available "observations" should be integrated;

• self-calibration should be used only when the geometrical configuration is sufficient.

3.4 THE RECOVERY ABILITY OF CALIBRATION PARAMETERS

Mathematical theories frequently differ significantly from numerical reality when realized by the computing machines. Simultaneous bundle block adjustment with additional parameters, which simultaneously solves the intersection and resection problems, mathematically represents the state-of-the-art in analytical photo-triangulation. However, when realized by a computer executable software, the limited number of significant digits available results in numerical restrictions. With the increasing practical application of this technique, it happens that some important characteristics which require a more cautious treatment, are being overlooked; for instance, over-optimistically applying bundle block adjustment with reduced control in order to reduce the operational cost. Kubik (1987) points to this problem and states:

> A proper ground control arrangement should be such that it includes sufficient control points in one image (or model) to determine the systematic parameters by resection in space (or absolute model orientation).

Concerning the practice, Kubik (1987) continues:

> One needs as a minimum one additional piece of control information for every additional parameter. In order to ensure a well determined solution, this control should be positioned in one model (image). We arrived thus at the recommended minimum control distribution shown in Figure 4 (see Fig. 3.2). Preferably, this cluster of control should be repeated throughout the block in order to suppress error propagation in the additional parameters. In summary, block adjustment with additional parameters does no save any work. It equals in work a proper camera calibration done independently before (or after) the photo mission.

This can also be interpreted as preference for the *on-the-job* type calibration.
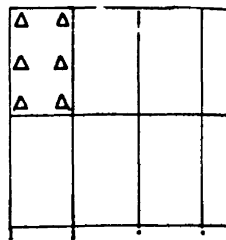
FIG. 4. Recommended
minimum control distri-
bution

Figure 3.2: Recommended control pattern by Kubik (1987)

With the intent on verifying Kubik (1987)'s statement, and clarifying what would

be the most essential factors for a block adjustment with APs and having some appreciation

on how well it would execute, a study with simulated block data was conducted. Since

block adjustments with independent models are generally considered as 2-step bundle

methods with some additional approximations (Ackermann, 1980), this study concentrates

on bundle block adjustments with additional parameters.

3.4.1 Self-Calibration and On-The-Job Calibration

Ever since photogrammetrists started using metric cameras, the procedures utilized

for the determination of basic interior orientation-, lens distortions-, and other image

geometry parameters of the camera are termed **calibration**. There are generally three

categories for calibration:

- test field calibration;
- laboratory calibration;
- bundle block adjustment with APs.

The laboratory calibration includes the use of collimator banks, and goniometer; while the

test field method utilizes either coordinates at test sites or known positions of stars (stellar

calibration). The bundle block adjustment can be realized as a two step approach: form the

photogrammetric system (internal) first, then link it with a specified datum by a similarity

transformation via the use of control points (external). Along with bundle block

adjustment with additional parameters, two basic modes can be identified: self-calibration

and on-the-job calibration (Faig, 1976).

While *on-the-job* calibration uses the *external* geometry, i.e., control points or

features in object space, to support the calibration; *self-calibration* uses the *internal*

structure, i.e., the intersecting geometry of bundles for image points appearing in several

overlapping photographs (Faig, 1976). It should be noted though, that *self-calibration* and

on-the-job calibration referred here are conceptual terms within bundle block adjustments

with APs. They can be applied together in a real block, i.e., both the image geometry and object space control could be strong. Meanwhile, the term *on-the-job* calibration also implies the in-flight calibration, i.e., no separate calibration is performed, and the calibration is done together with the current project: *on-the-job.*

Under the *self-calibration* concept, all the internal characteristics of the camera can be defined by the bundle geometry. Only the datum definition has to come from control quantities, e.g., control points, distances, or other entities in the object space (El-Hakim, 1979). Therefore, the self-calibration bundle block adjustment can also be realized in a free net (Papo & Perelmuter, 1982; Fraser, 1983). However, this does not mean that the same level of accuracy can be reached in all cases, because of the numerical realities, where the numerical condition differs from case to case. Granshaw (1980) has shown some very interesting examples, which indicate that a good image geometry would be indispensable when strong control information is not readily available; while a strong configuration of high quality control always provides good results.

Computationally, the difference between self-calibration and on-the-job calibration is not significant. However, self-calibration has to be realized with a much more powerful algorithm to solve for the often rather ill-conditioned systems. Many schemes have been developed in the past 15 years to handle this ill-condition problem, for instance the segmentation technique developed by Moniwa(1977), the weighted constraint for unknown parameters by Heikkila & Inkila (1978), the ridge regression technique and other techniques as reviewed in Fraser (1980). In practice, both good image geometry and highly accurate object control are required for successful aero-triangulation work. Due to economical as well as other important considerations, the image geometry usually is easier and cheaper to obtain than high quality ground control information. That means, good image geometry is essential for reducing expensive object control requirements.

It is well-known to surveyors that when there is more high quality control information, the overall quality of the work will also be higher. For bundle block

adjustments, strong ground control provides better conditions, at least for numerical aspects. However, the question remains as to the cut-off point for optimum benefits. Meanwhile, the accuracy of image coordinate digitization on precision instruments like modern analytical plotters or stereo-comparators can be estimated as 2-5 μm with well defined image points. On the other hand, the matching quality of required object control is becoming more difficult to obtain. For 1:5000 photography, 3 μm in the image is equivalent to 15 mm. When the image scale is reduced to 1:10, as in some medical applications, the corresponding value becomes 0.03 mm. It has been experienced in many cases, that when the control points are not of good quality, highly constraining them will distort the image. A proper weighting scheme can circumvent this problem, and then the concept of self-calibration can be properly applied.

3.4.2   Numerical Tests

In order to provide a more illustrative example for demonstrating the recovery ability of APs, a numerical study with simulated data is performed. The test data were generated as:

The image:
- Image format: 23x23 cm (standard format);
- Principal distance: 152.3 mm;
- Approximate image scale: 1/5000;
- Image resolution: 1 μm;
- Principal points: $(x_0, y_0) = (0.1, 0.2)$;

The flight:
- The flight : 60% side- and over-laps (double block);
- Flying height: 800 m;
- Arrangement of photos : 3 strips, 3 photos in each strip;

The object:
- Point spacing: 200 m along x and y;
- Degree of relief: 50 m (generated in uniform distributions);

The block:
- Number of photos: 9;
- Number of image points: 292 (only the non-singular ones);
- Number of object points: 88.

The test data:
- data 0: no distortion included
- data 1: radial distortion included
- data 2: affine distortion included

The control pattern:
- pattern A: 8H 12V
- pattern B: 4H 4V
- pattern C: 83H 83V

The tests have been executed on the IBM 3090 mainframe computer at U.N.B. GEBAT and UNBASC-2 were used. For GEBAT, only the data 0 was processed. For UNBASC-2, data 1 and data 2 were also processed. The tests were configured with 3 control patterns, (see Figs. 3.3, 3.4), combined with two calibration cases: with basic interior orientation only, and including all additional parameters.

The control pattern A consists of 8 full control points along the perimeter, and 4 height control points in the centre. This represents the dense perimeter control with vertical control in the centre. The control pattern B consists of 4 corner control points. The pattern C represents the full control, with 83 of 88 points used as control- and 5 as check points. With UNBASC-2, the values of the recovered parameters are stressed. Therefore, pattern A is compared with full control (88H 88V).

+ centre of each photo
- (ground points: every 200m x 200m)
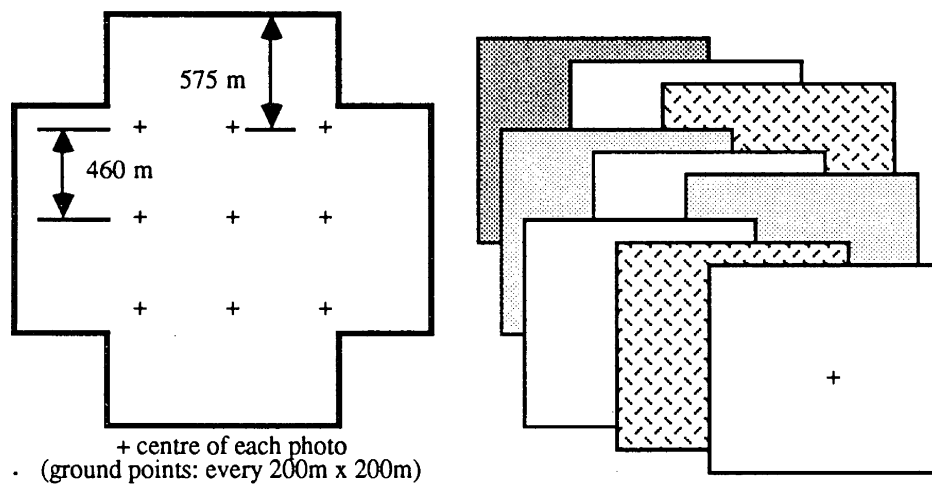
Figure 3.3: The Simulated Block

71

Pattern A

Pattern B

Pattern C

Δ 3-D control points

•   vertical control points
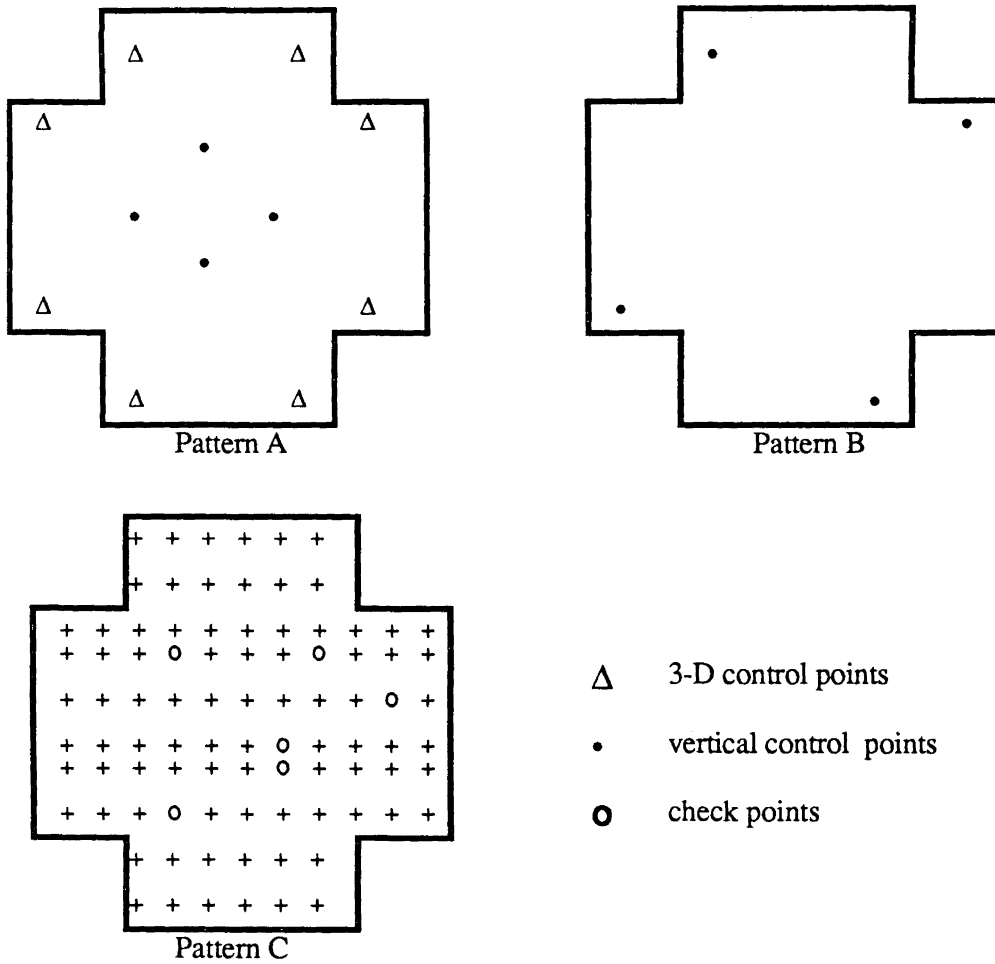
O   check points

Figure 3.4: The Control pattern

TABLE 3.9
GEBAT: RMSE from Image and Check Points
The RMSE of image residuals (unit: mm)

case pattern	(x_0, y_0, c) only x	y	(x_0, y_0, c) and all APs x	y	without $(x_0, y_0, c,$ APs) x	y
A	0.000	0.000	0.000	0.000	0.659	0.346
B	0.000	0.000	0.000	0.000	0.707	0.345
C	0.000	0.000	0.000	0.000	0.642	0.363

The RMSE of check points (unit: cm)

case pattern	(x_0, y_0, c) only X	Y	Z	(x_0, y_0, c) and all APs X	Y	Z	without $(x_0, y_0, c,$ APs) X	Y	Z
A	0.23	0.22	0.38	0.24	0.29	0.46	3.26	2.72	3.06
B	0.28	0.27	0.66	0.27	0.28	0.88	3.12	3.41	4.36
C	0.19	0.08	0.24	0.17	0.07	0.18	1.53	1.49	1.78

72

3.4.3 Test Results

From here, one can see that the larger RMSEs in pattern A, B, compared with the one in pattern C, are caused by the datum definition, not because of the including of APs. When a large number of controls are used, the photogrammetric network is tied tightly to the datum specified by the geodetic control network.

Other observations are stated as follows:

1. Block-invariant (see Table 3.9)

For this group of tests, the RMSE values from the control pattern are of major concern, because the recovery of unknown parameters is much easier than with the photo-variant approach. Therefore, only data 0 are tested.

    a) All the parameters are reasonably recovered in terms of actual values. Considering the number of significant digits, one may say that they are fully recovered. Judging by the resulting influence of these values of the additional parameters, there are essentially no differences.

    b) Patterns A, B and C, provide the same level of accuracy in terms of image coordinates. Patterns A and B provide the same level of accuracy at the check points. As compared with pattern C, patterns A and B provide worse results in terms of the fit to the check points. This however is likely caused by a less efficient datum definition, not from the introduction of basic interior orientation- and additional parameters. Where only the exterior orientation is included in the adjustment, the trend is even more significant, as evident from the figures provided in Table 3.9. It can be further observed that one cannot expect point determination to an accuracy better than 3 mm in planimetry and 5 mm in height, from 1:5000 photography with an ordinary double block. Another observation is that the more the control pattern departs from the full control, the more important becomes the self-calibration technique.

73

2. Photo-variant (see Tables 3.10 and 3.11)

This group of experiments is mainly for investigating the recovery ability of additional parameters. Since all 9 photographs are introduced with the same amount of distortion, a cross comparison between the resulting parameters of each photograph would be even more interesting.

The accuracy of pattern A in image coordinates is very close to the fully controlled block. The resulting values of the parameters are also very similar. The RMSE values at the check points show the same trend experienced in the block-invariant case.

TABLE 3.10
UNBASC-2: RMSE of Image and Check Points

Data	pattern	image point		check point		
		x	y	X	Y	Z
0	A	0.000	0.000	0.003	0.003	0.005
	full control	0.000	0.000	0.000	0.000	0.000
1	A	0.001	0.000	0.006	0.006	0.006
	full control	0.000	0.000	0.000	0.000	0.000
2	A	0.000	0.000	0.003	0.003	0.006
	full control	0.000	0.000	0.000	0.000	0.000

TABLE 3.11
UNBASC-2: Recovered (x_0, y_0, c) & APs Values

	pattern A			full control		
	x_0	y_0	c	x_0	y_0	c
true values	0.1	0.2	152.3	0.1	0.2	152.30
photo1	0.105	0.198	152.263	0.099	0.199	152.279
2	0.081	0.207	152.297	0.094	0.208	152.294
3	0.099	0.201	152.303	0.101	0.198	152.306
4	0.101	0.211	152.309	0.104	0.202	152.301
5	0.090	0.205	152.294	0.098	0.198	152.297
6	0.098	0.207	152.320	0.102	0.196	152.307
7	0.101	0.197	152.305	0.104	0.195	152.295
8	0.089	0.206	152.307	0.1	0.203	152.301
9	0.093	0.201	152.304	0.101	0.203	152.306

Radial distortion from data 1

No.	pattern A			full control		
	$K_1(10^{-6})$	$K_2(10^{-10})$	$K_3(10^{-14})$	$K_1(10^{-6})$	$K_2(10^{-10})$	$K_3(10^{-14})$
	0.100000	-0.2	0.13	0.1	-0.2	0.13
1	0.11661	-0.159092	0.134174	0.116060	-0.157242	0.133404
2	0.169521	-0.219199	0.153742	0.173138	-0.221937	0.15439
3	0.152370	-0.200733	0.147968	0.150201	-0.198722	0.147456
4	0.134630	-0.180254	0.141428	0.128510	-0.173720	0.139434
5	0.160814	-0.212976	0.152770	0.165071	-0.217205	0.153993
6	0.1352	-0.178813	0.140156	0.130959	-0.174884	0.139362
7	0.147146	-0.193288	0.144927	0.147621	-0.193320	0.145259
8	0.161682	-0.216069	0.154220	0.171130	-0.222948	0.155493
9	0.143765	-0.1841	0.141026	0.128990	-0.172794	0.138573

3.4.4 Concluding Remarks

While the block-invariant type additional parameters are suitable for aerial photography, where metric cameras are almost always in use; the photo-variant type additional parameters are suitable for non-metric imageries. Both of them show good results when the image geometry is good and do not depend on the number of control points very much. It is worthwhile to mention that the examples presented are generated without random noise, the only analytical error sources are the round-off errors in the system process and the chopping errors in the image coordinate generation.

Since the image coordinates were generated from ground coordinates with given orientation parameters, the ground coordinates represent the true values. The RMSE of the chopping error in the image coordinates was 0.6 μm from 646 coordinates of the 9 photos. This error is caused by the specified 1 μm resolution and should follow a uniform distribution. When random noises exist, as in real data, the discrepancies shown in these tests will be much more insignificant. However, the error propagation of random noises is also characterized by the geometrical configuration in the same way. It should also be recognized that some parameters are better for a block-invariant arrangement, while others are better in photo-variant cases.

The role of control points is mainly to define the datum, and also to numerically stabilize the system. A well-distributed control pattern for datum definition is justified as good control configuration for bundle block adjustment with additional parameters. A dense control cluster in the first image cannot substitute for well distributed control throughout the whole block.

In conclusion, self-calibration makes use of the *internal* strength of the image geometry. It is however recommended to be applied only when the **image** geometry is strong.

3.5   THE FINITE ELEMENT APPROACH

The Finite Element Approach (FEA), which instead of examining the physical characteristics closely, approximates the situation by breaking the object into many small cells, has gained importance almost everywhere in Engineering (Becker, et al., 1981). The application of FEA for camera calibration has been reported in Munji(1986a,b) for a single image case. Better accuracy than with the conventional additional parameter method was reported.

3.5.1   Basic Concepts of FEA

1. The image coordinates are taken as with no systematic error. Image coordinates remain unchanged except for random noises.

2. Distortions are modelled as a variation of the principal distance for each image point.

3. The variations of the principal distance are assumed to be governed by the shaping function (trial function) in each cell. These cells are formed by the "known" points as the nodal points.

3.5.2 Single Image Case

This approach is characterized by the separate adjustment for space resection and space intersection.

Triangular Method --- using triangular cells.

Stage 1: space resection

The collinearity equation:

$$x_{ij} - x_{0i} = f_{ij}(m_i/q_i)$$
$$y_{ij} - y_{0i} = f_{ij}(n_i/q_i)$$

...(Eq. 3. 9)

Observations : 2xn for n image points;

Unknowns:

> 6 --- for exterior orientation;
> 2 --- for (x_0,y_0);
> n --- for f_{ij}.

Therefore, 8 points provide a unique solution.

Stage 2: Form cells and find values for the shaping function

After stage 1, the variations on each nodal point are known. With an assigned shaping function, the values of the coefficients for the shaping function of each cell (triangle) are calculated. However, before doing that, the triangles have to be formed. They should be non-overlapping, and all nodal points should be used.

This triangulation could be done manually off-line and input to the program, or by using one of the auto-triangulation routines.

The most commonly used shaping function for triangles is:

$$a_1 + a_2x + a_3y = v(x,y)$$

...(Eq. 3.10)

where :
> a_1, a_2, a_3 are coefficients,
> (x,y) are global coordinates of the image point,
> v(x,y) is the variation value on each point.

The coefficients are calculated by:

$$a_1 + a_2 \, x_a + a_3 \, y_a = v_a$$
$$a_1 + a_2 \, x_b + a_3 \, y_b = v_b$$
$$a_1 + a_2 \, x_c + a_3 \, y_c = v_c$$

...(Eq. 3.11)

where the a,b,c are the 3 nodal points of the triangle.

Stage 3 : Intersection

The intersection is performed by defining a point in triangle and locating it to a specific shaping function. Then the value for principal distance of that point is obtained, and the intersection is computed in the usual way.

Rectangular Method

The form of the collinearity equation becomes :

$$x_{ij} - x_{pi} = g(f)(m/q)$$

$$y_{ij} - y_{pi} = g(f)(n/q)$$

...(Eq. 3.12)

where $g(f)$ is the shaping function.

There seem to be two ways to use it. One is to perform a space resection to get the variation value for each control point first, then do the interpolation to find the variation value for each nodal point via the nearest points. In the case of using a bilinear function as the shaping function, the nearest 4 points will provide a unique solution. Another way is to directly solve for the variation value for each nodal point. The second approach needs further clarification, while the first one is stated as follows.

Stage 1: space resection

Same as the one used in triangular method.

$$x_{ij} - x_{0i} = f_{ij}(m_i/q_i)$$
$$y_{ij} - y_{0i} = f_{ij}(n_i/q_i)$$

...(Eq. 3.13)

Stage 2: form cells and find values for shaping function

In this case, the cells are regularly formed with given width (a) and length (b). As used in Munjy (1986a,b), the whole image was divided into 4 rectangles, and a bilinear function was used, expressed in global coordinates as:

78

$$v(x,y)= a1 + a2(x) + a3(y) + a4(x\ y)$$

...(Eq. 3-14)

If expressed in local coordinates:

$$v = (1- x/a,\ x/a) \begin{vmatrix} v(i,j) & v(i+1,j) \\ v(i,j+1) & v(i+1,j+1) \end{vmatrix} \begin{vmatrix} 1-y/b \\ y/b \end{vmatrix}$$

...(Eq. 3-15)

where:
   the (a,b) is the size of the grid in (x,y);
   (x,y) element local coordinate with the origin at point (i,j);
   v(.,.) is the variation value on the nodal point.

Stage 3 : intersection

The point-in-polygon procedure could be much simplified with regular grids. After the point is translated to the local coordinate of the grid, the principal distance for the point can be determined.

$$f = (1- x/a,\ x/a) \begin{vmatrix} f(i,j) & f(i+1,j) \\ f(i,j+1) & f(i+1,j+1) \end{vmatrix} \begin{vmatrix} 1-y/b \\ y/b \end{vmatrix}$$

...(Eq. 3.16)

3.5.3 Multi-Image Case

The extension of FEA to the multi-image case has not been reported yet. The case of applying image distortion corrections prior to the block adjustment would be simple. For on-the-job- and self-calibration case, it may be performed by specifying certain points as the nodal points. These points can either be object control points or points of strong geometric configuration.

3.5.4 Some Remarks on the Use of FEA

1. Munjy (1986a) stated that the accuracy provided by the triangular method is 15% better than the one achieved with a 4 grids rectangular method. However, the accuracy is actually heavily related to the number of cells, i.e., the fineness of the mesh, rather than the form of the cell.

2. While the triangular method requires more work in the auto-triangulation and point in triangle procedures, the rectangular method requires extra work in computing the nodal variation value. However, the rectangular method seems to have a smaller computing load.

3. Munjy (1986a) mentioned that "higher accuracy in the finite element results for camera calibration depends very much on the accuracy of the image coordinate measurements". The question is: will it work with lower accuracy measurements? and what is the influence from the object coordinates?

4. Because FEA monitors all deviation from the basic functional model by the focal length variation on each point, and in each cell this variation is governed by one analytical function, the noise and the systematic errors from both the image space and object space will be included. Bouloucos & Molenaar (1987) have indicated clearly that the systematic deformations of photogrammetric blocks caused by undetected gross errors in the terrestrial control networks impose the doubts on the reliability of bundle blocks with additional parameters. For the current FEA, undetected gross errors and a large noise component are more troublesome.

5. Concerning shaping function, its complexity may be related to the size of the cell and the number of points included in the cell. Conceptually, the conventional APs approach takes the entire image as one cell, and the physical model serves a good **shaping function**. However, in the conventional APs approach, the image coordinates are subjected, while in FEA the focal lengths are subjected.

6. Munjy (1986b) showed that for a single image approach by triangular method, FEA yields better accuracy than bundle method with an odd-polynomial of three coefficients. If this is generally true, and includes the multi-image cases, then the justification of its use seems to depend on increased computation vs. improved accuracy.

The general idea of FEA is to model all systematic errors in small cells. Therefore, other additional parameters are not necessary. The high correlation between the principal distance variation on each node is overcome by introducing weights to principal distances. The proper weighting scheme may require further research, especially in the non-metric camera case, where the nominal focal lengths are generally uncertain within a few milli-meters.

FEA seemingly provides a good model for the pre-block-adjustment camera calibration. Either using instruments, e.g. goniometer, stellar photography, or test field, the camera can be pre-calibrated in terms of specified cell structure and the coefficients of a specified shaping function. These results can then be introduced to a mapping project. However, much more research is required for a publicly recognized specification. Although the advantages and disadvantages of FEA compared to the calibration in terms of "physical parameters", e.g. radial-, decentering- distortions, remain for further study, FEA provides another alternative.

3.6   THE POTENTIAL THEORY AND CONCLUDING REMARKS

As stated in 3.4, while *on-the-job* calibration uses the *external* information, *self-calibration* utilizes *internal* strength. What would be the meaning of the *internal* strength? Meanwhile, as stated in the last chapter, many different algorithms can be applied for camera calibration and model reconstruction. Is there any general concept to provide a unifying theoretical background?

Through a series of theoretical investigations, a unifying concept for analytical photogrammetric block adjustment was developed by Okamoto (1986) and named **Potential theory**. The objective of this development is to provide a unified model for photogrammetric analysis. It explains the why and how of self-calibration.

This theory starts by interpreting the 3-D to 2-D perspective transformation, i.e., the DLT model, with two 4-D transformations, namely, the orthogonal transformation

81

between the measuring space and the image space, and the central perspective transformation from image space to object space. Finally, 6 exterior orientation parameters, 3 basic interior orientation parameters and 2 affinities were interpreted for the general equation. For the 2 photo case, there are then 22 perspective parameters. Seven of them provide the datum definition, and have to be determined with external information, e.g., observed coordinates of control points. These seven pertain to exterior orientation. Another seven of 22 can be solved for by the coplanarity conditions which are provided by the stereo-pairs. These seven contain 5 exterior orientation parameters and 2 interior orientation parameters. The remaining 8 parameters are interior orientation parameters which can be determined either by observed distances or coordinates in the object space, and are named "similarity conditions". In brief, for a set of image points and object points in a stereo-pair, there should be at least 7 datum definition parameters (similarity transformation), 7 coplanarity conditions, and 8 similarity conditions, in order to solve for the 22 perspective parameters.

The relation between measuring space and object space is realized as coplanarity conditions and intersection conditions. The second part includes a 3D general affine transformation:

$$
\begin{vmatrix} x' \\ y' \\ z' \end{vmatrix} = \begin{vmatrix} a_1 & b_1 & c_1 & d_1 \\ a_2 & b_2 & c_2 & d_2 \\ a_3 & b_3 & c_3 & d_3 \end{vmatrix} \begin{vmatrix} x \\ y \\ z \\ 1 \end{vmatrix}
$$

...(Eq. 3.17)

where 12 parameters are realized; plus the central perspective rotation elements which give the other 3.

It is well known that the relative orientation includes 5 exterior orientation parameters, and in the absolute orientation 7 exterior orientation parameters are included. Examining the 22 projective parameters, there are 12 exterior orientation-, and 10 interior orientation- parameters. Therefore, in the coplanarity condition, there are 5 exterior and 2 interior; while in the intersection condition, there are 7 exterior and 8 interior.

82

All parameters pertaining to the coplanarity condition can be determined without external object information. However, as experienced in ordinary stereophotogrammetry, while 6 exterior orientation parameters of one photo are given, the number of the exterior relative orientation parameters remains at 5. This explains that when some parameters are constrained, the information required from either internal or external environment may not be changed. Since the relations of exterior orientation parameters are well-known, only the interior orientation parameters are discussed.

The three rotation parameters of central perspectivity in the intersection condition are functions of 6 parameters, namely

$$(x_{01}, y_{01}, c_1, x_{02}, y_{02}, c_2).$$

In the 3-D general affine transformation, the five independent interior elements relating to this process can be classified into 2 pure affinities and 3 translations[3.4] . The two affinities can be expressed as a function of 8 parameters, namely

$$(x_{01}, y_{01}, a_1, b_1, x_{02}, y_{02}, a_2, b_2).$$

The three translations and the 2 interior orientation parameters in the coplanarity condition can be expressed as function of 10 parameters, namely

$$(x_{01}, y_{01}, c_1, a_1, b_1, x_{02}, y_{02}, c_2, a_2, b_2).$$

From these sets, it can be observed that the principal point coordinates (x_0, y_0) pertain to both central perspective and affinity characteristics and are present in all 4 parameter sets.

This leads to the potential equation:

$$qt = (6n - 7) + (5n - 8)$$

...(Eq. 3.18)

[3.4] One way to physically interpret the 3D affine transformation, is identifying the 12 parameters as 3 translations, 3 rotations, 3 scaling parameters, and 3 non-orthogonalities. The translation and rotation here, plus one scaling parameter are classified as exterior orientation and represent the datum definition through a similarity transformation. The 2 **rotation** parameters mentioned in the text come from the use of the 4-D transformation concept. They are the same as the 3 **translation** parameters, as they are all termed from the 4-D transformation concept.

where n is the number of photos, and qt is called the **potential** of the photogrammetric system. The first part states the exterior orientation and is well-known to photogrammetry. The second part states that all interior orientation parameters can be provided if 8 external pieces of information, either 8 distances or coordinates, are available. These 8 conditions can be provided from the parameter constraints as well, not only from object space information. When 8 of 10 interior parameters are constrained, the interior orientation can be solved completely without object space information.

This explains the *internal* strength, and why the strength of the geometric configuration is the most important factor for self-calibration.

CHAPTER 4

THE STOCHASTIC MODEL AND NUMERICAL PROCESSING

SCHEME

Mathematical models, including the functional and the stochastic, are the tools people use to **model** the real world. Due to the complexity of nature, there are many different ways of interpreting physical phenomena, and none of them can be **perfect**.

In approximation theory, a general concept has been introduced to visualize the relations via the theory of functional analysis (Vanicek, 1983). Three basic spaces can be identified:

- parameter space $\mathcal{X}$;
- model space $\mathcal{F}$;
- observation space $\mathcal{L}$.
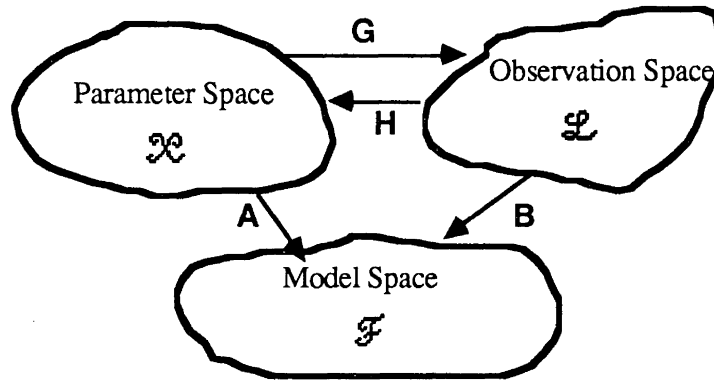
Figure 4.1: Block Diagram of Spaces in Adjustment

This basic model has been generalized through the concept of **collocation**, as introduced in Moritz(1972, 1980).

Mathematically, the observation equation is written in a general form :

$$\ell = H x + P(T)b - v - s + w$$
$$= \ell'' - p - v - s$$

...(Eq. 4.1)

In this equation, the first item represents to "the expected value of observable" (ℓ"), and the second, **systematic components,** in which the general form of the constituents is known but not their magnitude. The last two items represent statistically independent and dependent stochastic quantities[4.1] . Therefore, the method of bundle adjustment with additional parameters is one of the "simultaneous adjustment and regression" approaches. When the signal is counted, the problem is referred to as "2 components simultaneous adjustment and regression". When the prediction of the signal, i.e., predicting the values on points other than those used for computing the coefficients of the covariance function, is applied, it is termed **collocation.** In other words, collocation is the two-component adjustment combined with a prediction of the signal. Mikhail & Ackermann (1976) stated that "collocation means combining estimating the trend simultaneously with interpolation and filtering".

Diagrammatically, it is visualized by introducing **signal space** ($\mathcal{S}$, statistical dependent observation space), which is projected onto observation space via a transformation, plus the "prediction space" ($\mathcal{P}$) (Vanicek & Krakiwsky, 1982).
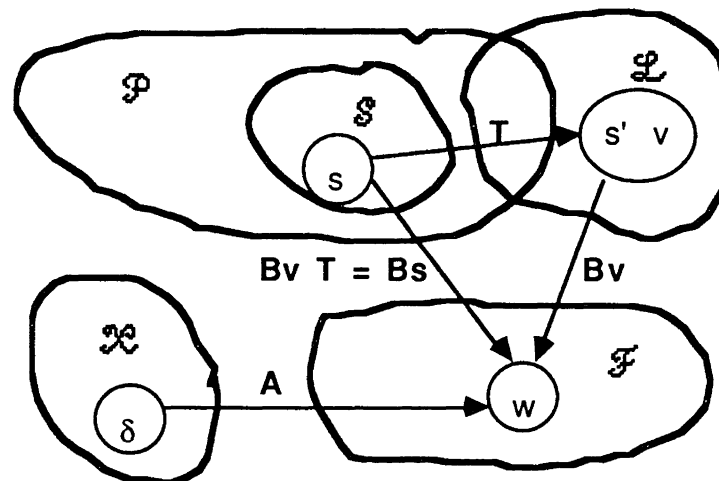
Figure 4.2: Block Diagram of Spaces for Collocation

4.1 The first two parts together are referred to as "trend", and classified as the deterministic part; the last two are "residual", and classified as stochastic.

Referring back to the basic model, there are only the parameter-, model-, and observation- spaces, but no "systematic error space", because the systematic errors are not "modelled". The systematic errors can be defined as caused by the imperfections of the functional model. It has been well experienced that if some "nuisance" parameters, which are designed for modelling "systematic errors", are removed, then high correlation will result between the adjustment residuals. This can be improved by a refinement of the functional model and/or with sophistication in the stochastic model. With respect to the basic functional model, such as the collinearity equations with exterior orientation parameters only, the application of additional parameters represents a method used to refine the functional model, while collocation would be one method to refine the stochastic model. Several studies on the application of the collocation technique to photogrammetric block adjustments have been made, e.g. Kraus (1972), Kraus & Mikhail (1972), Rampal (1976), El-Hakim (1979). Although improvements in terms of accuracy were reported, practical applications in photogrammetry are rare, mainly because of the computational overhead.

The objective of applying collocation is to take account of the correlation between observations. However, there are other approaches. "Kriging" would be one method which is close to collocation but more sophisticated. Dermanis (1984) shows that, when the mean function is unknown, or say, when a zero mean is used, the result of collocation equals to standard kriging. Other methods which have been applied in photogrammetry, include variance analysis, variance-covariance components estimation and the Box-Jenkins' time series analysis technique. The first two produce the covariance matrix for observations, which is the same as obtained with collocation but in a different way. The last one introduces time series concepts.

Ebner (1975) applied the covariance analysis technique; Foerstner & Schroth (1982), Kruck & Lohmann (1986) applied variance-covariance component estimation methods in different ways to improve the weighting scheme. Schroth (1984) applied the Box-Jenkins' time series analysis technique to examine the behaviour of additional

parameters and found the AR(1) process to be quite suitable. It should be noted that Foerstner & Schroth (1982), and Schroth (1984) mainly use the extension in the stochastic model for modelling local variations caused by the block-invariant additional parameters.

In this chapter, the basic stochastic models, namely, the combined model, the parametric model with additional observations, and the weighted constraint model are investigated first. The extension by collocation, variance-covariance-component-estimation and the Box-Jenkins' approach is discussed next. Finally, numerical data processing scheme for gross-error detection, the least squares solution method, and the aspect of software engineering are studied.

4.1 OBSERVATION OR UNKNOWN

The regression, known to surveyors as the least squares method, has been the main optimization scheme since its introduction by Gauss in the 18th century. There are three general stochastic models, namely the parametric model, the condition model, and the combined model. This section examines several concerns that surface in the literature.

For the sake of better numerical processing speed, the control information is introduced to a bundle block adjustment either in the form of weighted constraints, or as additional observation equations. Since in the optimization process, both the weighted quadratic forms of the residuals and the corrections are minimized, weighted constraint and additional observation equation models are essentially equivalent (Wells, 1985).

Another linear model has been devised by Ali & Branderberger (1982); however, the comparison of results obtained from the different stochastic models was not provided in this publication.

This section intends to examine the equivalence and difference between these stochastic models. The best achievable accuracy, rather than the processing speed, is considered most important.

4.1.1 Introduction

In the past, the control information, which mainly is in the form of 3-dimensional coordinates of the control points, is introduced to the bundle block adjustment by either weighted constraints or by additional observation equations. In the first approach, all object coordinates are considered as unknowns, and control points are differentiated from the others by much higher weighting. In the second approach, the control information is taken as observation in an additional observation equation, but as unknown in the collinearity equation. The reason for this lies in the computational efficiency. The above stated schemes could both be designed in the form of the so-called parametric adjustment model.

Ali & Brandenberger (1982) explored this problem by asking why the observation is treated as unknown, because if it is observation, then the collinearity equation will be no longer linear in the observation space. Would this simplification reduce the expected accuracy? Based on this, they devised a scheme to treat the coordinates of the control points as observations, and the coordinates of the pass points as unknowns. They "hoped that such a system would produce better estimates". Two methods based on the same stochastic concept were tested and successful results were reported.

In this study, three models are compared. The models are:

1. The weighted constraint model

$F(X_1, X_2, L) = 0$, with C_{x2}, & C_l.

With:

X_1: unknown object point coordinates, camera orientations, etc.;

X_2: control point coordinates;

L: image observations.

2. The additional observation equation model

$F(X_1, X_2, L) = 0$, and

$F'(X_2, L_2) = 0$.

L_2 : control observations.

3. The Ali-Brandenberger model

$$F(X_1, L, L_2) = 0$$

4.1.2 A Numerical Test with a Simple Example

The investigation is performed using a simple functional model:

$$abc + d = 0$$

where the a and b are observations, c is unknown, and d is constant. The relations between the observations are non-linear.

1. Combined model: taking a, b as observations

$$(a + v_a)(b + v_b)(c + \delta c) + d = 0$$

...(Eq. 4.2)

2. Parametric model with additional observations

$$(a + v_a) + d/((b + \delta b)(c + \delta c)) = 0$$

...(Eq. 4.3)

$$(b + v_b) - (b + \delta b) = 0$$

...(Eq. 4.4)

The following test data were used:

$b_0 = 6$ and $c_0 = 10$ were selected as initial values. The test conditions were established such, that all observations have identical weights, and are independent of each other (diagonal weight matrix). The iteration process was continued until the estimates have exactly the same values as in the previous iteration. The number of iterations required for the final values are listed in Table 4.1 under "ite".

4.1.3 Summary

1.   When all observed (b) are taken as observations along with all observed (a) in pairs, the mathematical meaning of this adjustment states that 5 pairs of observations are used, i.e., there will be 5 adjusted values for (a) and 5 for (b). While in the parametric

90

model used as above, the adjustment states that there are 5 observations for (a), and 5 observations for (b), i.e., there will be 1 adjusted value for (a) and 1 adjusted value for (b). This difference is well justified from the results. This is not caused by the stochastic model; instead, it is caused by the way of forming observation equations. If 5 pairs of parameters for (a) and (b) are used, the second model is exactly the same as the first model in this test.

TABLE 4.1
A Test for Combined and Parametric Models

All observations of b are treated as different parameters						
	combined		parametric		parametric-x	
item	ite	value	ite	value	ite	value
a_1	6	1.972532668	9	2.6	3	3.293846154
a_2	6	2.02771741	9	2.6	3	3.293846154
a_3	6	2.990234488	9	2.6	3	3.293846154
a_4	6	4.989140372	9	2.6	3	3.293846154
a_5	6	0.975542918	9	2.6	3	3.293846154
b_1	6	4.989140372	1	5.04	1	5.04
b_2	6	4.853359902	1	5.04	1	5.04
b_3	6	3.291127305	1	5.04	1	5.04
b_4	6	1.972532668	1	5.04	1	5.04
b_5	6	10.08796455	1	5.04	1	5.04
c	6	-1.016131896	9	-0.7631257631	3	-0.6023739092
qc	8	0.06424620462	10	0.02181484363	4	0.01133088575
σ_0	6	0.03671229498	8	46.962	3	49.35911243

Only one parameter is set for b						
item	ite	value	ite	value	ite	value
a	7	2.6	9	2.6	3	3.293846154
b_1	1	5	1	5	1	5
c	8	-0.7692307692	10	-0.7692307692	2	-0.6071929005
qc	8	0.04117502889	10	0.04117502889	3	0.02335739923
σ_0	6	9.02	8	9.02	3	11.42711243

Note: parametric-x stands for cases iterating in the parameter space only.

2.   In the case where only one (b) is observed, both models convey the same meaning. Identical results have been achieved for all estimates. The only difference is the numerical condition, which is reflected by the different number of iterations required for

convergency. Correlated observations have also been tested. Identical estimates have been achieved from these two models. This proves that they are **equivalent** models.

3.   The parametric-x case is the parametric model iterating in parameter space only. The results show significant differences. The adjusted observation for (a) is not equal to the mean value of the observed (a). Since identical weights were used, this states that this adjustment process is not correct.

In the parametric case,

$$L = F(X).$$

After the linearization

$$L = F(X_0) + (\partial F / \partial X)X, \qquad \qquad \text{...(Eq. 4.5)}$$

and the observation equation becomes:

$$\ell - F(X_0) + v = AX. \qquad \qquad \text{...(Eq. 4.6)}$$

If the first term is taken as L, then it has to be iterated during data processing. In the combined case:

$$F(X,L) = 0.$$

After the linearization

$$(\partial F / \partial X)X + (\partial F / \partial L)L + F(X_0, L_0) = 0. \qquad \qquad \text{...(Eq. 4.7)}$$

The observation equation is then

$$AX + Bv + W = 0. \qquad \qquad \text{...(Eq. 4.8)}$$

During the iteration,

$$A_n X_{n+1} + B_n(L_{n+1} - L_b + L_b - L_n) + f(x_n, L_n) = 0, \qquad \qquad \text{...(Eq. 4.9)}$$

or rearranged:

$$A_n X_{n+1} + B_n(L_{n+1} - L_b) + W_n = 0. \qquad \qquad \text{...(Eq. 4.10)}$$

W_n becomes :

$$W_n = f(X_n, L_n) + B_n(L_b - L_n).$$

...(Eq. 4.11)

The iteration in both observation and parameter spaces is necessary when both of them appear in the observation equation. This iteration is required for numerical processing because of the non-linearity of the functional model. The iteration in the observation space in the second model (parametric model), could be neglected when the residuals of the observations are small (negligible), and this is what we usually do. We learned from this simple exercise that a rigorous numerical processing scheme has a more significant influence than the "rigorous" stochastic model in some cases. In fact, the test shows that these models are equivalent when they are properly interpreted. The first and the second model, which stands for the combined model and the parametric model with additional observation equations respectively, provide exactly the same estimates. The only difference is the numerical condition which is reflected by the number of iterations required for convergence.

One intuitive observation on the additional observation equation model is that it is not possible to include the correlation between X_1, X_2, because the models are separate. However, this is not true, since both the original model and the additional observation model contribute to the same system. The difference between the weighted constraint model and the Ali-Brandenberger model lies in the role of the control coordinates. What one takes as observation, the other takes as weighted parameter. The additional observation model actually is the same model as the other two but written in separate form for each functional model.

This simple example indicates that the non-linearity between observations will likely cause no differences. Under the Gauss-Newton numerical process, these three models are expected to be equivalent. The only difference is the numerical condition.

4.2 THE EXTENSIONS OF THE STOCHASTIC MODEL

In the 1980-84 period between Congresses of the International Society of Photogrammetry and Remote Sensing, the refinement of the stochastic model was identified as one of the three main topics of Working Group III/1. Concerning this topic, Ackermann (1984) reported:

> The general task, however, of establishing a comprehensive stochastic model for photogrammetric determination still remains to be solved. Related with this general task is the delimitation of the stochastic error properties against systematic image errors and gross observation errors. It is felt, however, that the problem formulation is not yet clear enough.

As the objective, Ackermann (1984) stated:

> It is not expected that a refinement of the stochastic model of photogrammetric point determination will result in spectacular accuracy improvements. Nevertheless it is necessary to establish a complete and realistic mathematical model. It will also allow performance prediction for special applications and promote the further development of computational methods.

Reviewing literature, the stochastic behavior of observations in photogrammetry has been investigated in a number of papers. Ackermann & Schilcher (1978) studied the auto- and cross- correlation of image coordinates; image coordinates within photographs and between photographs were found to be considerably correlated. The magnitude of correlation depends on the extent of the systematic error removal. Kraus (1972), Kraus & Mikhail (1972), utilized collocation to interpolate the "signal" on each image point from reseau image data, then remove it prior to further data processing. Rampal (1976) and El-Hakim (1979) utilized the collocation technique in the form of 2-component simultaneous adjustment and regression with the aid of control points. Ebner (1975), Schroth (1982), Foerstner & Schroth (1982) used variance analysis, principal component analysis, and variance component estimation correspondingly; while Schroth (1984) implemented Box-Jenkins' time series analysis technique to model series of photographs.

It is assumed that if there are no systematic errors, the high correlation between observations will no longer exist. That is, with a "perfect" functional model, there will be

no systematic errors. In practice, after an efficient trend removal, the correlation will be significantly reduced. Therefore, it is justified to say, that the refinement in stochastic modelling is another way to improve the imperfectness of mathematical modelling.

In this section, three methods will be discussed:

- Collocation

- Variance-Covariance-Component-Estimation

- Box-Jenkins' time series analysis technique

It should be noted that this research is not intended to exhaustively cover all approximation methods, nor to detail the three selected approaches. The cases of present photogrammetric applications will be the only concern.

4.2.1   Collocation

4.2.1.1   Introduction of Basic Formulation

Following Vanicek & Krakiwsky (1982), the mathematical model for collocation can be written as:

$$f(x, \ell") = f(x, \ell + s + v) = 0.$$

...(Eq. 4.12)

Then the observation equations can be written as:

$$Ax + B_v \, V + B_s \, S + W = 0$$

...(Eq. 4.13)

The variation function on which the normal equation system is based, reads:

$$\Phi = SC_s^{-1}S + VC_v^{-1}V + 2K(A_x + B_sS + B_vV + W)$$

...(Eq. 4.14)

Assuming that signal and noise are independent from each other, i.e., $C_{sv} = C_{vs} = 0$, this leads to:

$$S = -C_s \, B_s \, L \, W$$

$$V = -C_v \, B_v \, L \, W$$

$$X = -(A \, M \, A)^{-1}(A \, M \, W)$$

...(Eq. 4.15)

where $\quad$ $L = (MAN^{-1}AM - M)$

$$M = (B_s \, C_s \, B_s + B_v \, C_v \, B_v)^{-1}$$

For the case of decomposition of a random series, as utilized in Kraus (1972),

$$B_s = B_v = -I, \quad A = 0, \quad W = -\ell,$$

which leads to:

$$S = -C_s(C_s + C_v)^{-1}\ell$$

$$...(Eq. \ 4.16)$$

4.2.1.2 $\quad$ Photogrammetric Applications

Based on the error analysis of reseau points, i.e., the difference between the calibrated reseau coordinates and the measured coordinates, Kraus (1972) and Kraus & Mikhail (1972) computed the coefficients of an analytical function which governs C_S. This analytical function is known as covariance function. Then, this function is utilized to estimate the signals on other image points.

Rampal (1976) and El-Hakim (1979) analyze the residuals on the control points which result from a space resection computation, and then compute the coefficients of a specified covariance function. The resulting function is subsequently used to generate the covariance matrix C_S, which is then introduced into other adjustment procedures, e.g., a photogrammetric adjustment with a combined stochastic model.

Concerning the covariance function used, Rampal (1976) derived one function based on harmonic analysis; the other three mainly used exponential and Gaussian functions, with the Gaussian function reported as experimentally better.

As a summary, the covariance functions are:

Gaussian function:

$$C(d) = C(0) \exp(-k^2 d^2)$$

$$...(Eq. \ 4.17)$$

where, C(0) and k are constants, and d is the distance between points;

Exponential function:

$$C(d) = C(0) \exp(-k\ d)$$

...(Eq. 4.18)

Rampal's (1976) 9 term working function:

$$C(d) = A_o^2 + [(A_1^2 + B_1^2)((a-d)/K)^2]/3 + (8A_2^2 + 10B_2^2)((a-d)/K)^4/45$$

$$+ (49A_3^2 + 48B_3^2)((a-d)/K)^6/70 + (944A_2^4 + 384B_2^4)((a-d)/K)^6/1575$$

where, A_o, A_1, A_2, A_3, B_1, B_2, B_3, K are constants.

...(Eq. 4.19)

All constants as included in the covariance functions, are obtained from the residual analysis. For Gaussian and exponential functions, the following equations are solved:

$$C_{xx}(d) = (1/n_p)\Sigma(x_i\ x_j) \text{ for } i < j;$$

...(Eq. 4.20)

where x_i, x_j are residuals of point i and j; n_p is the number of point pairs.

The covariance matrices corresponding to C_{yy}, C_{xy} are solved in the same way:

$$C_{yy}(d) = (1/n_p)\Sigma(y_i\ y_j) \text{ for } i < j;$$

$$C_{xy}(d) = (1/n_p)\Sigma(y_i\ x_j) \text{ for } i < j.$$

...(Eq. 4.21, 22)

For Rampal's (1976) formulation, the following equations are solved:

$$e_x = \Sigma\ (A_n \cos n\theta + B_n \sin n\theta)(R/K)^n$$

...(Eq. 4.23)

The same is performed for C_{yy}.

4.2.2　Variance-Covariance-Component-Estimation

The subject of variance-covariance component estimation is one of the central research topics for mathematical statistics, geodesy, and many other scientific fields. Concerning its application in surveying, Chen (1983) provides an extensive review.

In this subsection, the definition and solution of the problem are reviewed first, then a particular method: MINQUE is discussed.

4.2.2.1   Definition and Solution of the Problem

While in surveying measurements, no matter whether photogrammetric or geodetic (Chen, 1983):

1. there are frequently many different types of observables involved;

2. the same observables might be obtained with different instrumentation;

3. each type of observable may be contaminated with errors having several components corresponding to different characteristics.

In order to:

1. estimate unknown parameters, e.g., coordinates of points, in a least squares adjustment;

2. further investigate other derived parameters, e.g., displacement, strain or strain rate, relative movement between blocks, etc., in deformation surveying;

3. aid further design by supplying information on the behaviour of the instruments and on the influence of the environment conditions;

we require:

1. the variances of observations, or at least their weight relationships; and

2. their mutual correlations.

Conventionally, this requirement is fulfilled by:

1. accuracy of the instruments as claimed by the manufacturers;

2. analysis of the observations prior to the network adjustment, e.g., estimation of angle accuracy from the Ferrero formula (Chrzanowski, 1983), or distance accuracy from the "double observation method";

3. separate adjustments of the network using individual groups of observations;

4. trial and error method, in which different combinations of the suspected variances of the observations are entered into the adjustment until the a-posteriori variance factor passes the test on its compatibility with the a-priori one.

However, these methods obviously have their limitations :

1. The accuracy of an instrument claimed by the manufacturer is generally an average one and may significantly differ from the actual one.

2. Methods (2) and (3) may not always be possible and may not take full advantage of the available observations.

3. The last method usually requires many combinations of the suspected values of the error components and suffers by not having a very clear theoretical background.

Therefore, a more general method is required. Variance-covariance-component-estimation (VCCE) is one of those solutions.

Essentially, there have been three approaches as reviewed by Searle (1971).

1. **Maximum-likelihood estimation**

Principal concepts: This approach is based on the assumption that the variable is normally distributed, in which case the likelihood function can be written in terms of variance-covariance components and mean values. Then the maximum-likelihood estimates can be obtained by setting the partial derivative of the likelihood function with respect to unknown parameters (the components of the first order and the second order moment) to zero and solving the equations for them simultaneously. (The Bayesian estimation method could be viewed as generalized maximum-likelihood estimation method.)

Disadvantages: The equations involved in this approach are complicated and have to be solved by iterative techniques. Futhermore, very little is known about the properties of the maximum likelihood estimators in this case.

2. **Analysis of variance**

Principal concepts: In this approach, variance-covariance components are obtained by making calculated mean squares of some kind equal to their expectation values and solving linear equations for these components. Different methods along this line can be found in Searle (1971).

<u>Disadvantages</u>: As pointed out by Rao (1971), the theoretical basis of the approach is not clear, the procedures suggested are ad hoc in nature, and much seems to depend on intuition.

3. Methods based on optimization theory

<u>Principal concepts:</u> In this group, all methods are based on optimization theory. The Minimum Norm Quadratic Unbiased Estimation (MINQUE), which was proposed and developed by Rao, is the most general method (Chen, 1983).

<u>Advantages and Disadvantages</u>: This method does not need additional distributional assumptions. The only possible problem is that negative estimates of variances may arise. If this happens, one may infer that a negative estimator corresponds to a small positive true value or that the assumed model is not correct. But, this is a rather arbitrary and symptomatic treatment. Therefore, many authors have made contributions to overcome this drawback by disregarding certain properties of the MINQUE, e.g., the condition for unbiasedness (Chen, 1983). In the real world, the case of a negative definite matrix rarely happens, provided there are a sufficient number of observations, which has been considered as essential for most types of estimation work.

<u>Applications</u>: Sjoberg (1985) studied the case of a singular covariance matrix with MINQUE. Chen (1985) applied MINQUE to model errors in a levelling network. Schaffrin (1981) used BIQUE.

<u>Relation with the Helmert method</u>: MINQUE and the Helmert method are equivalent on variance estimation, but differ on covariance components estimation. Theoretically, the MINQUE method is better and more general than Helmert's method (Chen, 1983).

4.2.2.2 MINQUE: The Method and Examples

MINQUE, which stands for MInimum Norm Quadratic Unbiased Estimation, is an estimation method for variance-covariance components. This method has the following characteristics:

1. Invariance of translation of the unknown parameters x;

2. Unbiasedness;

3. Minimum Norm.

This method can be applied for parametric-, condition-, and combined models. The cases with a singular covariance matrix, either caused by the datum defect or not, can also be handled (Shih, 1985). The computational scheme for the parametric model is presented in Fig. 4.3. The functional model and the covariance matrix structure have to be selected prior to the computation. The covariance matrix can be a diagonal matrix, or a full matrix, or anything in between. It is introduced by selecting a proper component basis, and the corresponding structure matrix T_i. In practice, IMINQUE (iterative MINQUE), is frequently applied.

Two tests are included. The first one composes variance components only. The data are from a real triangulateration network. Two types of EDM (Electronic Distance Meters) instruments and one type theodolite were used (Table 4.2). Four cases were analyzed:

$$\text{Case 1:} \quad = \{ \ a_1{}^2, \ b_1{}^2, \ a_2{}^2, \ b_2{}^2, \ \sigma_\beta{}^2 \ \}$$

$$\text{Case 2:} \quad = \{ \ a^2, \ b^2, \ \sigma_\beta{}^2 \}$$

$$\text{Case 3:} \quad = \{ \ \sigma_{d1}{}^2, \sigma_{d2}{}^2, \sigma_\beta{}^2 \}$$

$$\text{Case 3:} \quad = \{ \sigma_d{}^2, \ \sigma_\beta{}^2 \}$$

where a, b are the components of EDM precision function, $\sigma_d{}^2$, $\sigma_\beta{}^2$ are the standard deviation of distance measurements and angle measurements respecttively. The results are listed in Table 4.3

<div align="center">

TABLE 4.2

Measurement numbers of the tested network

</div>

	Distances by EDM_1	Distances by EDM_2	Angles
# of observations	59	40	101

<div align="center">

TABLE 4.3

Component estimates from MINQUE: Triangulateration

</div>

Case	Components of Distances				σ_β^2
1	7.3×10^{-6}	1.7×10^{-5}	2.3×10^{-5}	1.1×10^{-5}	10.53
	7.1×10^{-6}	6.6×10-6	1.4×10^{-4}	5.6×10^{-6}	1.5×10^{-2}
2	1.5×10^{-5}	1.3×10^{-5}			10.39
	7.1×10^{-6}	6.6×10^{-6}			1.5×10^{-2}
3	4.6×10^{-5}		5.5×10^{-5}		10.40
	9.3×10^{-6}		1.3×10^{-5}		1.5×10^{-2}
4	4.9×10^{-5}				10.40
	7.7×10^{-6}				1.5×10^{-2}

Note: the second line for each case is the standard deviation of the estimates.

$$\ell = Ax + v \qquad\qquad C_\ell = \Sigma\, \theta_i\, T_i$$

$$D = I - A\, A^T\, C_\ell^{-1}\, A\, A^T\, C_\ell^{-1}$$
$$\hat{v} = D\, \ell$$

$$s_{ij} = tr\{\, RT_i\, RT_j\, \} \qquad\qquad q_i = \hat{v}\, C_\ell^{-1}\, T_i\, C_\ell^{-1}\, \hat{v}$$
$$R = C_\ell\, D$$

$$\hat{\theta} = S^{-1}\, Q$$
$$D(\hat{\theta}) = 2\, S^{-1}$$
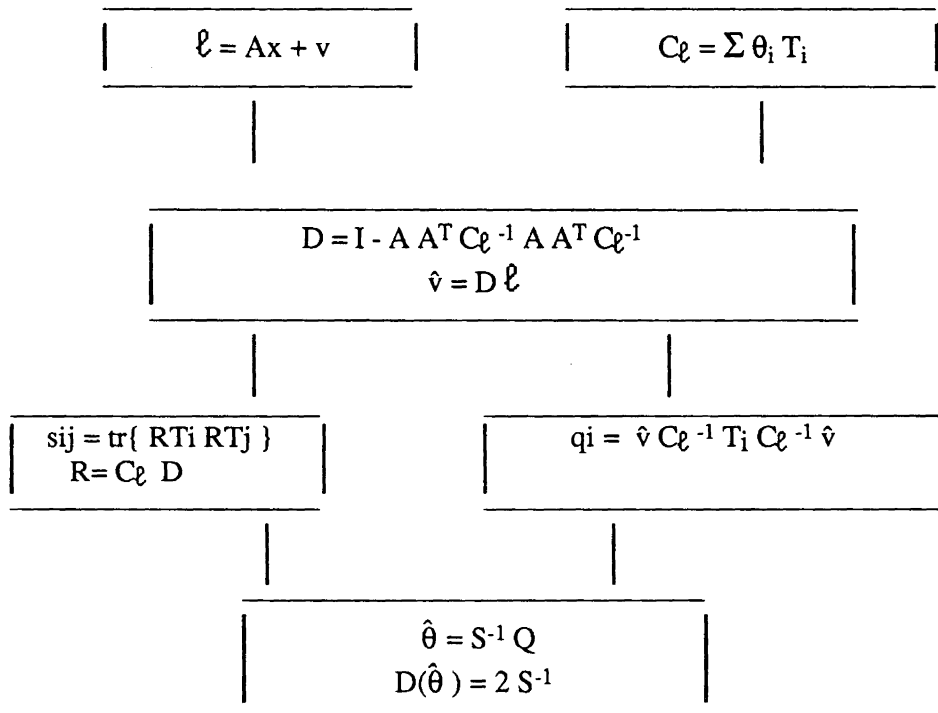
Figure 4.3: Computational scheme of MINQUE for parametric model

The second test is a 3D-2D perspective transformation case with non-metric camera. Three cases were studied. The first case assumes no correlation and assigns x- and y-coordinations with different components. The second assumes the same variance component for x and y. However, correlation is assumed to be a Gaussian function of the image distances. The same component is used for both x and y, and no correlation between x and y is assumed. The third case is the same as the second, however, the exponential function is applied.

Gaussian Function:

$$C(d) = k^{d^2}$$

Exponential Function:

$$C(d) = exp(-k\ d).$$

The results are listed in Table 4.4. A subsection of the resulted correlation matrix is listed in Table 4.5.

TABLE 4.4

Component estimates from MINQUE: Photogrammetry

Case	σ_x^2	σ_y^2	k
1	8.1×10^{-5} 2.1×10^{-5}	1.1×10^{-4} 2.7×10^{-5}	
2	9.8×10^{-5} 1.9×10^{-5}		0.588 0.121
3	1.2×10^{-4} 4.4×10^{-5}		0.425 0.228

Note: the second line for each case is the standard deviation of the estimates.

TABLE 4.5

Part of the resulting correlation matrix from MINQUE: Photogrammetry (Case 2)

1.00E0	3.56E-7	1.82E-15	3.54E-42	1.19E-1 .
3.56E-7	1.00E0	2.44E-2	1.07E-15	4.21E-5 .
1.82E-15	2.44E-2	1.00E0	2.09E-7	8.84E-12 .
3.54E-42	1.07E-15	2.09E-7	1.00E0	1.69E-35
1.19E-1	4.21E-5	8.84E-12	1.69E-35	1.00E0
...	...	...	...	...

4.2.3   Box-Jenkins Time Series Analysis Technique

4.2.3.1   Introduction of Box-Jenkins Time Series Analysis Technique

Box-Jenkins' approach is a method which deals with the time series for forecasting.

Four steps can be identified:

- Identification
- Parameters Estimation
- Diagnostic Checking
- Forecasting

There are several stochastic process models recommended by Box & Jenkins

(1976), namely:

1. Autoregressive
2. Moving average
3. Autoregressive and Moving Average

The model identification is performed by analyzing the autocorrelation and partial-autocorrelation functions of the data (time) series.   A brief identification table is summarized as follows:

TABLE 4.6

Brief Summary of Model Identification

Model	Autocorrelation function	Partial-Autocorrelation function
AR(p)	Tails off	Cut off at lag p
MA(q)	Cut off at lag q	Tales off
ARMA(p,q)	Tails off	Tails off

Frequently encountered models on a stationary basis are giving in Table 4.7(Lin, 1982).

For detailed discussion, the reader is referred to Box & Jenkins (1976).

TABLE 4.7

Frequently Used Stochastic Process Model

Model	Mathematical representation
AR(1)	$z(t) = A\ z(t-1) + a(t)$
AR(2)	$z(t) = A1\ z(t-1) + A2\ z(t-2) + a(t)$
MA(1)	$z(t) = a(t) - B\ a(t-1)$
MA(2)	$z(t) = B1\ a(t-1) - B2\ a(t-2)$
ARMA(1,1)	$z(t) = A\ z(t-1) + a(t) - B\ a(t-1)$

4.2.3.2   Schroth's (1984) Application

Applying the time series analysis concept, the variation of additional parameters between each photograph of a block is interpreted as governed by a stochastic process. In Schroth (1984), a set of block-invariant interior orientation parameters and additional parameters is utilized, and after model identification, parameter estimation, diagnostic checking, AR(1) was found to be appropriate. Compared with the photo-variant mode modelling, this process requires a limited number of parameters, which saves computational time and also improves the numerical condition of the computational system.

Schroth (1984) started from the extension in the stochastic model, but resulted in a functional model, more precisely, a dynamically "tuned" functional model. It is in the realm of the functional model because the coefficients of the process can be solved in the same way as other parameters, if the model of this process is defined, e.g., AR(1). However, in practice, the coefficients of the stochastic process can be obtained from the residual analysis, and are introduced as constants to the adjustment.

This provides the connection with the functional model as formed by Fraser (1979), where the lens distortion effects of multiple photos, taken from the same camera with different focus setting, are constrained. That is, a block-invariant radial distortion parameter set is used for different photos with different focussing, where the radial distortion is a function of this parameter set and the focus setting. This improves the fidelity of the functional model through the constraint in parameter space and could be taken as a typical example on mathematical model extension in functional models. However, it is noticed that the focus is fixed in the Schroth (1984) case; therefore it is not simply a stochastic realization of Fraser's (1979) functional constraint, at least not within the extent of current knowledge.

4.2.4 Concluding Remarks

While a block adjustment with additional parameters clearly constitutes a refinement of the functional model, collocation, variance-covariance-component-estimation, stochastic process, are all classified within the extension of the stochastic model. It is now apparent, that collocation separates observations into two dependent and independent parts, while other methods take observations inclusively. In collocation, one is looking for the coefficients of the covariance function, to use it to model the "signal"; while the other approaches either find the components of variance and covariance and use them to model the observations' weight matrix, or model the correlation through parameter space. It should also be noted that not all systematic errors can be compensated by the refinement in the covariance matrix. In fact, experiments indicate that the random field of the residuals turn out to be non-stationary when the additional parameters are not included.

Both MINQUE and collocation require a-priori knowledge on the formation of the covariance matrix; however, MINQUE utilizes all observations. Since Schroth's (1984) approach models the photo variation rather than the photo-variant parameters by a stochastic process, it can be conceived as a stochastic simplification for the analytically defined photo-variant approach. It represents another way of parameter formulation. This meaning is quite different from the others.

4.3 THE NUMERICAL PROCESSING SCHEME

The numerical processing scheme discussed in this section, is a procedure for data manipulation which was implemented after or during the data acquisition stage. Three aspects were of concern:

- gross error detection;
- least squares solution method;
- software engineering.

4.3.1 Gross Error Detection

Gross-errors, which may be caused by mis-identified image points during the image digitization procedure, or by a careless measurement in the ground control survey, have been of major concern in practical photogrammetry. Along with the development of many different statistical schemes, as well as of operational schemes, a precise quantitative definition for "gross error", "blunder" or "outlier" remains difficult. However, one may qualitatively define "gross errors" as measuring quantities which have "significantly larger errors" as compared with others.[4.2]

In this subsection, statistical methods for gross error detection will be outlined first, and then applied in operational approaches. Detailed discussion and extensive development on the statistical methods, is the subject of another PhD research presently underway in the Department of Surveying Engineering at the University of New Brunswick (see Owolabi, 1989).

4.3.1.1 Some Aspects of the Statistical Methods

For the assumption that "quantities are of $N(\mu,\sigma)$ distribution", three cases can cause its invalidity:

- the mean is not μ, but shifted to $\mu + l''$;

- the variance is not σ, but inflated to $a^2\sigma$;

- the distribution is not $N(.,.)$, i.e., not normal.

[4.2] According to Caspary (1987), the gross error is defined as the result of a malfunctioning either of the instrument or the operator. Gross errors are those errors, at least theoretically, which can be avoided by due care or can be detected by carefully designed observation schemes. An outlier is defined as a residual which, according to some test rule, is in contradiction to the assumption. Despite this fundamental difference between the definitions of outlier and gross error, it is naturally expected that the detected outliers are caused by errors. A more mathematically flavored interpretation will be adopted later.

Since the normality assumption generally holds[4.4] for surveying quantities; the last one is excluded. Therefore, two models can be established for "gross-errors":

- the Mean-shift model;
- the Variance-inflation model.

For the first model, an outlying observation has the distribution of $N(\mu+l,\sigma)$, instead of $N(\mu,\sigma)$, where μ is the expected value, l is the mean shift value. In the second model, the outlier comes from the distribution $N(\mu, a^2\sigma)$ with $a^2 > 1$.

The statistical method based on the first concept includes Baarda's (1968) data snooping, and Pope's (1976) τ-distribution test; while the second includes the Danish method, and the least sum method (Chen, et al., 1987).

For many years, statistical testing has been utilized to provide probability measures for surveying data. Vanicek & Krakiwsky (1982) stated:

The role of statistical testing is to determine whether or not:

1. the postulated probability density function for the sample is likely to have been correctly postulated;

2. the estimated value of a population parameter is to be trusted; and

3. the estimated value of a population parameter is consistent with the known (a-priori) value of the parameter, if it is available.

As observations and the model are concerned, the so called global test utilizing χ^2 distribution can be performed. When a single observation is tested for outlier, several cases can be identified:

- mean known;   variance known: normal test;
- mean known;   variance unknown: Student test;
- mean unknown;   variance known: normal test;
- mean unknown;   variance unknown: τ test.

[4.3] Although exceptions have been reported in many places, e.g. electronic navigation data (Mertikas, et al., 1987), this normality assumption is still generally justified, at least, in photogrammetric blocks.

108

The last test was introduced by Pope (1976). The concept is that when both mean and variance are unknown and estimated from the same sample, the statistic follows a τ–distribution. Along this line of thought, Vanicek & Krakiwsky (1982) Chap. 13 provides excellent guidance.

While Pope's test assumes that the variance factor is unknown; Baarda's data snooping follows a different line of thought. He assumed that the residuals are normally distributed and that the variance factor is known. The standardized residual is tested against a critical value. In the calculation of this critical value, a constant is introduced which connects the type I and type II error measures.

This testing scheme has been applied widely, e.g., by El-Hakim (1979), Chen (1985). Kavouras (1982) provides an extensive treatment and practical realization. Caspary (1987) gives a clear conceptual review and practical examples.

Robust methods are very different from the previous two concepts, as they do not have distribution assumptions. By definition, robust methods are methods which are relatively insensitive to limited variations in the frequency distribution function of the measurements. They include the least sum-, Danish-, and Andrew sine wave method and have one common characteristic, namely, they do not minimize the (weighted) square sum of residuals, but minimize the sum of a specified functional value of the residuals:

Σ f(r) --> min, instead of

Σ r^2 --> min; r: residuals.

Numerically, this is realized most frequently by "the iteratively reweighted least squares method" (Kubik et al. 1988; Faig & Owolabi, 1988). Therefore, in practice, a robust method is a least squares method with a weighting function which generates the weights for observations from the residuals of the previous iteration. As examples, the Danish method utilizes the following weighting function:

1                         $|r| < D$

$\exp(-|r|^2/D^2)$ $|r| \geq D$;

109

while Andrew's sine wave robust estimation uses:

$$(r/A)^{-1}\sin(r/A) \qquad |r| \leq \pi A;$$

$$0 \qquad |r| > \pi A.$$

In which, D and A are the tuning constants which play a similar role as the significance level in classic statistical testing.

Ackermann (1984) stated that "in the final stage, error detection methods which are based on or are more or less equivalent to a statistical test (data snooping or something similar) give generally best results". The reason for this lies on the weighting scheme, which is used in robust estimation and may cause weights for observations deviating from their expected values. If a weighting function results in a weight of either 0 or 1 times their original weight, then the robust estimation will be equivalent to least squares estimation.

The need for requiring an iterative procedure comes from the nonlinear nature of the weighting function. Although there are other methods, i.e., Huber's method, Newton's method, to overcome this problem, the iterative reweighting scheme is the most favoured one (Holland & Welsch, 1977). It is also worth noting that this scheme provides not only the localization of the gross-errors, but also the estimation, i.e., robust regression. Concerning the weighting function, Faig & Owolabi (1988) provide a collection of 11 common functions, all of which belong into the category of M-estimators[4.3]. Concerning photogrammetric applications, Kubik et al. (1988) presented an excellent illustration. Examples with cases of relative- and absolute- orientations are provided. Owolabi (1989) deals with detailed analysis in the application to photogrammetric systems, particularly the bundle block adjustment. Problems concerning how to choose the best weighting function, as well as a suitable tuning constant, and correspondent problems associated with point

---

[4.4] Robust estimators can be classified into 3 classes: M-estimators, which are related to the maximum likelihood estimation method; L-estimators, which are linear combinations of the ordered statistics; and R-estimators, which are based on ranks or scores of the observed data (Faig & Owolabi, 1988).

density, control configuration, multi-outlier presentation, etc. are extensively investigated there.

4.3.1.2 Aspects of the Operational Schemes

Compared to throwing all data into a bundle block adjustment which is directly equipped with a gross-error detection function, the step-by-step gross-error detection scheme is a much more favorable operational scheme. The step-by-step approach means that the outlier detection is handled in a smaller unit or with a simplified mathematical deduction procedure. Since large scale outliers can cause failure in the convergence of a bundle block adjustment, removing them prior to the block adjustment is essential.

Step-by-Step Scheme Concept

El-Hakim & Ziemann (1984) differentiated gross-errors into 4 types:

A. very large blunders in image coordinates, the size of error is larger than the dimensions of a photograph;
B. very large blunders in the control points' coordinates;
C. relatively smaller errors in both image and object;
D. remaining small errors, which are not very distinct from systematic errors in size.

Correspondingly, 4 stages of gross-error detection were designed:

A. conformal transformation between photos with at least three common points;
B. polynomial strip and block adjustment with minimum control and lowest degree of polynomial;
C. bundle block adjustment (without data snooping) with 4 full control points at corners, and 2 height control points inside the block, also another adjustment with all control points;
D. bundle block adjustment with data snooping.

Meanwhile, Chen, L.C.(1985) developed a selection scheme for non-metric close-range photogrammetric systems. A three phase module was recommended. Concerning the error detection, the DLT approach with data snooping stands on the first line. The mis-connection and some other large scale errors can be detected at the space resection stage, while mainly the gross errors in image coordinates can be detected at the intersection stage. Then, a bundle block adjustment with data snooping is performed.

On-Line Detection Scheme Concept

With the advances in data acquisition systems, particularly analytical systems, including the analytical plotter, which allows on-line registration of measured data to a numerical computing device, the necessity of an on-line error-detection scheme has been brought up. Jacobsen (1986) explained this clearly:

> A really on-line blunder detection implies a check immediately after registration of a photo point. Usually this is not necessary. It is sufficient, to have a check after finishing the registrations in a stereo model when the photos are still on the carrier and the remeasurements can be done at once. Also the second type of check is named on-line.

As its realization, the BLUH (Blockausgleichungsprogramm der Universitaet Hannover) on-line data check scheme was reported as a 3 phase check prior to the final block adjustment.

1. Point measuring stage

   If any prevalue of the point location is available, the new measurement will be compared with the prevalue according to a chosen criterion. Blunders are instantly noticed.

2. Model check

   After completing a model, a relative orientation including data snooping is computed.

3. Strip, sub-block check

   The completed model is transformed into the previous model within the strip by a 3-D similarity transformation, and the linkage of strips is done by a 2-D similarity transformation.

Any suspected or detected point can be checked by typing the point index which invokes the computer drive.

Experiences Obtained

Based on practical experiences obtained in this research, it was found that the pre-adjustment check has significant importance, particularly for the averaging of repeated observations. Two major experiments were conducted.

1. Enlarger-Digitizer test

In this test, 13 photographs with 2548 coordinate pairs of measurements were processed. Each point was digitized at least 3 times. Due to reasons such as unfamiliarity with the operation procedure, operator's fatigue caused by long term continuous measuring operation, etc., about 1/10 of these measurements were found to be contaminated by gross error. Most of them were mis-identifications, some suspected to have been caused by sending the registration signal accidentally before precisely locating the target. A sorting routine was called for point number, x coordinates, and also y coordinates. Human interference was utilized to justify the error correction/removal operation. An averaging routine was then called, and pre-specified criteria were implemented for another check. The screened data were then processed with DLTSNP (DLT with data snooping), followed by GEBAT-V, a bundle block adjustment with data snooping.

As far as the entire operation of this particular example is concerned, the pre-screen procedure cleared all gross-errors. Although several gross-errors were missed at the first stage and discovered by GEBAT-V, this was caused by human operation error in the pre-screen. In other words, they should have been detected in the pre-screen process judging on their size. However, DLTSNP did not work as expected.

2. Antenna test

Three photos, with 3045 measurements were processed. The measurements were performed on a Zeiss PSK stereo-comparator in the mono mode. In this test, the data check was conducted on-line, which includes the pre-screen by averaging, and DLT space resection. However, the averaging in this test was done by a 2 parameter transformation, i.e., the origin of each measurement set was set different. After this, DLTSNP and GEBAT-V were executed. Successful results were obtained; however, no error has been detected in the DLTSNP stage.

Remarks

Based on these experiences and the analysis of several operational schemes reported by other authors, several remarks are in order:

1. The pre-screen by averaging has been shown to be very useful. This simple and basic operation has removed almost all blunders in these two experiments. However, these two particular examples may only serve as examples for non-metric close-range cases, and only demonstrate that the averaging process could be important and worth performing. This procedure is recommended to be performed separately with any other procedure.

   Shifting the origin may have some advantages in some cases; while rotating the film may change the direction of approaching target points with the measuring mark, which may improve the precision of the measuring process.

2. The DLTSNP can detect the gross-error in image observations as well as blunders in ground control points. However, the power of detection is limited by the geometry of the investigated photogrammetric system. Although DLTSNP did not show its significance in these two experiments, it has been confirmed as a good scheme in other studies, e.g., Jodoin (1987). It is conceived that in cases of no large scale gross errors, and when the pre-screen procedure by averaging is not performed, the use of DLTSNP would be significant.

3. In cases where not all photographs have a sufficient number of control points, the relative orientation would be an important procedure for data checking. In the formulation stage of relative orientation, either equipped with data snooping as used by Jacobsen (1986), or implemented with robust estimators as reported by Kubik et al. (1988), can serve the second line data check after the averaging. However, it is worth noting that Jacobsen (1984) stated "because of the large differences in the partial redundancy, the method of robust estimators cannot be used for relative orientation".

114

4. Besides the error detection by the model/strip transformation as Jacobsen (1986) stated, Molenaar (1978b) proposed another scheme utilizing two invariant entities: the space angle, and the distance ratio between model points. This scheme is originally designed for the preadjustment error detection in independent model block adjustment. Errors in both model- and ground- coordinates can be detected. Although this scheme is more suitable when the points are evenly distributed, such as in the regular aerial case, it has been found to be helpful as an optional procedure to double check the detected points. This procedure was found to be particularly useful in an interactive editing environment, such as the one provided by using APL.

5. A conformal[4.5] transformation between photographs, as well as a polynomial adjustment, as used in El-Hakim & Ziemann (1984), are found to be of less significance in data screening than model formation by relative orientation. However, these transformations are designed for detecting errors in point numbering (e.g. assigning the same point number to different points) (Jacobsen, 1984), and they may be significant when this kind error occurs which might be missed by other procedures.

    One reason why these procedures were not significant in the two conducted experiments may be, that each photo has been measured at least 3 times and therefore, the chance for leaving mis-identified points to a latter stage is reduced significantly.

6. Bundle block adjustments without data snooping, but using two different control patterns, which are designed for multi-error detection of medium size, can be used as options, although a bundle block adjustment program with robust estimators, such as the one developed by Owolabi (1989): ROBUD, seemingly answers this question. Meanwhile, extra computing effort can be saved. It should be noted though, that the

---

[4.5] For convergent photography, affine or perspective transformation can be used.

reason why El-Hakim & Ziemann (1984) selected the reported scheme is mainly to make use of the currently available software. It would be intuitive to us, that the environment does play an important role, and that there is always another way to get around the problem.

4.3.1.3   Summary

As a summary, the commonly used gross error detection schemes in terms of statistical methods can be classified as:

- τ test,
- data snooping,
- robust methods;

while in terms of operational procedures, the step-by-step approach may be justified as the only available solution. The main theme is that the data should be processed starting from as small as possible units, e.g., from the repeated measurements of each point, to photo, stereo-model, strip, sub-block, and eventually to block.

Although the comprehensive statistical methods are favored by the academic world lately, another "old" method is still widely in use among industry, namely the "three sigma limit" (Erio, 1988, personal communication). For both data-snooping and the τ-test, the inverse of the normal equation coefficient matrix has to be obtained in order to calculate the "local redundancy". Besides time consuming computations, the method is limited by the reliabilities. In the case of a homogeneous reliable network, the local redundancy would be close, and then the "three sigma limit" would not be "inferior" to the τ-test or data-snooping. Concerning the robust test, Jacobsen (1984) stated:

> If the range of the partial redundancy is very large, smaller blunders
> in observations with small partial redundancy cannot be detected.

Especially for error detection by relative orientation the robust estimators can lead to wrong results[4.6].

Therefore, if the local redundancy is homogeneous, the situation will be the same as before. Meanwhile, the robust method is generally utilized to locate multiple blunders of relatively larger scale. With a step-by-step approach, the data will be "cleaned" to a decent stage. Another argument is that the statistical methods only provide a **statistically subjective** evaluation for reference of decision making. The best way is to judge the observation itself in order to decide whether it is wrong or not. This is ideally performed at an early stage of the step-by-step blunder detection scheme.

Apparently, the main concern is still the computation overhead. For the package ALBANY (Adjustment of a Large Block of Anything) which is marketed by ERIO technologies, 4400 photos can be included in one adjustment.

This may serve as a complement to the academic thought.

4.3.2　The Least Squares Solution Method

Traditionally, the normal equation approach is used for almost all surveying and photogrammetric adjustments. However, this is not the only approach; and moreover, it may not be the best approach, because of numerical problems.

Numerically, singular value decomposition (SVD) is the most stable and precise approach. For a usually ill-conditioned photogrammetric adjustment system, the good precision one can achieve from SVD is very appealing. Concerning the large storage of the first design matrix, an iterative approach can be developed; essentially, it is a type of matrix updating (Knight, 1988). Other Q-R decomposition approaches are starting to gain significance in surveying as well, e.g., Givens transformation (Blais, 1983, 1985).

[4.6] This statement is made by referring to the estimator used in Danish method. For those robust estimators which include local redundancy number in their formulation, this statement shall not be valid. However, the same drawback as τ-test and data snooping method will then be even more serious.

Another generalization comes from mathematical programming. It is well-known that the least squares method is one special case of the mathematical programming, where a least squares criterion is used as the object function. However, linear constraints may be introduced in practical photogrammetric applications as well. For instance, the maximum range of radial distortions, the known range of rotation elements, and other parameters, etc., can all be introduced as linear constraints to the least squares system. In this case, a quadratic programming technique is called for.

Even in the normal equation approach itself, a new solution scheme has been developed. The multigrid method, which has been developed during the last decade for the solution of boundary value problems in physics, is a very efficient iterative procedure for the solution of large sparse systems of linear equations. This approach is applied to grids of different mesh-size to remove the weakness of the relaxational procedures. Its photogrammetric application has been demonstrated in Ebner & Fritsch (1986).

No intention has been made in this study to explore the details of the linear system solution schemes. This subsection only intends to briefly state the current status of this subject which may become significant in the very near future. However, one operational comment on the use of the APL language can be made. Since a primitative function $\boxminus$ (domino) has been implemented in APL with the Household transformation algorithm, the formation of a normal equation is no longer necessary, as long as the dimensions of the workspace allow it.

4.3.3   The Software Engineering Aspect

Software engineering is defined to be "the systematic approach to the development, operation, maintenance and retirement of software" (ANSI/IEEE Std 729-1983). In this field, various aspects of software, including its specification, design scheme, testing, management, etc., are of concern. Since modern analytical photogrammetry heavily relies on digital computers, in practice, the majority of photogrammetric operations is realized

through computer executable software, the need for the adoption of "software engineering" into the photogrammetric system is becoming significant.

In this subsection, the presently available programming languages will be reviewed. First, a combined use of APL and C is recommended. Then, the software reliability and management is discussed.

4.3.3.1 Programming Languages

The selection of the programming language would be most important for software development. Reviewing the software configuration, an analytical photogrammetric data processing system can be decomposed into 3 groups:

- data acquisition and on-line data checking;
- data deduction for object information;
- down-stream applications.

The first group includes the data registration, pre-screening for gross-errors, etc. The last group includes, graphic output, GIS (Geographic Information System) data management, driving numerically controlled machinery, etc. The second group includes mainly the computations to obtain object coordinates from image coordinates, e.g., a bundle block adjustment.

Sarjakoski (1986) analyzed several procedural languages: FORTRAN, C, Pascal, Modula-2, Ada, BASIC, as well as symbolic manipulation languages: LISP, PROLOG. The Pascal series, which all are the successors of ALGOL, are favored due to their structured programming, type checking etc. One other advantage of Pascal is the relatively smaller compiler size, which is very significant for micro-computers. However, it is predicted that Pascal will be overtaken by Ada in the near future. FORTRAN is strongly supported by its giant user group and the existing software backup; while BASIC found its way in desk-top computers. C has received its largest popularity among UNIX-users. Its efficiency in execution and the great portability in UNIX environment rendered it a

significant role in today's programming language world. WILD, a major mapping instrument manufacturer, chose a UNIX-based Sun-3 as their workstation. One language, which may not be popular today, but has the most appealing and advanced features, namely APL is not included in Sarjakoski's (1986) evaluation.

Returning to software engineering knowledge, the programming languages can be classified into five categories (Sommerville, 1985):

- Assembly languages;
- Systems implementation languages, such as BCPL and C;
- Static high-level languages, such as COBOL and FORTRAN;
- Block-structured high-level languages, such as ALGOL, Pascal, and also Ada and Modula;
- Dynamic high-level languages, such as APL, PROLOG, and LISP.

The last class of programming languages is distinguished by the requirement that all storage management is carried out dynamically. That means the execution of individual language statements can cause certain storage to be allocated and de-allocated. Dynamic languages tend to be tailored for particular applications and are not usually general-purpose programming languages. Among them, APL is mainly applied in pure and applied sciences and in statistics. It is also predicted that "by the 1990s, a significant number of applications will make use of this type of language" (Sommerville, 1985).

Because of its mathematically oriented nature, APL has been well accepted as algorithm presentation (Crowder, et.al, 1979); and because of its efficient program writing, it is ideal for prototyping (Sommerville, 1985). APL usually is disadvantaged by its run-time overhead and because "its syntax does not permit readable, well-structured programs to be written". However, the run-time problems are not significant when a personal computer is utilized, since the computing cost is essentially nil, as long as real-time response is not required. Moreover, efficient compilers are on their way, e.g. IBM has announced and released its new version APL: APL-2, which contains native support of the vector facility; STSC marketed APL*PLUS 7.0. Both of these newly released compiler

have great improvement as compared with their predecessor, e.g., the dynamically allocated working space.

Concerning the "readability", it has been conceived that any language, including natural languages and programming languages, should be used according to good **style**. A piece of badly written or poorly styled program would be difficult to read regardless of language used. In fact, APL does allow very good style programming, i.e., the proper use of defined functions. If no programming trick is played, the APL language provides concise and clear self-documentation.

This concept is also justified in industry. Mills (1987) proposed: "APL: a better image processing language", in which the APL language, supported by C language, is proposed for the image processing and GIS applications software development by Decision Images, Inc. Logically, it follows that the frequently used part, which has been well-developed, should be written in the most running-efficient language, i.e., the C; while those parts, which are under development or project oriented should be written in the most flexible and written-efficient language, i.e., the APL. Within the APL program, C routines can be called when required. In practice, an interface package between APL*PLUS and C has been developed by Decision Image Inc.[4.7] Excellent efficiency has been achieved as compared with systems developed with other languages, for both execution and program development.

With respect to the re-usability of software components, APL provides excellent options. Since the storage is dynamically arranged, the defined functions are limited to have a maximum of 2 arguments, and each defined function can be easily re-used. It is the author's feeling, that APL is mostly like our natural language; there are words (primitative functions), idioms (phrases of primitive functions, also called idioms in the APL

[4.7] Decision Image Inc. is a Princeton, N.J. based Ameraicn company, marketing image processsing and GIS work-stations.

universe), sentences (defined functions); one has to learn how to properly use them and it will then be as flexible, concise, readable, as our natural language.

Besides, for micro-computer applications, APL*PLUS from STSC, Sharp-APL, and WATAPL from WATCOM provide commercialized implementations[4.8], and also various application software packages, e.g. for accounting, graphics, data base management, etc.

Finally, it may be stated that during this research, a group of APL defined functions has been written, namely APT, which stands for APL version Photo-Triangulation. The speedy programming, concise mathematical presentation, and user interactive feature provide an extremely comfortable environment.

4.3.3.2 Software Reliability and Management

Sommerville (1985) stated that "reliability and maintainability are considered to be the most important attributes of a well engineered software system". It is also addressed that "the principal criterion for system quality is reliability rather than efficiency". Referring back to photogrammetric literature, Kilpelae (1980a) reported on an international joint study on self-calibration. The following paragraph is quoted:

> A comparison of the absolute accuracies achieved with the same data in the different institutes is somewhat difficult, because even the results of the reference adjustments differ (against expectations) from each other in many cases.

Although many reasons such as different rounding errors in different computing facilities, different weighting schemes, different ways of solving normal equations, etc. can be excused, this still implies the question: are these programs reliable?

[4.8] STSC Macintosh version APL, STSC APL*2 (specially designed for Intel 80386 based personal computer), and Digital VAX-750/UNIX APL would be another important implementation.

Besides these international experiences, it has also been noted that some routinely used packages result in unreasonable output in some cases. Part of these reasons are due to the incomplete debugging procedure, part are due to unspecified limitations. This brings up the issue of experiments and reports on software.

It is well-known that a well engineered program must be a structured one, written in good style with sufficient self-documentation. In contrast to many negative examples, PTBV (Armenarkis, 1987) serves as a good example.

Besides the programming style and external documentation, the computational experiments and their report would be another important concern. Sommerville (1985) stated that: "correct mathematically verified software is sometimes less reliable than tested but unverified software".

On the experiments and their report, Crowder, et al. (1979) provide extensive analysis and practically important guidelines.

CHAPTER 5

THE FAMILY OF GENERALIZED PHOTOGRAMMETRY

Within the scope of photogrammetric measuring systems, a variety of methods has been devised for shape or anthropologic measurements. These methods can be categorized as:

1. (conventional) stereo-photogrammetry;

2. light sectioning;

3. Moire topography;

4. raster-stereography;

5. line-sensing.

These close-range applications have certain general characteristics which differ from conventional aerial photogrammetry, namely

1. Object distance

   The sensor (camera) is relatively close to the object (<30m).

2. Coordinate system

   Rather than using an absolute coordinate system, a local coordinate system is normally utilized, because relative positions of the measured points and features satisfy the measuring objective. In this case, the parameter space is homogeneous and isotropic (not affected by the translation and rotation of the coordinate system). In some applications, the scale is also excluded.

3. Dynamic requirement

   Unlike terrain or topography, objects in close-range photogrammetry sometimes change with quite high speed. For instance, anthropological measurements are generally made in a dynamic mode, i.e., shape and position are changing with the posture (gesture) and with time. In fact, the shape of the human body in

different time realizations will not be the same (non-stationary) because it is a living body. Therefore, the two stereo-images (in the broad sense) for photogrammetric measurement should be taken virtually simultaneously.

4. Pattern-less

Similarly to the problems encountered in aerial photography when monotonous objects are photographed, surfaces of close-range objects may be naturally patternless, e.g. the human body. This situation happens relatively more frequently than in topographic mapping due to the large variety of close-range applications.

Among the 5 methods stated at the beginning of this chapter, the last four are classified in some literature as utilizing **structured light** and are preferred in many cases. In this chapter, the basic concepts of the different methods, together with stereoscopic interpretation, an accuracy factors, as well as advantages and disadvantage are briefly reviewed.

5.1 STEREO-PHOTOGRAMMETRY

For this project, stereo-photogrammetry is defined narrowly as a process in which objects are imaged on a pair of common overlapping photographs which form a virtual model of the object.
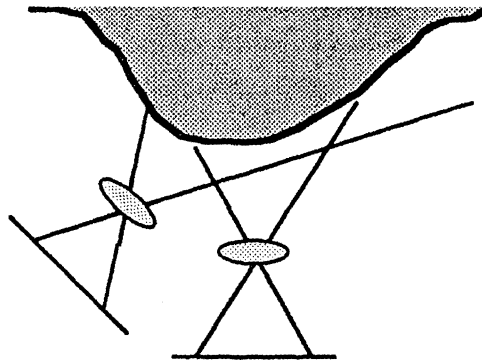
Figure 5.1: Stereo-photogrammetry

This is a singular process to transform a three-dimensional object space to two two-dimensional image spaces. In conventional stereo-photogrammetry, an inverse-perspective transformation of at least two overlapping photographs is used to recreate three-dimensional object information in the stereo-model space.

Accuracy Factors

The accuracy relies heavily on the geometric configuration and on the accuracy of the image coordinates, where the geometric configuration includes the imaging system itself (interior) as well as the arrangement of the imaging system (exterior orientation).

Pre-analysis for the normal case can be performed according to El-Hakim (1979). The accuracy of the convergent case has been extensively studied in Faig (1973), Abdel-Aziz (1974), and Marzan & Karara (1976).

Advantages and Disadvantages

—— This technique has the full benefit of the excellent resolution of a lens-film system. However, a pattern must be generated on the object, either by direct marking, or by optical projection.

—— Practical application of this method follows standardized procedure,but usually an expensive photogrammetric resituation instrument is required, and real-time auto processing is almost impossible.

—— With proper geometrical configration and object space control arrangemant, the edge problem could be solved by a multi-station approach. This problem is caused by the 3-D nature of objects such as the human body, where overlapping photographs can only cover one side.

—— While dynamic studies are possible by using a high speed imaging system, e.g., a movie camera (van Wijk & Ziemann, 1976), restrictions exist, such as, in the

digitization process of the large volume of analogue data (photos), the time resolution of the high speed process, and in synchronization.

——— More than two photographs could easily be implemented, which provides higher reliability as well as accuracy.

——— The geometric fidelity, both in image and station configuration, together with a satisfactory mathematical model development, provide generally the best accuracy potential in today's technology.

5.2   LIGHT-SECTIONING

Light sectioning is a technique based on the projection of light through parallel slits onto an object and the subsequent photography of the object using a single camera whose axis is aligned at 90 degrees to the direction of projection (Atkinson, 1980).

Only one photographic image results, and relief information is displayed in the form of profile lines defined by the light planes.
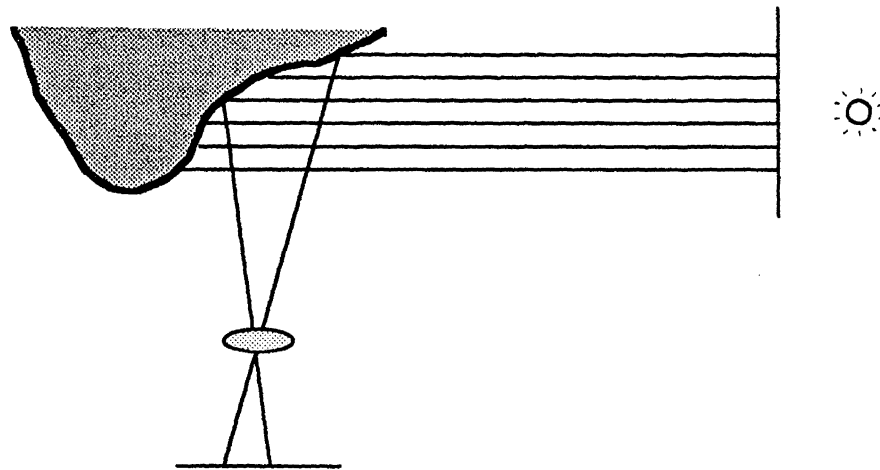
Figure 5.2: Light Sectioning

This system could be viewed as consisting of one perspective projection (camera) and one parallel projection (light planes). Often the image is not formed simultaneously, but one section at a time, in other words, one profile or contour line after the other.

Accuracy Factors

The performance of the system depends on mechanical characteristics, largely the parallelity when generating the light planes.

The perspective characteristics of the camera and thus existing perspective distortions, are usually neglected in the interpretation,because of low system accuracy.

Advantages and Disadvantages

—— It is easy to operate, easy to interpret, and free from the problem of targeting.

—— Concave and convex features cannot be fully covered.

Figure 5.3: Concave and Convex feature

—— The method is sensitive to object movement. Therefore, dynamic study is restricted.

—— The output is only in analogue form.

—— The edge problem cannot be avoided.

5.3 MOIRE TOPOGRAPHY

The system is composed of one light source, one image recording device, and one grating plane. The case of one grating plane is called "the shadow moire method". In some cases, two separate pieces of grating plane are used; referred to as "the projection method" (see Figure 5.4).

128

In this technique, contours are produced on the object as interference fringes whilst it is illuminated by a point source[6.1] of light through a plane grating of equally spaced lines. The fringe pattern is produced by the interference of the grating (from the view side of the image recording device) and its shadow (from the view side of the light source) on the object, and this pattern may be recorded either monoscopically or stereoscopically.

Moire topography could be physically interpreted by either two perspective projections, in the case when radiating light is used (Takasaki, 1975); or one perspective projection and one parallel projection, in the case when parallel light is used (Terada & Ikeda, 1978).

the shadow Moire method   the projection method
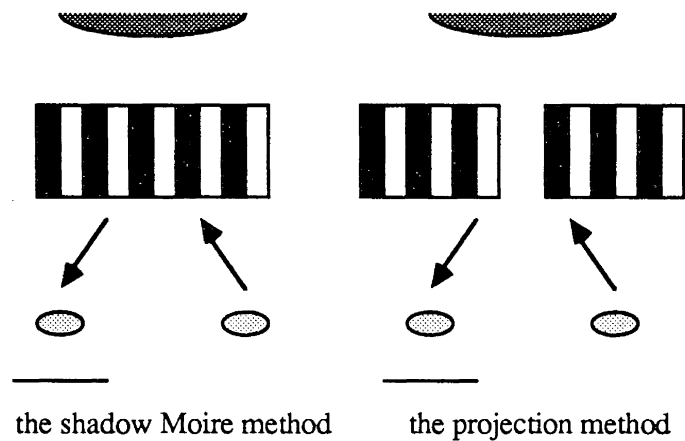
Figure 5.4: Moire Topography

Due to the fact that the grating is opaque to light and that the interference from an equally spaced grating produces a pattern of iso-lines, the 3-Dimensional information can be condensed into one single photograph. In other words, the height information is assessed by "optical computing", and recorded on one photograph (Frobin & Hierholzer, 1982).

6.1   In some cases, a linear light source is used.

Accuracy Factors

The geometrical quality of a Moire photograph depends on the accuracy with which the various components of the instrument, i.e., the camera, the light source, and the screen, are aligned and the distances between them are defined. Other possible error sources are imperfections of the screen, and camera distortions. The accuracy analysis of a conventional Moire topographic instrument has been discussed in van Wijk (1979).

van Wijk (1979) also provides some ideas on iso-line resolution. When using 1700 mm for the distance from the camera and the light source to the screen; 710 mm for the distance between the camera and the light source, and 2 mm for the screen interval (line thickness plus spacing), then a fringe interval of 5.0 mm at the distance of 40 mm from the screen is obtained.

Advantages and Disadvantages

—— The operation and interpretation is simple, instantaneous, and fast.

—— Dynamic study can be easily done by using recording devices such as a high speed photographic device or a video camera.

—— The problem for measuring the edge of a model remains unresolved.

—— High resolution and high accuracy are not easily obtainable.

—— The digital automated process is difficult due to the analogue nature of its output. However, as a pre-screening device for diagnosis, e.g., of spinal deformity, Moire topography is an excellent visual method.

5.4   RASTERSTEREOGRAPHY

This technique is illustrated in the Figure 5.5. It is a stereophotogrammetric method with one of the two cameras replaced by a projector. Depending on the pattern projected, rasterstereography can be further identified as grid or line rasterstereography. The

projected pattern acts as a pseudo-photo. Together with the real photo, a stereo-pair is obtained.
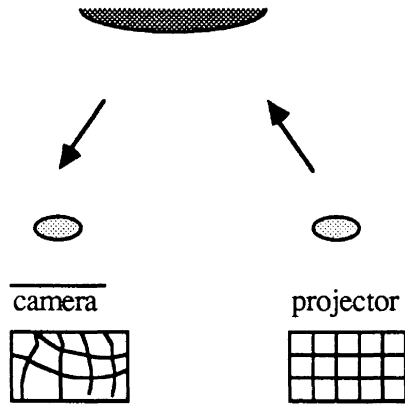
Figure 5.5: Rasterstereography   Figure 5.6: Line sensing
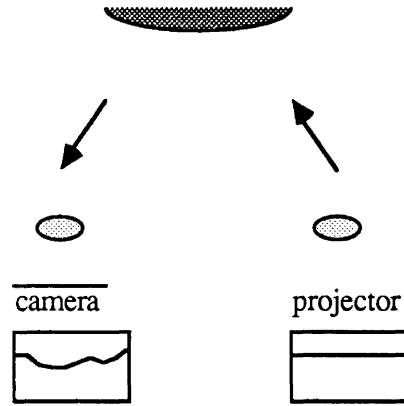
Rasterstereography is similar to conventional stereo-photogrammetry. Two perspective projections are used. The only difference is that one image is reversely projected from "image" space to "object" space. With this condition, only one image has to be digitized. Meanwhile, the image pattern which could be stereoscopically evaluated by this **pair** is limited in the pattern which has been projected and simultaneously photographed.

The perspective projection type projector can also be substituted by an orthogonal projection type. This is particularly suitable for small objects with significant relief, such as the human face. Practically, the shading problem from a high relief object is removed, see Johnson et al.(1983).

Accuracy Factors

The accuracy is also similar to that of conventional stereo-photogrammetry. However, in this case, the mathematical model used has to be more general. The **camera** has totally different characteristics; this implies that each **camera** should have its own

calibration parameters. The precision of the projected "image" coordinates will be generally different from the precision of the sensed (real) image.

The accuracy gained from the multi-station approach is not practical because then the merits gained by reducing the image digitization are virtually lost. Also the distribution of the stations is heavily restricted.

The multi-realization in the time domain has the potential to improve the reliability and stability of the system. Both a sophisticated mathematical model and data handling algorithm are required which to the author's knowledge still need to be developed.

Advantages and Disadvantages

Three major reasons for applying rasterstereography are:

1. synchronization

Due to the fact that only one camera is used for "freezing" the information flow onto an image, synchronization of the imaging system is no longer necessary.

2. reduced digitization work

Because the pattern projected can be digitized beforehand and retained as unchanged during all other measurements, the image coordinate digitization work is reduced to half of the conventional stereophotogrammetric case.

3. signalization

The signalization of a patternless object is waived, because the projected pattern can be used as targets.

Another advantage of rasterstereography lies in the automation considerations. Since one "image" is essentially a fixed pattern, the feature extraction from the digital image is easier than the conventional stereographic case.

Therefore, the great merit of this technique is its simplicity and flexibility, which are well suited for automated evaluation. Only one image has to be digitized. When a linear projected pattern is applied, the digitization is simplified from point digitization to line

digitization. With a "well calibrated" stabilized system, the computational requirement is significantly reduced to a direct space intersection.

In most applications, as in Frobin & Hierholzer (1982, 1983), a solid-state linear camera was used as the sensor. In the data analysis, the point detection (control points) and raster line extraction were automatically executed. In Frobin & Hierholzer (1985), the linear camera was replaced by a metric film-based camera for better geometric quality and stability which would simplify the computational work; the image scanning and feature extraction procedures remained the same. In these examples, the fully automated data reduction is very impressive.

Disadvanges also exist. The image pattern which could be stereoscopically evaluated by a "pair" is limited in the joint set of projected and photographed patterns. Because projection from one point can cover only one side of the object, there are heavy restrictions on the geometrical configuration selection of camera stations. Moreover, the edge problem still remains. Besides, the mathematical model and analytical processing scheme still need further refining and investigation.

5.5   LINE-SENSING

This technique utilizes a *projector* (or a *scanner*) and one *camera*. The pattern is projected once for each line, and the camera senses the image one line per frame. After the projector completes all the line projections, all the sensed frames are "superimposed" into one frame.[6.2]   The resulting image is the same as in linear rasterstereography.

This technique could be viewed as piecewise (line-wise) linear rasterstereography. However this step-by-step image formation will result in characteristics that differ from those of the techniques previously described, because each frame essentially is composed of many frames of single line in a certain time span.

[6.2]   There is no physical superimposition, only in the sense of analytical data handling.

Accuracy Factors

According to today's data processing procedures outlined in El-Hakim (1984), the accuracy is heavily affected by the stability of this system and the completeness of its calibration.

Advantages and Disadvantages

This technique simplifies the feature extraction algorithm. One bright line on a black background is easily detected. This permits the parallel processing of image sensing, feature extraction and parameter determination, resulting in a "real-time" process. Its most significant application potential for this technique is in robot-vision. In anthropological shape measurement field, the ISIS Scanner developed by Oxford Orthopaedic Engineering Centre, University of Oxford, falls into this category. Successful applications have been reported (Turner-Smith & Harris, 1986).

There are many aspects of the technique that have not been well understood. This may be so because of its more recent development. Its metric information quality also relies on the sensor technique and on the analytical evaluation model. The existing instrumentations are also relatively expensive.

CHAPTER 6

CLOSE-RANGE PHOTOGRAMMETRY WITH NON-METRIC PHOTOGRAPHY

The solutions for non-metric camera imagery applied in close-range photogrammetry are studied. Rather than classifying them methodologically as analogue, semi-analytical, and analytical, the operational system is taken into account as well. Along with other criteria, different methods are evaluated from the economical point of view.

It appears that an approach composed of photo-coordinate digitizing, analytical reduction, and analytical plotting becomes favorable in many cases, especially for close-range applications with non-metric cameras.

6.1 BASIC CONSIDERATION

Definition

A non-metric camera is a camera whose interior orientation is completely or partially unknown (Faig, 1976); however, the "unknown" varies with the requirement of individual applications. Therefore, the lack of fiducial marks conventionally serves as the classification standard. In this case, all the "amateur" cameras are considered to be non-metric.

Characteristics

Because of their general flexibility in focusing range, as well as usually smaller dimensions, lower weight and cost, non-metric cameras are indispensable for many users (Faig, 1986). However, while data acquisition is unrestricted, the amount of evaluation effort is increased. Because of the lack of fiducial marks and other metric data, the evaluation method of the non-metric camera imagery is relatively limited and has to be more generalized.

135

Solution

Referring to the methodology for solving the problem of extracting photogrammetric information, the data could be processed and evaluated either analogically, semi-analytically, or analytically (Faig, 1976). The instruments which have been used are the: analogue plotter, analytical plotter, mono- or stereo comparator, and cartographic digitizer. Because of the significant role the instrumental system played, the solutions are reviewed in the classes of instrument:

1. analogue plotter/ analogue mode; semi-analytical mode;

2. hybrid plotter/ semi-analytical mode;

3. analytical plotter/ analogue mode; analytical mode;

4. mono- or stereo comparator/ analytical mode;

5. cartographic digitizer/ analytical mode.

The analytical plotter may be used in a number of different ways, however, here the analytical plotter is used as a **plotter**; all functions are performed on-line. More specifically, the analytical plotter is used as a **stereo-plotter**, i.e., after certain procedures, we can work in the **stereo-model**, where all remaining parallax p_x is a function of height, while p_y is automatically eliminated by analytical means.

Compared with the plotter approaches, the last two cases deal with image data rather than model data.

The material that is utilized in the above systems could be either in forms of photographic originals, contact prints, or enlarged/reduced copies. The latter is of particular significance in close-range applications (Adams,1980; Shih & Faig, 1986).

6.2   THE METHODOLOGY

Kratky (1979) states :

From the operational aspect there are three basic phases in the process of an
on-line analytical operation :
    --- definition of the image geometry;

136

--- reconstruction of the photogrammetric model, and
--- detailed photogrammetric compilation of the model.

Dorrer (1986) approaches the first two parts of the analytical operation from a transformation point of view. The transformations are:

1. from real stage to ideal stage and vice versa;
2. from ideal stage to real image stage and vice versa;
3. from real image to ideal image and vice versa;
4. from ideal image to regional Cartesian coordinates and vice versa;
5. from regional Cartesian coordinates to Geodetic coordinates and vice versa.

The first four could be summarized functionally as: calibration, interior orientation, image deformation, and perspective.

These approaches are not only valid for on-line operations with the analytical plotter, but may also be used for all photogrammetric "solutions". In an analogue plotter, the image geometry is characterized by the design and construction of the hardware, i.e., the plotter, and its relation to the image itself. The calibration (from real stage to ideal stage) and the image deformation compensation (from real image to ideal image) are very difficult to achieve on an analogue plotter. However, these become much more easily achieved by using hybrid plotters, where the analogue plotter part is connected on-line with a computer (Lanckton, 1970). The reconstruction of the photogrammetric model is realized by the procedures of relative- and absolute orientation. Then, the image space is transformed to the model space by the hardware of the plotter. In other words, the perspective relation is retained by the "analogue computer". The detailed compilation is done visually by human stereo-perception in the model space. Continuous line drawings are generated mechanically.

A system where a computer is connected to an analogue plotter (Zeiss C-8) for the semi-analytical evaluation has been evaluated extensively by Drees (1985). The term **hybrid** is used for the system while the method is called **semi-analytical**.

In the case of analytical plotters, the image geometry and perspective relations are defined or formed analytically with greater flexibility. In the compilation stage, the analytical plotter works in much the same way as an analogue plotter.

The comparator and cartographic digitizer approaches are quite different from the plotter approaches. Image geometry definition and model reconstruction are performed analytically; however, they usually work in the batch mode. The detailed compilation is done analytically, i.e., contours are interpolated from spot-heights, and horizontal features are plotted by the connection of characteristic points.

6.2.1 Utilization of an Analogue Plotter

For interior orientation, there are two approaches for the application of non-metric camera imagery whether the analytical calibration is used or not.

The calibration referred to here means the analytical solution for the setting value of interior orientation.

1. Without analytical calibration

    Photo corners, or the intersection of photo-edges, are used instead of fiducial marks, and the nominal focal length is used as the principal distance. Then, all orientations are performed according to standard procedures.

2. With analytical calibration

    The coordinates of the principal points and the principal distances are computed by either space resection or photo-triangulation. Then, the computed principal points are used to centre photographs by various procedures.

The approach which does not utilize analytical calibration could be viewed as analogue method with the analogue plotter; the method which uses analytical calibration could be viewed as a semi-analytical method.

The general difficulty arising from the limited range for principal distance could be overcome by either using an affinely distorted model, or by using an enlarger to fit the photo principal distance into the instrument range. The problem which arises from the limited range of rotation elements could be resolved by either using an approximately parallel pair of photographs or by using a rectifier.

138

6.2.1.1 Without Analytical Calibration

This approach provides an approximate solution for projects where high accuracy is not required. The advantage of this method is that it is easy to perform and does not require any computations.

Welch and Dikkers (1978) used a Zeiss Multiplex plotter, and selected a suitable lens for the non-metric camera such as to approximate the focal length of the Multiplex. In their case, a 21mm focal length lens was used, while the focal length of multiplex projector was 22mm. Thus, the reduction of the original negative became unnecessary and contact prints of the negative were used. Variations from the specified focus setting resulted in minor affine model deformations affecting the vertical scale of the model according to the relationship :

$$\text{vertical scale factor} = \text{planimetric scale factor} \times (c_1/c_2)$$

$$...(Eq.6.1)$$

A correction could be made if necessary. When the degree of relief is acute or obvious, then the magnitude of the correction is large. When the model relief is moderate, the affine deviation will not be significant.

The photo corners were used to locate the principal point. Then, relative and absolute orientation were performed according to standard procedures. A test of the topographic mapping of microscale landforms showed that for object distance ranging from 0.5 m to 3 m and plotting scales 1:1.5 to 1:8.5, planimetric and vertical accuracies of 1 mm to 5 mm could be expected, and contour intervals of 5 mm to 30 mm are feasible (Welch & Dikkers, 1978).

6.2.1.2 With Analytical Calibration

This approach requires analytical computations and higher accuracies are expected. This approach could be viewed as a counterpart to current topographic mapping with aerial camera.

Murai et. al. (1980) designed their approach in the following way:

1. Through space resection with on-the-job calibration, all interior and exterior orientation parameters are calculated.
2. The original negative is enlarged to obtain a diapositive which is applicable to the plotter. This procedure takes the flatness factor as a primary consideration.
3. The rotation angles of photos are reduced by rectification. This could be done together with step 2 on a rectifier.
4. Analytical orientation information is utilized; in this way, the true focal length could be computed for plotter setting.
5. The centering for interior orientation is done by overlaying a transparent film onto the glass plate, upon which control points have been plotted with their calculated coordinates. The fiducial marks are then generated and plotted with reference to the computed principal point.

This approach was applied to a mine excavation investigation. Using the same concepts, Adams (1980) offered another approach, in which the 3-D projective transformation (DLT) was used for calibration. A parallel stereopair was used in place of the rectifier. The steps used by Adams were:

1. Enlarge the negative into a 23x23 cm^2 format photo print;
2. Attach the enlarged photo to a digitizer to digitize the photo coordinates;
3. The digitized coordinates are used for the DLT type analytical calibration in order to obtain the principal point coordinates and the principal distance of each enlarged photograph.
4. The principal point is determined by moving the cursor of the digitizer, on which the photograph remains attached, until the required coordinates are displayed. The current position is then recorded on the photo.
5. Because the equivalent principal distance becomes too large for the plotter's range, half of its value is introduced for setting. The resulting differential Z is corrected by selecting the proper Z gear ratio.
6. Conventional normal empirical relative and absolute orientation is carried out afterwards.

6.2.2 Hybrid System

The model errors in the plotter operation caused by lens distortion, film unflatness, and the influences of imperfect relative orientation, have been well-known to the

photogrammetric world. A study on the effect of the most significant error source - radial lens distortion - has been conducted in Faig (1972).

Because of the limitation of the mechanical / optical/ optical-mechanical devices, it is very difficult to achieve a precise compensation for the above mentioned model errors. The analogue plotter is very accurate and very precise over small image areas, but where the entire stereomodel is accommodated, the accuracy is greatly degraded. Therefore, Lanckton (1970) proposed a Hybrid stereoplotter, which

> is a stereoplotting system employing an integration of analogue and digital computational techniques to solve the stereophotogrammetric problem. In particular, the hybrid stereoplotter uses any one of the conventional, optical-mechanical stereoplotting systems to solve the projective equations and a digital system to correct for the stereoplotter's inaccuracies, to remove any mathematically defined systematic errors and, within limits, to accomplish final relative orientation and complete absolute orientation.

Concerning the realization of such instrumentation, Forrest (1971) states that a hybrid stereoplotter uses an analogue instrument to perform the projection from photograph to stereomodel, and a digital computer is used to adjust the model coordinates of the floating mark during plotting. Therefore, in his stated system, the horizontal position of the pencil head (X, Y), and the tracing-table platen height (Z) are under computer control. The y position of one projector is computer-controlled as well, in order to enhance the stereoscopic vision.

The application of this concept has become progressively more important in recent times, because the wide implementation of analytical plotters frees a large number of existing analogue plotters, especially older types, from the first line of mapping. In order to upgrade the performance of the analogue plotter, as well as to fully utilize existing resources, the concept of the hybrid system has to be implemented, as reported in a recent extensive study by Drees (1985).

6.2.3 Analytical Plotter

Because the model is constructed (formed) mathematically instead of analogically on the analytical plotter, the plotting and contouring of non-metric imagery is relatively simple. Neither the setting of principal distance, nor the locating of the principal point should be problematic. However, for the interior orientation registration procedure, fiducial marks are conventionally used; for non-metric imagery either photo-corners or control points could be used as substitutes. The mathematical model, whether with calibration or not, can easily be selected.

When using the control points, it is recommended that the measured photo coordinates be used as image space registration, and the calibration data can then be directly referred to it. In this way, an initialization stage includes not only the registration, but also the interior and analytical exterior orientations.

Shortis (1982) suggests a sequential algorithm for using control points to define image geometry. A Zeiss Jena Stecometer online with PDP 11/23 were used for his test. This algorithm provides the combined use of either fiducial marks and/or control points to define the image geometry.

While the calibration data are keyed-in or taken from previously stored data files, the image coordinates of control points in the calibrated system need to be located for registration. Otherwise, the principal point coordinates (x_0, y_0) cannot be defined.

However, a great invention has overcome the stage registration, namely, the parallax conditions formed by combining collinearity equations and super-position conditions as applied to the design of the APY (Analytical Photogram-meter by Yzerman) system by Henk Yzerman, the inventor of Kern PG-2 (Yzerman, 1988).

A number of analytical plotters have been designed and produced. The UNB Digital Mapper, an analytical plotter designed at University of New Brunswick (Pepin, 1983), offers an excellent and economical option. This device is an image space primary plotter, where a 2-D cartographic digitizer is used as the image coordinating device in the

plotter system. This system was originally designed for a mapping agency to update maps with an existing 2-D cartographic digitizer.

With regard to hardware, the UNB Digital Mapper is economically excellent, but the software/firmware development is costly. For an application oriented mapping agency, developing a system alone is not generally practical. The Digital Mapper deserves a closer look regarding commercialization.

Advancing with computer technology, many personal computer (PC) based inexpensive analytical plotters are becoming available, such as MACO 35/70, Pentax PAMS, Nikon MPS-2, Carto Instrument AP190, Photogrammtric System APY etc. (Gillen, 1983. Charmard, 1987. Reutebuch, 1987. Yzerman,1988). Such entire systems, together with hard-ware, application soft-ware and data management package, cost from 30,000$US, to 50,000$US. This fits the category of "third order" analytical plotters: micro-processor based, accuracy 5 μm, costing less than 50,000$US, as suggested by Thorpe (1983). Besides, the Kern PC-PRO also use an IBM PC or its compatible as host, while the RT routine is residing on a specified processor. OMI is also working on a new model with a micro-computer (Klein, 1987). This trend is expected because of the fast expanding micro-computer technology, and the increasing user population.

MACO 35/70, Pentax PAMS, Nikon MPS-3, are particularly designed for close-range applications. PAMS could be viewed as a Pentax version of the Wild Autograph A-40. Although it is mainly designed for down-stream use of their stereo-camera ST-120V, the non-metric as well as the non-parallel image pair, can be handled. Basically, the PAMS is an image space plotter according to a definition proposed by Forrest (1971). PAMS uses a micro-computer as the host and does not have a feed-back control.

The Nikon MPS-2 is an object space primary plotter. Because photo-carriages are in a vertical position, the instrument is rather compact.

Both PAMS and MPS-2 have 4 stepping motors, yield resolution of 4-5 μm, and are controlled through tracking balls or joy-sticks. They are designed for small format

photographs, such as 35mm and 60mm imagery. These systems have fairly good optical quality; moreover, they are featured with a complete data management- and application software.

Carto Instrument's AP190 is designed for full format imagery, especially for working with paper prints. It is an open loop image space primary plotter. The measuring precision is 25 μm for left plate, and 10 μm for right plate.

The APY system as designed by H. Yzerman, also caters for large format image applications. By utilizing a super-position equation, 4 stepping motors, a micro-computer as host, and an open-loop object-space primary type plotter configuration, APY is a low priced system. A complete work station is currently priced at 40,000$US. The most remarkable feature of this system is that by using the super-position equation together with the collinearity equations, the stereoscopic model is maintained directly by parallax, and therefore the significance of photo coordinates is reduced (Yzerman, 1988).

It is worthwhile to note that the analytical plotter itself has moved from its expedition stage. The man-machine relationship has been realized as important (Dorrer, 1986). Optical quality, mechanical quality, as well as electronic quality are all of equal importance. As far as software is concerned, user friendliness, flexibility, as well as completeness of the application package have been stressed.

6.2.4   Photo-Coordinate Digitizer

Often a photogrammetric comparator is used as the photo-coordinate digitizer in this approach. In some cases, a stereoplotter is used to simulate either stereo- or mono-comparators (Ghosh, 1988). However, a 2-D cartographic digitizer or other coordinate measuring tools could be applied as well, especially when working with enlarged photographs. By this method, the low resolution of the measuring system could be largely compensated by the photographic enlargement. This method becomes even more practical when a micro-computer is serving as a working station, on-line with a digitizer. Adams

144

(1980), Murai et al.(1980), Welch & Jordan (1983a,b), Shih & Faig (1986), Kim(1987) reported on examples for such applications.

This approach, in some aspects, is equivalent to the image space plotter as stated by Forrest (1971). We only have to generalize the viewer recorder from the stereo-scopic device in order to include the monoscopic device as well. The general comparator-computer case is the same as the image space plotter without feed-back.

We usually recognize a stereo-plotter by that a plotter is working with a model, the p_y is removed by the relative orientation procedure then maintained by either an analogue computer, or a digital computer driven device, moreover, one has to have stereo-perception.

6.3   THE ENLARGER-DIGITIZER APPROACH

There are two factors which are important to the enlarged photo approach. First, a small format camera is cheaper, lighter, more easily available, and suitable for mapping of small projects, because for instance model aircraft and model helicopters have become more popular and available. Secondly, photogrammetric techniques have been found to be useful in many other professions. However, it is not advisable to invest in a comparator or a stereo-plotter for a small work-load. A good alternative would be to enlarge the photograph and then to use a simple coordinate measuring device. Photographic enlargement, which introduces some smaller errors, can improve the ratio of measuring resolution to accuracy. Shih & Faig (1986) reported on preliminary studies concerning the accuracy of analytical processing with the enlarger-digitizer approach. Further studies are reported in section 8.2.

The current resolution of high precision cartographic digitizers is 25 μm (0.001 inch), while the absolute accuracy is approximately three times the resolution. Rollin (1986) recommended 127 μm (0.005 inch) as the acceptance criterion for a digitizer. Compared with a precision comparator, this is quite inferior. In order to compensate for

this relatively low resolution, the original negatives are enlarged, and then the enlarged prints are digitized. The idea is to effectively increase the resolution by working with a larger photo scale. Although the extra procedure introduces extra errors, the gain is expected to be larger than the trade-off.

The main advantages of this enlarger-digitizer approach are lower cost, comfortable working environment, and there is no need for stereo-perception.

1. Cost

As compared with specialized photogrammetric instruments, a digitizer is far less expensive and has much wider applications. The capital investment for a single task can thus be significantly reduced.

2. Comfortable working environment

Most photogrammetric measuring instruments utilize binoculars for viewing. When using them, the eyes have to focus to infinity. However, everything else, such as notes on the table, is at a much closer distance. Adjusting focus between infinity and close range all the time, introduces extra constraints for the eyes.

3. No need for stereo-perception

Although stereo vision is natural for human beings, precise measurements with stereo-perception require extensive practice. Schwarz (1984) reported that 3-9 months of training are required for an observer to reach a minimum proficiency. Most people do not have this training. Furthermore, for some physical reasons, such as acuity differences between the left and right eyes, stereo-perception can become rather difficult to achieve. Even with normal vision, the "weight" for the signals from the two sides is usually different, for example right-handed people are usually also "right-eyed" (Hilborn, 1984). Schwarz (1984) reported that "some 20-25% of the photogrammetry trainees, having passed successfully tests for their natural stereoscopic vision, do not have the measuring capability to make a good photogrammetrist".

The problem of applying a cartographic digitizer for photogrammetric projects lies in its low resolution and accuracy. This limits the direct application to certain circumstances such as when the paper prints are used or when such low accuracy is sufficient (Kim, 1987; Reutebuch, 1987). The enlarger-digitizer approach has more general applications, however, additional problems are introduced with the "super-imposed" two perspective transformations and the associated lens distortions and film deformations.

Concerning the first problem, the effect can be expressed by the following equation:

$$
\begin{vmatrix} x \\ y \\ 1 \end{vmatrix} = \begin{vmatrix} a_1 & b_1 & c_1 \\ a_2 & b_2 & c_2 \\ a_3 & b_3 & 1 \end{vmatrix} \begin{vmatrix} b_{11} & b_{12} & b_{13} & b_{14} \\ b_{21} & b_{22} & b_{23} & b_{24} \\ b_{31} & b_{32} & b_{33} & 1 \end{vmatrix} \begin{vmatrix} X \\ Y \\ Z \\ 1 \end{vmatrix}
$$

...(Eq. 6-2)

where the first matrix (3x3) on the right hand side represents the 2-D perspective transformation coefficient matrix of the enlargement, while the second one (3x4) models the 3-D to 2-D perspective transformation from object to image. Clearly, the dimensions of the resulting coefficient matrix are 3x4, which means that the "super-imposed" two perspective transformations are equivalent to another 3-D to 2-D perspective transformation. The unknown interior orientations of both physical projections will not cause problems. The resulting focal length can be determined by a simple scaling process, since the normal case is the most common situation of enlargement. However, in Shih & Faig (1987) a general solution for the single photo case in the closed form is given.

The joint effects of lens distortions and film deformations are more complicated. However, based on analytical analysis, the additional parameter approach is expected to be effective.

Due to the allowable original format of most commercial photographic enlargers, 35 mm and 60 mm format cameras are recommended for this approach. The original negatives are enlarged 4 to 10 times, with the enlargement ratio depending on the size of the image points, as well as on the resolution of the original film. Bolt & Atkinson(1984) and

Wester-Ebbinghaus (1980) have shown that the image resolution causes the major problem for the use of a small format camera for model aircraft and -helicopter photography. For the enlargement ratio, the best size for the next step, namely plotting, could also be considered.

The enlarged photos are digitized on a cartographic digitizer, and analytical processing commences. For example, a bundle block adjustment with additional parameters, or the DLT method may be used. Finally, the enlarged photos can be utilized for direct contouring and plotting with a photogrammetric plotter.

There are two types of instruments which could be used for enlarging a photograph: the rectifier, and the enlarger. The rectifier may be used not only to change the format of the photo but also to compensate for tilts; the photo could then fit into the tilt range of an analogue plotter. The enlarger is recommended primarily for two reasons :

1. The enlarger is cheaper and more commonly available. A rectifier may only be found in a photogrammetric environment, while an enlarger can be found in almost any photographic shop.

2. The rectifier does the perspective transformation from one 2-D space to another 2-D space, where the relief of the actual 3-D terrain is ignored. Therefore, the rectification used is only an approximation. This problem will be accentuated when the object has more relief, where the degree of relief is usually represented by the ratio between the object distance and the dimensional deviation in the depth direction. A high degree of relief is almost always the case in close-range photogrammetry. Although this does not imply that the introduction of rectification during the process will cause erroneous transforms, because the rectification used here is transforming a 2-D photograph into another 2-D photograph. When the enlargement- digitization approach is used, the requirement for image coordinates prior to the rectification indicates another photographic process. The conventional rectification process does not need the image

coordinates, but the result of the rectification is theoretically not all under control due to the relief effect.

6.4   JUSTIFICATION OF STEREO-PLOTTER

Plotting of planimetric features and contouring for the relief are two important functions for mapping and graphic representation of an object. This may be done in a direct or an indirect way. Direct contouring and plotting requires stereoscopic interpretation and absolute orientation, therefore, it is carried out on a stereo-plotter, and with respect to a specific datum. With this method, continuous line drawing is directly achieved from the semantic information. The indirect method usually takes measurements of points, then requires analytical means for connection to form features, and interpolation for contouring. In many circumstances, direct contouring and plotting is preferred.

In this section, the evaluation of these two methods is conducted from three points of view.

6.4.1   Model Error (Convergence Error)

The concept of model error which is caused by the imperfectness of relative orientation, has already been covered by some texts, e.g. Masry (1979).

Due to the larger lens distortion, film distortion, interior orientation uncertainty and other error sources, the relative orientation is usually much less perfect than for metric imagery. The generally applied convergent photography makes this effect even greater (Konecny, 1965). The problem may be under better control when a hybrid or analytical plotter is used. But it is expected to remain the significant error source when the ordinary plotting procedure is applied.

Konecny (1965) performed some analysis and concluded:

1. Systematic errors in interior orientation have no influence on relative orientation, only the differences $(dx_{pr} - dx_{pl})$, $(dy_{pr} - dy_{pl})$, $(df_r - df_l)$ act as error source. However, in the object space, the individual deviation will be effective.

2. In convergent photography, the error factors act differently as in the normal case. For the 6 standard v. Grueber points, in the normal case $(\phi = 0)$, only the b_z and b_y will be affected by interior orientation. In the convergent case, mainly κ, b_y, b_z are influenced. When the convergent angle increases, the uncertainty of the relative orientation parameters increases.

6.4.2 Stereoscopic Viewing Difficulty

6.4.2.1 Relief Model

The problems of stereoscopic vision in terrestrial photogrammetry have been extensively studied in Dalsgaard (1978). It was found that the acceptable length of the photo base is a function of the slope towards the photo base in addition to the object distance and the calibrated focal length.

Conventionally, the base-height ratio is governed by two factors - one is the accuracy, which usually serves as the lower boundary of the criteria; another is the stereoscopic perception limits which usually serve as the upper boundary (Finsterwalder & Hofmann, 1968).

$$\frac{Y_{min}}{4} \geq b \geq \frac{Y_{max}}{c}$$

b = the camera base length;
c = the principal distance;
Y_{min}, Y_{max} = the minimum and maximum object distance;

...(Eq. 6-3)

The fidelity of this equation has been queried because its upper limit cannot explain the aerial photogrammetric case. This problem was solved by Dalsgarrd (1978). An equation is suggested based on the human vision:

150

$$b = k\,y\,\tan \phi$$

where:

    b: the camera base length;
    k: a constant which varies from person to person; and less than 1 is recommended;
    ϕ: the angle of slope of the object plane;
    y: object distance.
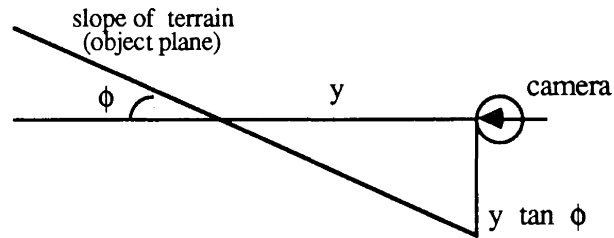
Figure 6.1: Diagram illustrating the base formula

Besides, in where is a large variation of height in the model, the stereoscopic vision can only be maintained at a time within a very limit area. This phenomenon has been experienced when plotting aerial photography as well; e.g. when the top of the hydro-pole is in stereoscopic vision, the ground is blurred. This encourages the use of the photo-digitizer approach.

6.4.2.2 Stereo-viewing Difficulty Caused by Non-parallel Pair

Stereo-vision of normal eyes is similar to the stereo-pair of normal case photography. The differences in tone, tint, texture, and brightness between two pictures will cause problems in stereo-viewing, because the bio-perception depends heavily on **cue**, rather than **metric** (Cerella, 1986). The non-parallel imagery will cause larger variation in the scene thereby worsen the problem.

Actually, in the analogue plotter, the tilted image has to be accordingly tilted, not only because of the requirement of recovery of the perspective relation by the analogue computer, but it also provides the projection of the tilted images onto the same plane, which makes the stereoscopic vision possible.

From this aspect, the photo-digitizer approach once again is justified for convergent photography.

151

6.4.3   Instrument Support

There are two major advantages for the use of a stereo-plotter :

1.   Direct plotting and contouring is available and is not so mathematically complicated as its analytical counterpart.

2.   The stereoscopic vision provides a better environment for the interpretation and for human **image understanding**.

However, the advantages are no longer relevant. With the major advance of personal computers in the last decade, analytical plotting and contouring is now flourishing. This is not only due to the development in hardware, but largely in the correspondent software.

On one hand, the direct contouring requires an experienced operator for a better job and needs specific instruments. On the other hand, the use of a personal computer is universal, and it is indispensable to the modern laboratory. Besides, the presentation format of the data varies considerably; e.g., the bird view, the perspective viewing, and contour display from any specified datum, for instances. The popularity of digital data actually is also reflected in today's mapping environment with stereo-plotters.

Together with the hardware advance, all of the above software could be purchased or even free-copied for a micro-computer from a micro-software exchange center. Therefore, the analytical process is necessary, and far less complicated than in former times.

6.5   REMARKS

In many instances, the 3-D spatial coordinates are essentially important for investigation, study, or/and analysis. Photogrammetry has been justified as a useful methodology for this purpose, by its non-destructive, non-contact, time-frozen, and permanent recording characteristics.

152

The use of a non-metric camera in close range photogrammetry is very handy, because of its fidelity, low cost, and availability. For a non-photogrammetric laboratory, a 2-D cartographic digitizer and a commercial photographic enlarger could compose a very inexpensive system for data reduction. However, when a graphic output is required through analogue plotting, a stereoplotter is generally still required. An economical, proper resolution analytical plotter, such as the UNB Digital Mapper, offers a very appealing solution. The Pentax PAMS, Nikon MPS-2, etc., indicate that there is a market potential for a well-equipped work station.

However, the use of these systems leads to another purchase or hardware development. The Digital Mapper is relatively inexpensive in terms of hardware, but the development is expensive especially in software, and there is currently no commercial model available. On the other hand, the other system requires some new investment. Meanwhile, the changing environment for analytical plotting by (micro-)computer is becoming more favorable.

For stereo-plotting purposes, parallel pairs are preferred. The pre-calibration procedure with a fixing frame and a suitable control field for the initial setting of exterior orientation, is an advisable approach. This has been practically used by Ruether & Adams (1984). The problem with it lies in the extent of the pre-setting needed and in the stability of the system.

The enlarger-digitizer approach, along with analytical plotting is highly recommended for non-photogrammetric laboratories[6.1]. When the process of analogue plotting with the analogue plotter is taken for small-format imagery, enlargement rather than rectification is recommended. However, the scale of newly introduced problems by rectification is still under investigation. In aerial photography and for he reproduction of minor relief objects, this problem should be totally negligible.

[6.1] It should be mentioned that an analytical system composed of a tablet digitizer and a personal computer has been commercially marketed, i,e. the MR-2 from Rollei.

Gillen (1983) summarized the advantages for the use of small format (35mm/ 60mm) non-metric camera as:

1. low cost for the camera itself;

2. film and processing are readily available and are inexpensive;

3. interchangeable lenses are readily available;

4. accessories, such as filters, auto-flash units, auto-winders, etc. are commercially available. In total, small format camera systems already exist in state-of-the-art form at a relatively low cost.

Following the same scheme, the application of a personal computer as host, has the advantages :

1. the PC itself is inexpensive;

2. the user's training and computer maintenance are readily available and are inexpensive;

3. supporting application software is readily available, much cheaper, and of great variety;

4. accessories, communications, as well as consulting are readily available.

It could be arranged in the same way for a cartographic digitizer instead of a stereo-plotter :

1. the system itself is relatively inexpensive;

2. no stereo-perception training is required, operators are readily available;

3. a parallel-pair is not required, any geometric configuration can be applied without considering human stereo-perception, the photos are readily available.

Solutions to an engineering problem usually are not unique. All of them have advantages and also disadvantages. While the 35 mm format non-metric camera has its significant advantage in the economical aspect, the image quality is not always sufficient. There are also many limitations imposed on micro-computers, as well as the enlarger-digitizer approach. However, a detailed understanding would be helpful for arriving at the best decision.

CHAPTER 7

CLOSE-RANGE PHOTOGRAMMETRY WITH VIDEO CAMERA

In the generalized sense, an image is a record of the energy signature of the scene. In either passive or active mode, the recording device receives the energy radiation from the object to be measured. For film based systems, the recording device is a light-sensitive chemical layer; for electronic camcorder, a light-sensitive metal plate. As far as the image can be recorded, photogrammetric methodology can be applied.

Similar to the significant contribution which amateur non-metric cameras made to close-range photogrammetry, video cameras are making their impact now. Together with the fast growing use of the regular video camera, the electronic counterpart of the camera- the still video camera (SVC) has a high future potential. In fact, several commercial models have been developed, e.g. Sony Mavica, Cannon RC-701.

The major advantages of these *electronic imaging devices* are the instant image formation, no need for chemical processing, overwhelming flexibility on transmission, simplicity in A/N conversion, and re-usable recording media. For the surveying and information fields, the simplicity in providing *digital images* makes electronic imaging devices particularly important. The reason lies in the on-going trend of processing images with digital methods and the growing importance of digital images in an information system. In fact, several Geographic Information Systems (GIS) in the market have implemented image information into their products.

This chapter focuses on close-range applications of home video equipment. The devices, the resolution and accuracy, and the processing procedures are studied.

155

7.1 THE DEVICES

Based on the theory of image formation, video cameras can be classified into the scanning tube type and the solid-state type. In the second category, the linear array camera and matrix camera can be further identified. A linear array camera utilizes linearly arranged solid-state sensors, and mechanically scanning over the focal plane to obtain a complete frame; while the matrix camera has a matrix of solid-state sensors and there is no need for any mechanical movement. The significance of a linear array camera lies in its less expensive price compared with a matrix camera of the same level resolution. However, the distortions caused by mechanical movement are heavily dependent on the calibration and are difficult to model (Robertson, 1986). In spite of its applications in the past, e.g. Frobin, W., & Hierholzer, E. (1982), and in space-imaging, its significance in close-range photogrammetry is decreasing. Thus, it will not be covered in this study.

7.1.1 Scanning-Tube Type Camera

Scanning-tube is the major component of the television technique. Concerning the image formation, the light from a scene is focussed first by the zoom lens of the video camera. A set of prisms inside the camera splits the light into the three primary colors. Each prism sends an image in one color onto the front of a camera tube. Each tube turns the image into electrical signals that become part of the TV signals and are recorded onto a video-tape.

The tubes in most color cameras are Plumbicon tubes, an improved version of a tube called the vidicon. A vidicon tube has a glass faceplate at its front end. At the back of the faceplate is a transparent coating called the signal plate. A second plate, called target, lies behind the signal plate. The target consists of a layer of photoconductive material that conducts electricity when exposed to light. At the rear of the tube is an electron gun.

Light from the image reaches the target after passing through the faceplate and the signal plate. The light causes electrons in the photoconductive material to move towards

the signal plate. This movement leaves the back of the target with a positive electric charge. The strength of the positive charge corresponds to the brightness of the light shining on that area. The camera tube thus changes the light image of positive charges on the back of the target.

The electron gun shoots a beam of electrons across the back of the target. The beam moves across the target in an ordered pattern called *scanning pattern*. As the beam moves across the target, it strikes areas with different amounts of positive charge. The electrons from the beam move through the target and cause an electric current to flow in the signal plate. The voltage of this current changes from moment to moment, depending on whether the beam is striking a bright or dim part of the image. This changing voltage is the video signal from that camera tube.

Concerning scanning pattern, in North America, NTSC (National Television System Committee) standard is generally used, which utilizes 525 lines and 30 frames per second. To avoid flicker, each part is scanned twice in alternating strips, i.e., each frame is composed of 2 fields. In Europe, a system of 625 lines with 25 frames per second is commonly used (World Book, 1979).

The problems of tube are:

1. its inability in pointing to a bright object for long;

2. "comet tail" effect, when passing by a bright object, e.g., candle light (largely

    improved by the latest type tube, Super Band Saticon).

For photogrammetric applications, the noticeable effect on the scanning path of the electronic beam from the surrounding magnetic-electronic field creates another problem.

7.1.2   Solid-State Camera

The major imaging sensors for today's commercial solid-state camera/camcorders are CCD (Charge coupled device) and MOS (Metal oxide semiconductor). The difference between these two is very limited. In fact, every CCD is also an MOS. Hitachi is the

largest manufacturer of MOS pickups. It installs them in its own productions as well as for other brands including Minolta, RCA, Pentax, Radio Shack and Kyocera. Most other manufacturers, including Sony, NEC, Toshiba, and Matsushita, favor the CCD pickup.

Compared with a scanning-tube, there is no movement, i.e., no scanning. The electronic picture of the scene is formed directly by the electronic wells constructed by the photo-diode of each cell. The signals are collected to the vertical register first, and then to the horizontal register. For color images, the same scheme as used in scanning-tube type cameras, can be applied. However, the most often applied scheme is to arrange CCD cells for different colors in an alternate manner, i.e., only one chip is used for a color camera.

Compared with a scanning-tube, the chips require less power and no warm-up time. They are almost impervious to damage from shocks and are almost completely free of the annoying comet-tails of light that would stream out from bright lights or hot spots. For photogrammetric application purposes, solid-state cameras are particularly of interest due to their smaller electronic distortions and stable geometrical characteristics. However, the drawback of the current CCD as compared with scanning-tubes is less sensitivity.

7.2   RESOLUTION AND ACCURACY

Compared with films, small format and limited resolution are the major constraints of electronic imaging devices. For commercial camcorders, prior to Super VHS and Extended Definition Beta, pickups with 210,000 to 250,000 pixels were common. Today, chips of 380,000 pixels are dominating. Compared with film, they are all inferior (see Table 7.1, data compiled from Jones (1987)).

Although Kodak's break-through significantly increases the resolution (pixel size: 6.8 x 6.8 μm), this type of chip is too slow and costly to be used in a consumer-oriented system (Schaub, 1988). Besides, it is still 20 times less than imagery from ordinary 35 mm camera. Reseau-scanning and Mosaic-focal-planes seem to provide a solution. Reseau-scanning is using a sensor scanning over the image, then each image is registered

into a frame by a perspective transformation utilizing the four grid points of the reseau. Rolleimetric RSC 70mm from Rollei Fototechnic is the first commercial model implementing this technique (Luhmann & Ebbinghaus, 1987). A Mosaic-focal-plane is formed by arranging individual chips into a linear array, each of which is a smaller subarray (Chan, 1981).

TABLE 7.1
Resolution of Films and CCD Pickups

Media	Type	Included pixels[7.1]
film	35mm	25 000 000
	110	2 500 000
	disc	1 500 000
SVC	Cannon RC-701	187 200
	Sony Mavica 1981	250 000
	Sony Mavica 1987	380 000
	Konica KC-100	300 000
	Minolta SB-70S, -90S	380 000
	Chinon CP-9AF	380 000
Camcorder	JVC GF-S1000 (S-VHS)	380 000
	Minolta V-2000 (S-VHS)	390 000
	Hitachi VM-6000 (S-VHS)	400 000
	Kodak Megapixel	1 366 200

While the resolution of solid state cameras is limited by the number of photosites, the resolution for tube cameras is limited by the diameter of the electron scanning beam (vertically) and bandwidth (horizontally). Additionally, the vertical resolution is limited by the number of scan lines defined by the RS-170 standard, i.e., 242.5 lines/field or 485 lines/frame. (Not all 525 lines/frame are used for the image resolution).

It should be noted that, in the videography case, i.e., when the pro or consumer type camcorder and VCR equipment are used, the resolution lost during the data transmission has to be considered. Because the current write-read speed of hard disk drives for micro-computers is not sufficient for many applications, the video signal is stored through VCR then played back for image digitization. Vlcek (1988) reported experiences on image deterioration in this process.

[7.1] For SVC and Camcorder, the listed numbers of pixels are the gross number.

In general, a standard VHS camcorder/VCR delivers 240 lines of resolution[7.2] in color. The 3/4U[7.3] VCR will deliver 240-260 lines of resolution. Superbeta VCRs push this to 290 lines. Superior-performance 3/4U VCRs have 340 lines of resolution. And, 330 lines would be the upper limit of the NTSC Broadcasting system. For the new generation, 420 lines for JVC S-VHS in Standard Play (SP) mode, and 500 lines for Sony ED-Beta are provided. All VCRs will make sharper B/W pictures than color pictures. Many 3/4U VCRs have 300 lines of B/W but only 240 lines of color resolution (Utz, 1988).

As far as the accuracy in photogrammetric applications is concerned, Wong (1972) calibrated several scanning tube type cameras, and values better than 0.5 TV-line were reported with a 20-term polynomial calibration. Burner et al. (1985) reported the tests of several high resolution scanning tube type cameras with both Vidicon and Newvicon tube. Sub-millimetre accuracy in object space positioning were archived. Close-range photogrammetric applications with video cameras uncorrected for electronic or optical distortion was recommended as useful if the affine correction is allowed.

Curry et al. (1985) utilized a 128x128 pixels CID camera, where 0.2 pixel accuracy was obtained with calibration. El-Hakim (1986) used an IRI-D256 Vision system with a 256x256 pixels CCD camera, where 0.1 pixel accuracy was reached with calibration; while Wong & Ho (1986) reached 0.4 pixel with a 244x248 pixels CID camera. These examples indicate the feasibility of sub-pixel determination.

7.3   THE PROCESSING PROCEDURES AND GENERAL REMARKS

The processes involved in the photogrammetric use of electronic sensors can be identified into: image formation, image acquisition, preprocessing, recognition,

---

[7.2] Lines of resolution is the unit for evaluating the horizontal resolution.
[7.3] U stands for U'matic, a trademark. 3/4U VCR uses 3/4 inch width tape; while both VHS and Beta use 1/2 inch tape.

positioning, and three-dimensional information extraction (Gruen, 1986). Although the gathered digital image can be processed with its hardcopy form in the same way as photo-prints, complete on-line digital processing is more pleasing. This directs to a potentially complete-automated system.

In the process, image processing and pattern recognition techniques are heavily used. Feature identification and correlation between different images impose the problem of image understanding. The entire procedure also challenges the computational power, and expands the dimension of the photogrammetric information content. In order to reduce the complexity, structured light and specially arranged targets are commonly applied. Artificial intelligence and expert system techniques also provide possible tools for using non-positional and high-order image information. Much research in digital photogrammetry has been and is being conducted. General reviews are found in Gruen (1986) and Wong (1986).

The application of domestic video equipment is essentially a part of the subject of digital photogrammetry, i.e., image information is processed by pixels with digital values. However, besides the objectives for an automated mapping system and a near real-time robotic monitoring system, Video camera/camcorder is going to substitute for non-metric cameras in certain applications. One of the most appealing fields would be real-estate/architecture documentation with still video cameras (Jones, 1987). This field has long time been one of the major application of close-range photogrammetry.

CHAPTER 8

THE EXPERIMENTS

Resulting from Chapter 5, rasterstereography has been shown as an attractive method in today's environment; while from Chapter 6, enlarger-digitizer approach is practical and economical. In Chapter 7, the potential for applying video camera for image acquisition has been described.

In order to practically investigate the feasibility of rasterstereography in the non-metric environment, the reliability of enlarger-digitizer approach, and exploring the availability of utilizing a home camcorder for image acquisition, three experiments have been conducted and are reported in this chapter. The first one deals with a film-based rasterstereographic system utilizing a non-metric camera and an over-head projector. The one-plane-constraint method is introduced and tested. The second one investigates the enlarger-digitizer approach. The last one reports the preliminary investigation on the metric characteristics of a video-based image processing system. A currently available working scheme is proposed and utilized in practical experiments.

8.1 AN EXPERIMENT WITH A FILM-BASED RASTERSTEREOGRAPHIC SYSTEM

For the film-based system, a 2-phase approach could be chosen. That is, the calibration phase and the measuring (working) phase are separate. This application to a non-metric system was reported by Ruether & Adams (1984) when surveying whales by photogrammetric means. Although the concept of utilizing pre-calibrated camera data for a subsequent intersection procedure, was developed as early as the stereo-camera, the application of the 2-phase approach to this particular system still needs further investigation.

For regular maintenance re-calibration, the method applied in Armenakis (1983) could be adopted; where, the control points were used only once in consecutive photographic missions.

8.1.1   The One Plane Constraint Method

The lack of pseudo-image coordinates for control points is the major problem for the data processing of rasterstereography. However, by implementing certain procedures, the data processing can be done with conventional analytical photogrammetric software.

Frobin et al. (1982) provide a solution with interpolation by identifying the projected points surrounding a control point, measuring all these image coordinates on the camera image and then following with a perspective transformation.

Another approach has been developed by Ethrog (1987), who utilized two control planes. Raster lines are used for projection. The rear control plane is a flat white plate, while the front plane is a frame on which several white tapes are stretched, approximately perpendicular to the projected raster lines. With the camera image coordinates, the spatial coordinates of the intersection of the projected raster-lines and the two control planes can be calculated.

Ethrog's method provides a good way for solving the problem of control points on the pseudo photo, and also has been shown to be capable of compensating for deviations from ideal central perspective transformation. However, while the additional object information provides some helpful constraints, especially for the radial distortion control of the projector, it also implies additional work and conditions for the operation. Therefore, another approach following the same concept in object space design, was developed by the author.

Following Ethrog's method, the object space control is designed; however with only one plane, rather than two. Several control points are established on this plane, for

163

which absolute flatness is assumed (Z = 0). The number of control points should no less than three. The object is situated in front of the control plane. A regular grid pattern is projected from a projector located on one side, while the camera station is on the other, arranged for convergent photography. The convergence angle is depending on the characteristics of the undertaken project.

The space resection for the camera is performed with the aid of object space control points. The projected raster points on the control plane are calculated from the intersection of the bundles with the plane, and these intersected points are subsequently used for the space resection of the projector. An ordinary procedure for intersection follows for the other points.

The data processing can be carried out as described above, however, a simultaneous bundle block adjustment may be more favourable. In this case, one extra condition from the plane is added. This can be realized by assigning a constraint function; or better by assigning weighted constraints to the Z coordinates of points located in the plane.

In both cases, the initial values for the orientation parameters can be determined by utilizing a closed solution scheme developed in Shih (1987), Shih & Faig (1988).

8.1.2   The Experiments

In order to evaluate the capability of this scheme, a calibrated satellite antenna was used as test object. A pencil-follower flat-bed digitizing table provided the control plane.

It is not intended to imply that this proposed method can be used for ultra-precise surface measurements, such as antenna calibration, rather it was intended to use a well calibrated antenna to test the proposed system.

In order to avoid directional reflection from the glass surface of the flat-bed digitizer, and also to improve the contrast, six sheets of white paper were taped onto the table. Twelve control points were placed on the paper, and distances between them were

164

measured. Meanwhile, all signalized 317 points on the antenna surface had been measured with two Kern E2 electronic theodolites operating in an automated data collection system (Pedroza, 1987). Based on theoretical derivations, the magnitude of the propagated error in object space in the E-2 system is less than 0.05mm, which makes it an excellent reference.

8.1.2.1   Data Acquisition

A Cannon AE-1 camera with a standard 50 mm lens, and a 3-M Model 213 AKD portable overhead projector with 355 mm focal length were used. A grid pattern was generated by scribing onto thick scribing material with the WILD A-10 plotting table using a line-width of 0.6 mm. A contact print diapositive of the grid on Lith-film was used for generating the raster pattern on the projector.

Three photos were taken with different convergence angles, approximately 30° (see Fig. 8.1), and subsequently digitized on a Zeiss PSK stereo-comparator. At least three readings were taken for each image point. The repeatabilities in terms of RMSE are listed in the table 8.1, where photo 10 refers to the pseudo image, with its accuracy estimated from the line-width and the precision of the A-10 table. It is very interesting to note that photo 16 has significantly better repeatability. This is because of its better image quality, which arises from a relatively larger scale, and more importantly, a smaller depth of field. However, the repeatability is not equivalent to the accuracy. This can be observed from Table 8.2, which gives the RMSE for single photo calibration.

TABLE 8.1
Repeatability of digitization (unit: μm)

photo	10	14	15	16
$\sigma_x(\mu m)$	(300)	3.99	4.38	3.72
$\sigma_y(\mu m)$	(300)	4.72	3.90	3.36
scale	1:5	1:60	1:60	1:50
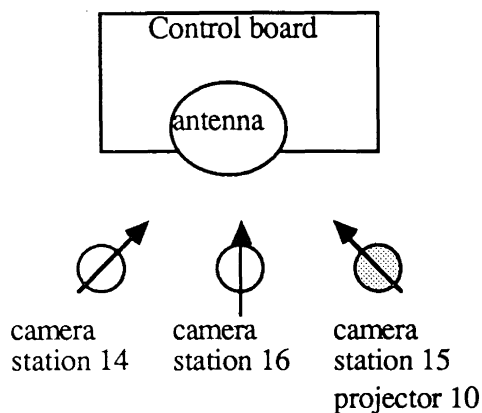
Figure 8.1: Test Arrangement
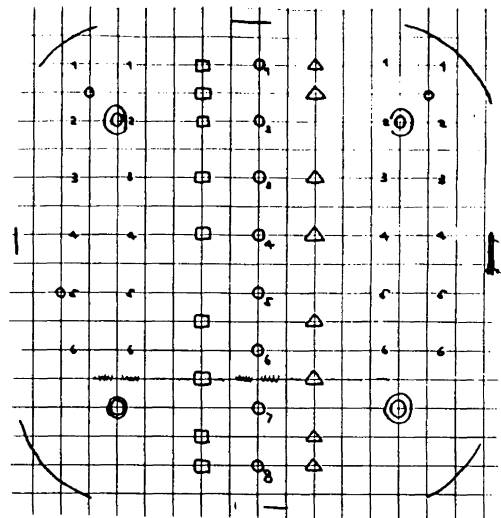
Figure 8.2: The Pseudo-image

8.1.2.2   Data Processing

The data were processed in three different phases:

• photo-triangulation with 3 real photos;

• single photo space resection/calibration;

• photo-triangulation with pseudo photos.

The first two are accomplished with the object coordinates measured with two Kern E-2. While the first provides another set of reference data which can be directly compared with, the second one is mainly processed for variance analysis. The variances were analyzed by system calibration. All 317 geodetically determined points were used to calibrate the non-metric camera imageries, and the 97 projected points were used to calibrate the pseudo image.

In the operating sequence, the single photo space resection/calibration for three real photos was performed first. A closed form solution scheme as introduced in Shih & Faig (1987) was used. Then the photo-triangulation with three real photos was performed with the self-calibration program UNBASC-2 (Moniwa, 1977). With the resulting object coordinates, the calibration for the projector was accomplished. Finally, based on the interior orientation parameters from the second phase, the rasterstereographic photo-

166

triangulation was performed with the one-plane constraint and the control points on the plane.

8.1.2.3 Results

Single photo calibration

Besides the interior and exterior orientation parameters, 2 affinity parameters were included. From the resulting parameters, the affine distortion of the real photo is much smaller. Since the resulting RMSEs are very close to the repeatability indicator, no further additional parameters were introduced.

Concerning the pseudo photo, with all 97 points scattered around the entire format, the RMSE values are extremely large. Further additional parameters were added, but resulted in no significant improvement. It is recognized that this big distortion may not be sufficiently modelled by the additional parameter model used, because of the configuration of the overhead projector. However, the affinity correction is quite effective, especially for the 97 point case.

The case 10b refers to the 33 central point case where the largest radial distance is 45 mm. Although the RMSE is still larger than the expected, it decreased significantly. The magnitude of the affinity parameters is also reduced.

TABLE 8.2

The RMSE from single photo calibration (unit: μm)

photo	10	10b	14	15	16
$\sigma_x(\mu m)$	2500	540	3.66	3.57	3.87
$\sigma_y(\mu m)$	3200	490	3.52	3.66	3.61

The photo-triangulation with real photos

The resulting RMSE in image coordinates from UNBASC-2 are in x: 2 μm, in y: 3 μm. All additional parameters according to Moniwa (1977), i.e., 3 for radial-, 2 for decentering-, 2 for affine distortions, were included.

167

Furthermore, the plane constraint was used for another accuracy investigation. Since the datum is defined by geodetic measurements, a plane fitting was performed. The resulting RMSE of the deviation was 0.282 mm. The largest deviation was 0.56 mm. This accounts for the unflatness of the taped-on paper, and also the relatively poor numerical condition from the extrapolation situation. Considering the paper sheets were just taped by their four corners, and undulation can happen in any place, especially the central part of the paper, this result is quite reasonable.

The rasterstereographic case

Based on the single photo calibration, the RMSE ratio between pseudo photo and the real photo is near 1:700 for the full format. Following photogrammetric reduction, a 3-D similarity transformation was performed for the goodness of fit to the 3-real-photo case. The RMSE values in planimetry and direction of depth are listed in Table 8.3.

TABLE 8.3
Checking the goodness of fit(unit: mm)

Case	Photos	RMSE(plani.)	RMSE(depth)	datum
1	14,16	1.	1.	plane constraint
2	10,14	20.	16.	plane constraint
3	10b,14	1.	1.	geodetic definition
4	14,15,16	1.	1.	plane constraint

The accuracy indicated by RMSE of fit, as compared with the single photo calibration, is even worse. However, the central 33 points, as controlled by 6 points whose coordinates were obtained from the 3-real-photo case, present promising results.

8.1.3 Concluding Remarks

The one plane constraint method developed in this study provides an alternative to other methods for rasterstereography, and also can serve as control for other photogrammetric projects. Although the control information is limited to one plane which does not allow for a full calibration for non-metric imaging devices, the "calibration" still

can be carried out with three dimensionally distributed object points by utilizing the "self-calibration" concepts.

It also should be noted that rasterstereography generally takes one camera and one projector. This arrangement does not provide as good a reliability for estimated parameters, as one can expect from conventional photogrammetry. For the self-calibrating case, the image geometry is not strong either. It can be viewed as a 2-station intersection as is the usual case of a stereo-camera.

The ordinary overhead projector as used in this experiment has shown large irregular distortions. This may be caused by its special optical configuration and non-metric lenses. However, in the central area of the format, good *metric* quality can be expected.

8.2 THE REPEATABILITY AND ACCURACY OF THE ENLARGER-DIGITIZER APPROACH

In this section, the reliability and accuracy of the enlarger-digitizer approach are studied and compared against comparator-digitized image coordinates in terms of the individual transformation as well as the performance within a bundle block adjustment.

8.2.1 Repeatability of Digitizer

Concerning the accuracy of the digitizer measurements, Masry (1984) stated that:

> The performance of the operator is highly dependent upon the skill, dedication, and stamina of the person. The limits imposed by human physiology are seldom approached. For example, the eye can resolve about 500 lines per inch under bright illumination at about 10 inches. If suitable controls are provided, the positioning accuracy will be a function primarily of visual acuity. For non-mechanical positioning, operator accuracy will typically be about 0.010 inch (0.25mm).

Experimentally, Rollin (1986) reported on a test performed at the British Ordnance Survey with 34 digitizers, some of which have been in service since 1972. The results range from 0.075 mm to 0.142 mm in terms of RMS in x and y as compared with precise grid coordinates. As a result, he recommended that, "the RMS vector error must not exceed 0.127 mm".

Independently, Oimoen (1987) tested a $2000 tablet digitizer with a resolution of 0.001 inch (0.025mm) and an accuracy to the nearest 0.01 inch (0.25mm), as claimed by the manufacturer. Each point on every photograph was digitized five times separately with a rejection criterion for remeasuring of 0.003 inches (0.076mm). The values were compared with the readings from a precision comparator with a least count of one micrometre. The RMS error in x and y respectively were 0.098 mm and 0.113 mm.

At the Department of Surveying Engineering at the University of New Brunswick (UNBSE), several tests have been carried out with different test objects. The standard deviations from the repeated measurements are listed in Table 8.4. The obvious differences between the first 9 photos and the last 4 photos are caused mainly by differences in targetting, i.e., the definition of the photo points. The first group is using a metal plate test body as used in Moniwa (1977), which has well-defined crosses as targets. The second one uses a box-string project from a UNBSE laboratory assignment; where depth of field problems cause the deterioration of the image quality. However, in both cases, a repeatability of less than 0.1 mm was achieved.

This manual digitization station was also utilized for a video project, in which the printed hard-copies from an ink-jet plotter were digitized (Faig & Shih, 1988). The results of which will be presented in the section 8.3. Without rejecting any measurements, the standard deviations of the averaging process are presented in Table 8.5. For the first object, a plane, all targets are well defined. For the second object, the same test plate for close-range application of non-metric camera was used. In the video image, the grid points are better defined than the bolt points, while both of them are less defined than points in the

images of plane object. For all prints, all image corners have good definition. Although the standard deviation of the averaging process can be reduced to 1/3 by implementing a robust estimation procedure, the listed figures provide an appreciation of how the pointing can disperse with different type of targets.

TABLE 8.4
The repeatability of digitizer

Test	Enlarge	Photo	No. of	σ_x	σ_y	σ_0		σ_0
object	ratio	no.	obs.	x10^{-3}"	x10^{-3}"	x10^{-3}"	μm	unit scale
1	4	16	180	1.9	2.9	2.4	62.7	15.7
	4	17	153	1.6	2.6	2.2	56.4	14.1
1	7	19	182	2.1	3.6	2.9	75.9	10.8
	7	18	134	2.2	3.3	2.8	71.5	10.2
1	10	16	182	1.9	3.1	2.6	66.5	6.6
	10	17	150	1.7	2.4	2.0	53.2	5.3
	10	18	135	2.0	2.6	2.3	60.3	6.0
	10	19	183	1.9	2.6	2.3	59.5	6.0
	10	20	182	1.9	2.6	2.3	59.0	5.9
2	8	13	211	2.6	3.9	3.3	85.9	10.7
	8	14	267	2.4	2.9	2.6	68.1	8.5
	8	15	274	3.1	3.9	3.5	91.3	11.4
	8	22	315	2.7	3.3	3.0	78.3	9.8

TABLE 8.5
The repeatability of points with different quality

Test	Photo	type	no. of	σ_x	σ_y	σ_0	
object	no.		obs.	x10^{-3}"	x10^{-3}"	x10^{-3}"	μm
plane	-	corner	64	1.9	2.1	1.9	48.4
	1	cross	105	2.3	2.3	2.3	59.3
	2	cross	105	2.6	2.6	2.6	67.4
	3	cross	105	3.1	2.6	2.9	74.5
plate	1	corner	16	2.0	2.4	2.2	57.5
	2	corner	20	2.6	3.0	2.8	72.5
	3	corner	20	3.1	3.5	3.3	84.2
	4	corner	20	3.6	3.1	3.3	86.1
plate	1	grid	180	3.9	3.4	3.7	95.0
	2	grid	144	4.1	4.0	4.1	104.2
	3	grid	144	4.6	4.8	4.7	120.6
	4	grid	144	6.3	5.3	5.8	148.9
plate	1	bolt	75	4.3	4.1	4.2	108.5
	2	bolt	100	6.1	8.6	7.4	190.4
	3	bolt	75	7.5	6.5	7.0	179.3
	4	bolt	100	6.2	6.0	6.1	156.1

8.2.2 Accuracy from Single Photo Transformation

The enlarger-digitizer measurements are transformed to the measurements of the original negative by using a 2-D affine transformation, and the results are compared with those obtained by using a perspective transformation. The resulting standard deviations are listed in Table 8.6, which show the perspective transformation effect in the enlargement as compared to the measuring error and other error sources. The figures are scaled to conform to the original negative. The enlarger-digitizer measurements are then transformed to object space via a 3-D to 2-D perspective transformation (DLT) (Abdel-Aziz & Karara; 1971) without additional parameters. In Table 8-6 and 8-7, 4a, 4b are two sets of independent image digitizations which were conducted by different personnel at different time on 4 times enlargement .

Gross errors are realized as an important issue. In order to have the results of transformations compared on a common base, those and only those observations which have been identified as gross errors in the bundle block adjustment are removed. All sets of prints, which have been analyzed, show a similar trend, thus only two of them are listed. It seems, that the perspective transformation of the imaging process composes the major part of the error budget, while the enlargement introduces a relatively small part.

TABLE 8.6

Standard deviation of single photo transformation

Photo	16					17				
Enlargement	Orig.	4a	4b	7	10	Orig.	4a	4b	7	10
Affine to Original	--	2.04	2.80	1.37	1.66	--	1.58	2.32	1.34	1.21
Perspective to Orig.	--	1.26	1.86	0.96	0.97	--	1.13	1.46	0.91	0.80
DLT to Object	13.06	25.26	24.71	10.63	9.16	12.94	14.76	15.49	11.66	7.72

8.2.3 Accuracy from Bundle Block Adjustment

Concerning the errors introduced in the enlargement, Shih & Faig (1986) have indicated that the pooled effect can be taken into account by the parameters in the final block adjustment. It has been found that the physical model for additional parameters as used in

172

UNBASC-2 (Moniwa, 1977) provides better results than a third order spherical harmonics model (El-Hakim, 1979), since the latter has shown no improvement over a bundle adjustment without additional parameters.

From Table 8.7, the results from the bundle block adjustment using UNBASC-2 are given. Two blocks were processed, one consisting of 3 overlapping photographs, the second of five. For the 4x enlargement, only three of five were used.

TABLE 8.7

The Resulting Accuracy from Bundle Block Adjustment

RMSE, unit: image (μm), object (mm)

| Data | Without APs | | | | | With APs | | | | |
| | Image | | Object Check Points | | | Image | | Object Check Point | | |
	x	y	X	Y	Z	x	y	X	Y	Z
Orig.3 photos	7.0	7.0	0.13	0.16	0.36	4.0	4.0	0.08	0.10	0.36
Orig.5 photos	7.0	8.0	0.15	0.14	0.20	4.0	4.0	0.07	0.07	0.12
4x 3 photos a	8.0	10.0	0.15	0.20	0.81	7.0	7.0	0.10	0.18	0.63
4x 3 photos b	7.6	8.9	0.13	0.22	0.76	7.0	7.6	0.10	0.21	0.76
7x 3 photos	6.5	6.5	0.13	0.15	0.36	5.1	5.1	0.09	0.09	0.34
7x 5 photos	7.6	7.6	0.12	0.13	0.23	5.8	6.9	0.06	0.08	0.14
10x 3 photos	5.3	5.8	0.11	0.14	0.20	3.5	3.5	0.07	0.06	0.17
10x 5 photos	6.1	6.1	0.13	0.13	0.17	3.8	4.3	0.07	0.06	0.14

Object: plate;
No. of control points: 18H20V;
No. of check points: 34H32V.

8.2.4   Concluding Remarks

The experiments have shown that the enlarger-digitizer approach is feasible. However, precise pointing has been found to be very subjective and depends not only on the characteristics of the targets, but also on the condition of the operator. Although this is true for any coordinate measuring device, it is felt to be more significant in this approach.

Concerning the pointing, Rollin (1986) stated that care must be taken, although being over-cautious can produce biased readings. A number of other precautions, such as constant orientation of the cursor because of eccentricity errors, and a warm-up period for

the instrumentation, which are suitable for all digitization projects, are all important for this approach.

The second perspective transformation introduced by the enlargement, can be combined with the 3-D to 2-D imaging perspective transformation, and both modelled together by one 3-D to 2-D perspective transformation. The effects from lens distortion and film deformation of the enlargement are not dominant and can be effectively compensated by additional parameters together with the distortions from the first imaging process. The physical model for additional parameters has been shown to be better.

8.3 AN INVESTIGATION INTO THE METRIC CHARACTERISTICS OF A VIDEO-BASED SYSTEM

For the purpose of studying fluid visualization, the Fire Science Centre at the University of New Brunswick configured a general-purposed image acquisition and processing system. Currently, a Sylvania scanning tube type video camera with 12-72mm zoom and autofocus function is used together with a Matrox PIP-1024 Image Digitizer Board. An IBM PC/XT compatible with 640K RAM is used as the host.

This section reports the investigation into the metric properties of this system and to set up a calibration procedure for the current configuration and its expected upgrading.

8.3.1 The Test Approaches

As a general concept, photogrammetric data reduction can be directly performed with high order features, such as curves, surfaces. However, the current photogrammetric techniques mainly work with the lowest order feature, the point. Therefore, before the metric properties in the digital image can be utilized, the image points of interest have to be extracted and their image coordinates have to be determined.

174

Concerning the procedures, El-Hakim (1986) divided the entire process into several stages: noise reduction and feature enhancement, image segmentation, feature extraction, target recognition, target location, matching, and object space coordinate determination. The accuracy of the final results depends primarily on how these procedures are performed. The process may be exclusively classified into two stages, namely, finding the point/target, and secondly obtaining its image coordinates.

For the first part, one scheme as used in El-Hakim (1986) performs the image enhancement first, then segmenting the image by thresholding. The noise reduction and image enhancement procedures as well as the thresholding play an important role in the proper functioning of this scheme. Another approach would be applying pattern recognition techniques to identify all special features. Several interest operators are available, such as the Moravec-, the Dreschler-, and the Foerstner operator (Luhmann & Altrogge, 1986). Both schemes have their advantages and disadvantages, and none of them can be generally suitable for all cases.

Concerning the image coordinate determination, the most straight forward way would involve the geometrical centre of gravity. This provides fast execution, but is highly influenced by the threshold value selected and may be biased. As a refinement, the weighted centre of gravity can be used as reported by Wong & Ho (1986). This leads to:

$$x = (1/M) \, \Sigma \, \Sigma \, j.g_{ij}$$
$$y = (1/M) \, \Sigma \, \Sigma \, i.g_{ij}$$
$$\text{where } M = \Sigma \, \Sigma \, g_{ij}$$

...(Eq. 8.1)

where g_{ij} is the grey scale value of pixel (i, j). Prior to performing this step, thesholding with the threshold intensity:

$$T = \text{Integer}(\, (\text{Mean} + \text{Minimum})/2 + 0.99)$$

...(Eq. 8.2)

was applied.

175

Mikhail et al. (1984) utilized the moment preserving method and the Fourier descriptor method. The two-sided gradient method with parabolic curve fitting have been utilized in Frobin & Hierholzer (1983) and in Curry et al. (1985). These methods provide a more sophisticated algorithm and are aiming for a higher locating accuracy.

8.3.2 The Tests

For this study, two test objects were used.

Test Object 1:

A piece of wooden board with ten centimetre grid lines at a line width of 1 mm, serves as the first test object. Three images from different angles were taken. The intersections of the grid-lines were used as the photogrammetric targets. Their locations were determined to sub-millimetre accuracy on a Wild A-10 plotting table. At least 35 targets were covered in each image. The zoom was selected to be between 20-23 mm.

Test Object 2:

A metal plate which has been utilized for close-range non-metric camera calibration for many cases (Moniwa, 1976), was selected as the second object. This plate contains 36 grid intersections and 25 bolt points. All grid points which lie on the metal plate, are assumed to be of the same height. The bolts are composed of three different classes of height ranging from 10 mm to 35 mm. Four images were taken. All 61 points were covered in each image. The zoom was initialized on 72 mm. A series of ordinary film-based images was also taken. Three of them were digitized on a Zeiss PSK comparator and served as comparison standard. The object coordinates were determined with a comparator for planimetry, and 0.2 mm precision was achieved; plus a micrometer for depth, to the precision of 0.1 mm.

Each image was taken by averaging 4 successive images to reduce the distortions. The converted image contains 512x480 pixels.

8.3.3   The Analyses

In this study, three approaches were configured. One follows El-Hakim's (1986) scheme, however, instead of dedicated hardware, software written with WATFOR, a FORTRAN77 compiler for IBM PC from WATCOM, was used. A general convolution filter routine was written with a changeable kernel function. Different kernel sizes are handled with different versions. Minimum filter, (weighted) central-mean low-pass filter, high-pass filter, and several other type filters are included.

For the second approach, a function defined kernel, i.e. the Moravec interest operator (Luhmann & Altrogge, 1986) was implemented. A Hough transformation (Ballard, 1981; Gonzalez & Wintz, 1987) for straight line representation is also implemented as an option. This selection is based on the characteristics of both test objects which contains intersections of long lines. The image is transformed into a parameter space consisting of radial distance and polar angles, and then the lines are selected and defined.

The third approach is interactive, off-line, and conventional-photogrammetrically flavoured. The images were dumped into an HP ink-jet plotter, and then the hardcopies were digitized on an Altek table digitizer.

After the image coordinates were obtained, an APL version Photo-Triangulation (APT) package was applied for data reduction.

8.3.4   The Results

The first two approaches were found to be very time consuming on the PC/XT. Due to heavy noise, Moravec's interest operator failed in most cases, and considerable effort in image enhancement was found to be required. The third approach is therefore utilized for further analysis.

Concerning image enhancement, among all implemented filters, no particularly one provided satisfactory results by its own, while a cascading process has shown better enhancement. However, in all studied cases only the look-up-table was adjusted, no filtering was applied.

8.3.4.1 The Repeatability of the Digitizer

For each image, the four corners were digitized at least four times, and the other image points were digitized at least 3 times. An on-line data checking procedure was performed along with the digitizing operation to detect outliers. The repeatability in terms of standard deviation is listed in Table 8.9.

TABLE 8.9
The Repeatability of Digitization (plane)

	Σv_x	Σv_y	σ_x	σ_y	σ
plane1	4.44×10^{-10}	1.50×10^{-10}	59.79	58.95	59.38
plane2	3.83×10^{-10}	1.34×10^{-10}	67.53	66.47	67.46
plane3	3.96×10^{-10}	2.69×10^{-9}	80.18	68.52	74.57
corners			50.72	53.44	48.41

(unit: μm)

It can be seen that the corners have a slightly higher repeatability than the rest of the points. This is realized by the fact that the definition of corners is better than for other points. However, affine transformations between these three images show that the digitizing accuracy is essentially the same (see Table 8.10).

TABLE 8.10
Transformation of Image Corners Between Images

	Image 1-2	Image 1-3	Image 2-3
σ	66.04	86.86	79.24

(Unit: μm)

These repeatabilities also agree with other investigations performed on the same system as stated in Faig et al. (1988). The first two items are the sum of residuals which

provide a certain indication on the existence of systematic errors because the random noise is assumed to be of zero mean (El-Hakim, 1979).

8.3.4.2 Test Object 1

For the plane object, a perspective transformation was performed, where the differential scale is modelled. The residuals were analyzed for normality and systematic errors (see Table 8.11). For an ideal normal distribution, skew would be zero and kurtosis would be 3.

In terms of pixel size, standard deviations of 0.58 pixels were reached; while in terms of relative accuracy, values are slightly better than 1/1000.

The residuals were also analyzed for the systematic components, e.g. radial distortion, however, no set of parameters was found to have an influence of more than 25.4 μm in terms of the standard deviation. The residuals were further analyzed for Gaussian and exponential functions as performed in El-Hakim (1979) for the collocation procedure. However, no significant off-diagonal component was found. This once again confirms the statement in Burner et al.(1985), that, in additional to the camera station parameters, affinity is most significant.

TABLE 8.11

Statistics of the Perspective Transformation

	Image 1	Image 2	Image 3
Sample size	70	70	70
Mean	-0.69×10^{-10}	-1.35×10^{-11}	1.68×10^{-11}
σ	187.70	187.70	321.31
Mean deviation	142.74	144.78	241.30
Median	-11.17	-0.177	0.508
Pearsonian skew	0.4369	-0.2592	-0.2967
Kurtosis	4.3574	3.7761	3.4928

(Unit: μm)

```
            H                              H      Image 2
            H      Image 1                 HH
          H H                            H  HH
          HHHH                           H  HH
          HHHH   H                       HHHHH  H
          HHHHH  H                       HHHHHHH
          HHHHH  H                       HHHHHHH
          HHHHH  H                       HHHHHHH
          HHHHHHH                        HHHHHHHHH
          HHHHHHH                        HHHHHHHHHH
        HHH HHHHHHHH                   H  HHHHHHHHHHHHHH
        HHHHHHHHHHHHHH      H
```

```
                    H
                    H      Image 3
                   HH
                   HH
               H  HHHH    HH
               H  HHHHH   HH
              HHH HHHHHHHH   H
              HHHHHHHHHHHHHHH
         HH   H HHHHHHHHHHHHHHHHHHH   H
```
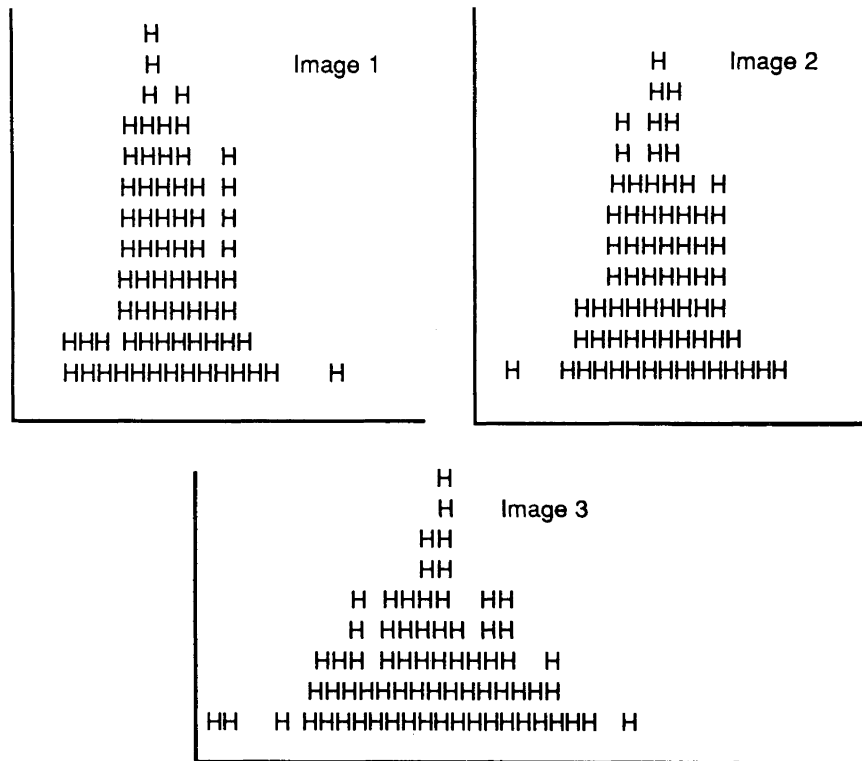
Figure 8.3
Histograms of the Residuals from Perspective Transformation
Class interval: 63.5μm

8.3.4.3 Test Object 2

With this object, 4 images were taken. The bundle block adjustment with additional parameters is used for analysis. Because of the relatively poor quality of point definition, the standard deviations of the measurements are relatively bigger (Table 8.5). Although by applying a robust estimation technique, these figures can be reduced to less than 0.1mm, the direct mean values without gross error removal were used. Analyzing by a 3-D to 2-D perspective transformation without additional parameters (DLT) (Abdel-Aziz & Karara, 1971), the standard deviation achieved for each image are less than but about 0.010 inch (0.25mm), which is equivalent to 0.79 pixel size.

As analyzed by a bundle block adjustment package with different additional parameter models, it is found that the photo-variant mode gives better results than the

180

block-invariant mode. This is particularly true for interior orientations. Three additional parameter models were tested, namely Moniwa's model (Moniwa, 1977), which includes 3 parameters for radial distortion, 2 for decentering distortion, and 2 for affinities; Schut's model (Schut, 1979) which includes 14 polynomial parameters; and Brown's model (Brown, 1976), which has 19 parameters. The third order spherical harmonic model was also tested, however, convergence was not reached.

TABLE 8.12
RMSE from Bundle Block Adjustment

	Image		Object check points			
	x	y	X	Y	Z	P
	0.33	0.40	0.41	0.54	2.16	1.31
Moniwa Model	0.22	0.22	0.63	0.58	0.62	0.61
Schut Model	0.18	0.18	0.46	0.51	0.15	0.77
Brown Model	0.15	0.15	0.38	0.42	0.80	0.56

(Unit: Image- pixel; object- mm)
$$(RMSEp = [(RMSEx^2 + RMSEy^2 + RMSEz^2)/3]^{1/2})$$

From the image residuals, the Brown's model provides the best results, while Schut's model placed next, and Moniwa's model the last. However, all of them provide significant improvement. It is impressive that Moniwa's model provides the best Z in comparison with check points. The individual influence from each component in the parameter set has not been studied in this experiment.

8.3.5   Some Remarks of On-Video Digitization

With the plate object, one image has been digitized on the image display screen with a software-driven cursor. Processing by a 3-D to 2-D perspective transformation with full control, the residuals have been analyzed as listed in Table 8.13. The corresponding standard deviation in object space is 0.3 mm. A weighted centre of gravity algorithm was applied, with 3x3, 5x5, and 11x11 windows. However, none of them improves the pointing accuracy obtained from the calibration in terms of standard deviation. This is

understood by the fact that the target shape in this project was not a closed figure, such as a disk or circle.

TABLE 8.13
The Statistics of On-Video Digitization

	Direct Video digitization	5x5 weighted c.g.	5x5 parabolic
Sample size	72	72	72
Mean	5.17×10^{-14}	5.20×10^{-14}	-1.12×10^{-5}
σ	0.77	0.80	0.66
Mean deviation	0.59	0.65	0.51
Median	-0.07	-0.09	0.007
Pearsonian skew	0.014	0.015	0.216
Kurtosis	2.729	2.470	2.519

(Unit: pixel)

```
      H    Direct v.d.                    w.c.g.                 H
      H                                                         H    parabolic
      HH                        H                               H
      HHHH                      H                               H
      HHHH  H                   HH                             H HH
      HHHH HH                   HHH H                          HHHHH
      HHHHHHHH                  HHHHHHHH                       HHHHHH H
      HHHHHHHHHHHHH             HHHHHHHHH                      HHHHHHH H
                               HHHHHHHHHHHHHHH                 HHHHHHHHH
```
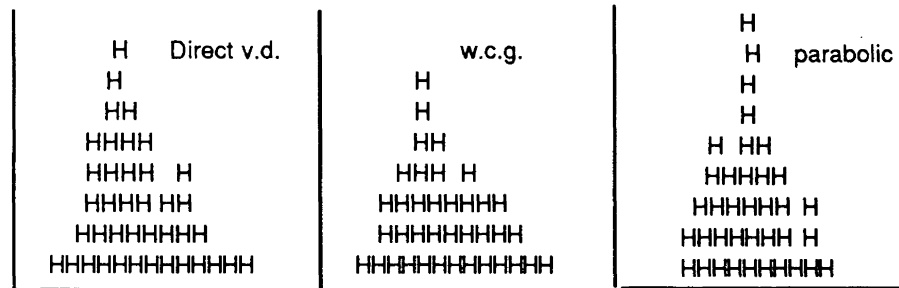
Figure 8.4
Histogram for Data from Table 8.13
Class interval: 0.3 pixel

Using the vertex of a parabolic curve which is fitted to the signal amplitudes along two axes improved the accuracy. However, this algorithm has been implemented for taking horizontal and vertical profiles, as well as profiles along two diagonals. The interpolated grey scale, as well as the fitting residuals were used to make selections on both observations and final results. Human interpretation is also applied. This has an effect similar to the gross error detection for the video digitization procedure. Because the current system does not allow for a zoom function for image display, this improvement may be insignificant if a zoom function is provided. This is supported by the fact that the standard deviation of the digitized data with gross error corrections has an even smaller value (0.60 pixels).

182

The inefficiency of these sub-pixel determination algorithms may mainly be caused by the heavy noise ratio. All images processed are original images without image enhancement.

8.3.6   Concluding Remarks

The potential for obtaining metric properties from digital images on a PC-based image processing systems has been shown. An automated fast processing system would be rather difficult to configure without dedicated hardware. About 0.5 pixel accuracy has been obtained for the hardcopy digitization approach with single image (photo) processing, about 0.2 pixel for multi-image by bundle block adjustment with additional parameters; compared with the 0.14 pixel accuracy reached in Mikhail & Mitchell (1984), this would be inferior. However, the sensor used in this study is a scanning-tube type camcorder. The converted 512x480 pixel image does not have the same quality as the same dimensional image provided by solid-state cameras. Meanwhile, the images were taken under normal working conditions, with ink-jet plotter and table digitizer.

Although a system upgrading is ongoing in the sense that a 80386 based PC and a commercial CCD camcorder have been ordered, it is conceived that the human interfaced on-video digitization with a software driven cursor, as well as the off-line hardcopy digitization provide practical means for utilizing metric properties of digital images from the present configuration.

CHAPTER 9

CONCLUSIONS

The solutions to an engineering problem are usually not unique. However, finding the optimal approach from all feasible schemes with proper instrumentation, is one of the most meaningful tasks for the engineer.

In the world of photogrammetry, as in many other technical fields, the nature is modelled by either analogue or analytical representations, and the solution schemes to the problem are established from them. In this research, three subgroups are classified: the functional models, the stochastic models and the operational aspects.

In this study, the meaning of broad class models was researched and evaluated. In the functional model aspect, the relation between the physical parameter space and the algebraic parameter space of perspective transformation has been fully explored. Better understanding is achieved and a closed form solution scheme is developed based on it. Several commonly used functional models were also comparatively studied. Equivalence theory has been successfully applied to configure a unified structure.

Concerning the basis for additional parameters, the physical model has been revealed as generally the best. From the functional evaluation aspect, physical model APs provide the best fidelity. In the numerical aspect, other models do not generally provide better numerical conditions. The results confirm experiments with real data reported by other authors. It is also recommended that additional parameters should be applied only, when the **image geometry** is strong, which has been shown to be the most important factor for self-calibration. For weak image geometry, the separability between blunders and systematic errors is low, which may result in un-reliable solutions. As a guidance for the introduction of additional parameters, the potential theory as proposed by Okamoto (1986) may serve as a first criterion, while the reliability of the network as addressed by

184

Foerstner (1985) may serve as the second. The condition number which reflects the numerical condition of the system, provides a further criterion if it is considered feasible.

Concerning the stochastic models, a dilemma concerning the basic stochastic models was solved. Equivalence theory is applied again. For the extended Gauss-Markov model, as far as the present photogrammetric application is concerned, the variance-covariance-component-estimation by MINQUE is highly preferred for estimating the covariance matrix of observations over the currently used collocation technique, not only because of its rigor but also because it can provide more measures on the estimates, e.g., the significance. On the practical application, it is more robust to the systematic errors. MINQUE has been accused of possibly providing negative values. This, however, mostly happens in cases with insufficient observations. Similar to the use of additional parameters, it is not recommended to apply any method which is based on residual analysis when the number of observations is not sufficiently large.

Concerning the quality control in data processing, statistical tests provide only an indication of possibilities, while a physical interpretation is essential when deciding about the removal of an observation. In practice, on-line data acquisition together with a step-by-step procedure provide a good working scheme to make this feasible.

As far as instrumentation for image data extraction and reduction is concerned, an economical approach utilizing a photographic enlarger and a cartographic digitizer has been extensively tested. Successful results point to a valid substitution to the conventional comparator approach.

In the hardware and software systems aspect, the application of photogrammetric methodology with various imaging sensors for different kinds of measurement proved to be very promising. Rasterstereography, which reduces the image digitization work as well as simplifies the image correlation/identification, has been shown as applicable and suitable in today's environment, particularly for measurements on a medium-sized patternless

object. The utilization of non-metric cameras as well as of digital cameras was also explored. A scheme termed "one plane constraint method" was developed and tested.

In the software engineering aspect, an interactive working environment is preferred by the author. The programming language APL, interfacing with C, is justified as an ideal scheme. A number of defined functions have been written for photogrammetric data reduction in this study and are named APT (APL version Photo-Triangulation). Although this software is in a preliminary prototype form, the convenience and speed in programming and operation can be felt.

Coming to the end of this study, it has become the author's strong feeling that if NATURE can be perfectly modelled, then it may not be NATURE any more. An ultimate model as well as an operational scheme may never be achieved. For different projects, the optimizing scheme would be different and the environmental factor has even greater influence. Only with full understanding of all aspects of the imaging- and data reduction systems, can an optimized set-up be ensured.

REFERENCES

Abbreviations
ASP(RS): American Society of Photogrammetry (and Remote Sensing);
DGK: Deutsche Geodaetische Kommission;
ISP(RS): International Archives of Photogrammetry (and Remote Sensing);
PE(&RS): Photogrammetric Engineering (and Remote Sensing).

Abdel-Aziz, Y.I. and Karara, H.M., 1971. Direct Linear Transformation from Comparator Coordinates into Object Space Coordinates in Close-range Photogrammetry. *Proceedings of the ASP/UI Symposium on Close-Range Photogrammetry* Urbana, Illinois, January 1971, 420-475.

Abdel-Aziz, Y.I., 1974. Expected Accuracy of Covergent Photos. *PE,* 40(11):1341-1346.

Ackermann, F., 1980a. Blockadjustment with Additional Parameters. *ISP,* 23(3): 1-10.

Ackermann, F., 1980b. Mathematical Models of Photogrammetric Point Determination. *Deutsche Geodatische Kommision,* Reihe A. Heft Nr. 98, 7-21.

Ackermann, F., 1984. Report on the Activities of Working Group III/I during 1980-1984. *ISPRS,* 25(A3a):10-15.

Ackermann, F., Schilcher, M., 1978. Auto- and Cross- correlation of Image Coordinates. *Nachrichten aus dem Karten- und Vermessungswesen,* Reihe B, Heft 36, 5-24.

Adams, L.P., 1980. The Use of Non-metric Cameras in Short Range Photogrammetry. *ISP,* 23(B5): 1-8.

Ali, M., and Brandenberger, A., 1982. Analytical Triangulation of Space Photography. *PE&RS,* 48(1):55-65.

Armenakis, C., 1983. *Subsidence Determination by Aerial Photogrammetry.* TR-93, University of New Brunswick, Fredericton, N.B.

Armenakis, C., 1987. *Displacement Monitoring by Integrating On-line Photogrammetric Observations with DynamicInformation.* PhD Thesis, University of New Brunswick, Fredericton, N.B.

ASP (American Society of Photogrammetry), 1980. *Manual of Photogrammetry.* 4th Edition (C.S. Slama, Editor), Falls Church, VA., Chap. 2.2.4.2 & 16.3.3.2

Atkison, K.B., 1980. *Developments in Close-range Photogrammetry--1'.* Applied Science Publishers Ltd. London.

Baarda, W., 1968. *A Testing Procedure for Use in Geodetic Networks.* New Series, Vol. 2, No. 4. Delft.

Baksalary, J., and Kala, R., 1981. Linear Transformations Preserving Best Linear Unbiased Estimators in a General Gauss-Markoff Model. *The Annals of Statistics,* 9(4):913-916.

Baksalary, J., 1984. A Study of the Equivalence between a Gauss-Markoff Model and its Argumentation by Nuisance Parameters. *Math. Operationsforsch u. Statist.*, 15(1):3-35.

Ballard, D.H.; 1981. Generalizing the Hough Transformation to Detect Arbitrary Shapes. *Pattern Recognition*, 13(2):111-122.

Becker, E.B., Carey, G.F., Oden,J.T., 1981. *Finite Elements, an Introduction.* Prentice-Hall, Inc..

Bjerhammar, A., 1973. *Theory of Errors and Generalized Matrix Inverses*, Elsevier Scientific Publishing Co., pp341-345.

Blais, J.A., 1983. Linear Least-Squares Computations Using Givens Transformation. *The Canadian Surveyor*, 37(4):225-233.

Blais, J.A., 1985. Least-squares Filtering and Smoothing Using Givens Transformations. *Manuscripta geodaetica*, 1985(10):208-212.

Boge, W.E., 1965. Resection Using Iterative Least Squares. *PE*, 31(4):701-714.

Bolt, M.F., Atkinson, K.B., 1984. Space Resection of 35mm Model Aircraft Photography. *ISPRS*, 25(A5):90-99.

Bopp, H., and Krauss, H., 1977. A Simple and Rapidly Converging Orientation and Calibration Method for Non- topographic Applications. *Proceedings of the ASP Fall Technical Meeting*, Little Rock, Arkansas, 425-432.

Bouloucos. T., 1986. Multidimensional Tests for Model Errors and their Reliability Measures. *ITC Journal*;1986(3):235-242.

Bouloucos, T., Molenaar, M., 1987. Systematic Deformations of Photogrammetric Blocks Caused by Undetected Gross Errors in the Terrestrial Control Networks. *ITC Journal*, 1987(2):134-137.

Box, G.E.P., Jenkins, G.M.,1976. *Time Series Analysis, Forecasting and Control.* Holden-Day.

Brill M.H. and Williamson, J.R., 1987. Three-Dimensional Reconstruction from Three-point Perspective Imagery. *PE&RS*, 53(12):1679-1683.

Brown, D.C., 1966. Decentering Distortion of Lenses. *PE*, 32(3):444-462.

Brown, D.C., 1971. Close-Range Camera Calibration. *PE*, 37(8):855-866.

Brown, D.C., 1976. The Bundle Adjustment - Progress and Prospects. *ISP*, 21(3).

Burner, A.W., Snow, W.L., Goad, W.K., 1985. Close-Range Photogrammetry with Video Cameras. *Proceedings of ASPRS 51st Annual Meeting*, Washington, 62-77.

Caspary, W.F., 1987. *Concepts of Network and Deformation Analysis*. Monograph 11, School of Surveying, The University of New South Wales, Australia. (Edited by J.M. Rueger).

Cerella, J., 1986. Pigeons and Perceptrons. *Pattern Recognition*, 19(6):431-438.

Chamard, S., 1987. The MPS-2 a Micro Analytical Photogrammetric System. *Proceedings of ASPRS 1987 Fall Convention*, Reno, Nevada, 233-238.

Chan, W.S., 1981. Focal Plane Architecture: an overview. *Optical Engineering*, 20(4):574-578.

Chang, B., 1986. The Formulae of the Relative Orientation for Non-metric Camera. *ISPRS*, 26(5):14-22.

Chen, L.C., 1985. *A Selection Scheme for Non-Metric Close- range Photogrammetric Systems*. PhD Thesis, University of Illinois at Urbana-Champaign.

Chen, Y., 1985. A New Space Resection Method and a Posteriori Weight Estimation. *Journal of Wuhan Technical University of Surveying and Mapping*, 21(3):61-68.

Chen, Y.Q., 1983. *Analysis of Deformation Surveys - A Generalized Method*. TR-94, University of New Brunswick, Fredericton, N.B.

Chen, Y.Q., 1985. Assessment of Levelling Measurements Using the Theory of MINQUE. *Proceedings of the 3rd International Symposium on the North American Vertical Datum*, Rockville, Md., pp 389-400.

Chen, Y.Q., Kavouras, M., Chrzanowski, A., 1987. A Strategy for Detection of Outlying Observations in Measurements of High Precision. *The Canadian Surveyor*, 41(4):529-540.

Chrzanowski, A., 1983. Supplementary Materials for Gedetic Surveying, SE3022. Surveying Engineering Department, University of New Brunswick, Fredericton, N.B.

Crowder H., Dembo, R., Mulvey, J., 1979. On Reporting Computational Experiments with Mathematical Software. *ACM Transactions on Mathematical Software*, 5(2):193-203.

Curry, S., Baumdind, S., Anderson, J.M., 1985. Calibration of an Array Camera. *Proceedings of the 51st ASP Annual Convention*, Washington, D.C.,331-340.

Dalsgaard, J., 1978. Stereoscopic Vision - a Problem in Terrestrial Photogrammetry. *Photogrammetria*, 34(1978)3-18.

Dermanis, A., 1984. Kriging and Collocation- A Comparison. *Manuscripta geodastica*, 9(1984):159-167.

Dorrer, E., 1986. Operational Aspects of On-line Phototriangulation. *Photogrammetria*, 40(1986) 257-298.

Drees, A., 1985. *Ein semi-analytisches Praezisionsauswertesystem fuer die Nahbereichsphotogrammetrie.* Doctoral dissertation, Institut fuer Photogrammetrie der Universitaet Bonn.

Drerup, B., W. Frobin, E., Hierholzer, (Editor) 1983. *Moire Fringe Topography and Spinal Deformity, Proceedings of the 2nd Internationsl Symposium.* Gustav Fischer Verlag.

Ebner, H., 1975. Analysis of Covariance Matrices. ISP, Commission III, Stuttgart, 1974; *DGK*, Reihe B, Heft 214.

Ebner,H., 1976. Self Calibrating Block Adjustment. *ISP*, Commission III.

Ebner, H., Fritsch, D., 1986. The Multigrid Method and Its Application in Photogrammetry. *ISPRS*, 26(3/3):141-149.

Ebner, H., Molenaar, M., Strunz, G., 1986. Report of Working Group III/I : Accuracy Aspects of Combined point determination. *ISPRS*, 26(3):210-211.

Ebner, H. and Mueller, F., 1986. Processing of Digital Three Line Imagery Using a Generalized Model for Combined Point Determination. *ISPRS*, 26(3):212-222

El-Hakim, S., 1979. *Potentials and Limitations of Photogrammetry for Precision Surveying.* PhD. Thesis, Surveying Engineering Department, University of New Brunswick, Fredericton, N.B.

El-Hakim, S.F., 1984. A photogrammetric Vision System for Robots. P-PR 54:13-27. National Research Council, Canada.

El-Hakim, S.F., 1986. A Real-time System for Object Measurement with CCD Cameras. *ISPRS*, 26(5):363-373.

El-Hakim, S.F., Ziemann, H., 1984. A Step-by-Step Strategy for Gross-Error Detection. *PE&RS*, 50(6):713-718.

Ethrog, U., 1984. Non-metric Camera Calibration and Photo Orientation using Parallel and Perpendicular Lines of the Photographed Objects. *Photogrammetria*, 39(1984)13-22.

Ethrog, U., 1987. Calibration and Model Reconstruction of Rasterstereographic Systems. *Proceedings of ASPRS 1987 Annual Convention*, Baltimore, 29-35.

Faig, W., 1972. Simple Method for Estimating Model Deformation Caused by Radial Lens Distortion. *The Canadian Surveyor*, 1972, 38-44.

Faig, W., 1973. Convergent Photos for Close-range. *PE,* 39(5):605-610.

Faig, W.,1976. Calibration of Close-Range Photogrammetric Systems: Mathematical Formulation. *PE&RS*,41(12):1479-1486.

Faig, W. 1986. *Handbook of Non-topographic Photogrammetry*, second edition, draft, Chapter 6. ASPRS.

Faig, W., Shih, T.Y., 1986. Critical configuration of Object space control points for the Direct Linear Transformation. *ISPRS*, 26(5):23-29.

Faig, W. and Shih, T.Y., 1987. Space Resection - A Comparative Study of Functional Models. *Proceedings of ASPRS 1987 Fall Convention*, Reno, 177-185.

Faig, W. and Owolabi, K., 1988. Distributional Robustness in Bundle Adjustment. *Proceedings of ASPRS, 1988 Annual Convention*, St. Louis, 3: 169-180.

Faig, W. and Shih, T.Y., 1988. An Investigation into the Metric Characteristics for a Video-based Image Processing System. *Proceedings of the First Special Workshop on Videography*, Terre Haute, 105-114.

Faig, W., Deng, G., Shih, T.Y., 1988. The Reliability and Accuracy of the Enlarger-Digitizer Approach. *Proceedings of ASPRS-1988 Fall Convention*, Virginia Beach, 281-288.

Finsterwalder, R. and Hofmann. W., 1968. *Photogrammetrie*, Walter de Gruyter & Co.. Berlin. p158-160.

Forrest, R.B., 1971. Image-space Plotter. *PE*, 37:847-853.

Foerstner, W., and Schroth R., 1982. On the Estimation of Covariance Matrices for Photogrammetric Image Coordinates. Symposium on Geodetic Networks an Computations, *DGK* Reihe B, Heft 258/VI, 43-70.

Foerstner, W., 1985. The Reliability of Block Triangulation. *PE&RS*, 51(6):1137-1149.

Fraser, C.S., 1979. *Simultaneous Multiple Camera and Multiple Focal Setting Self-Calibration in Photogrammetry*. PhD Disseration, University of Washington, Seattle, Washington.

Fraser, C.S., 1980. On Variance Analysis of Minimally Constrainted Photogrammetric Adjustments. *Australian Journal of Geodesy, Photogrammetry and Surveying*, 33:39-56.

Fraser, C.S., 1982. On the Use of Nonmetric Cameras in Analytical Close-Range Photogrammetry. *The Canadian Surveyor*, 36(3):259-279.

Fraser, C.S., 1983. The Analysis of Photogrammetric Deformation Measurements on Turtle Mountain. *PE&RS*, 48:561-570.

Frobin, W., and Hierholzer, E., 1982. Calibration and Model Restruction in Analytical Close-range Stereophotogrammetry. *PE&RS*, 48(1):67-72, 48(2):215-220.

Frobin, W., and Hierholzer, E., 1983. Automatic Measurement of Body Surfaces using Rastergraphy. *PE&RS*, 49(3) :561-570

Frobin, W., and Hierholzer, E., 1985 Simplified Rasterstereography using a Metric Camera. *PE&RS*, 51(10):1605-1608.

Fryer , J.G., 1986. Distortion in a Zoom Lens. *AutralianJournal of Geodesy, Photogrammetry and Surveying*, 44: 49-59.

Ghosh, S.K., 1988. *Analytical Photogrammetry*. 2nd edition. Pergamon Press.

Gillen, L., 1983. Analytical Photogrammetry from Small Format Photography. *Proceedings of ASP-1983 Annual Meeting*, Washington, D.C., 18-25.

Gonzalez, R. and Wintz, P., 1987. *Digital Image Processing*. Addison-Wesley Publishing Co.

Granshaw, S.I., 1980. Bundle Adjustment Methods in Engineering Photogrammetry. *Photogrammetric Record*, 10(56):181-207.

Gruen, A., 1978. Experiences with Self-Calibrating Bundle Adjustment. Presented paper of ASP 1978 Annual Convention, Washington, D.C.

Gruen, A., 1980. Precision and Reliability aspects in close- range photogrammetry. *ISP* 23(B11): 378-391.

Gruen, A., 1986. Real-Time Photogrammetry at the Digital Photogrammetric Station (DIPS) of ETH Zurich. Presented paper at ISPRS Comm. V, Ottawa meeting.

Hadem, I., 1981. Bundle Adjustment in Industrial Photogrammetry, *Photogrammetria*, 37(1981)45-60.

Haralick, R. and Chu,Y.H., 1984. Solving Camera Parameters From the Perspective Projection of a Parameterized Curve. *Pattern Recognition*, 17(6):637-645.

Heikkila, J. and Inkila, K., 1978. Self-Calibration in Bundle Adjustment *The Photogrammetric Journal of Finland*, 7(2):123-134.

Hilborn, W., 1984. Photo Interpretation, Lecture notes. Department of Forest Resources, University of New Brunswick, Fredericton, N.B.

Hofmann, O.,Nave, P., Ebner, H., 1984. DPS- A Digital Photogrammetric System for Producing Digital Elevation Models and Orthophotos by Means of Linear Array Scanner Imagery. *PE&RS*, 50(8):1135-1142.

Holland, P.W., and Welsch, R.E., 1977. Robust Regression Using Iteratively Reweighted Least Squares. *Communications in Statistics*, A6(9):813-827.

Horst, M., 1983. Skeletal Deformities and Trunk Shape: A Survey of Diagnostic Methods. *Proceedings of the 2nd International Symposium on Moire Fringe Topography and Spinal Deformity*, Gustav Fischer Verlag, 3-16.

Jacobsen, K., 1982a. Attempt at Obtaining the Best Possible Accuracy in Bundle Block Adjustment. *Photogrammetria*, 37(1982):219-235.

Jacobsen, K., 1982b. Selection of Additional Parameter by Program. *ISPRS*, 24(3): 266-275.

Jacobsen, K., 1984. Analysis of Remaining Systematic Image Errors. *ISPRS*, 25(A3a):426:434

Jacobsen, K., 1986. Operational Aspects of Data Aquisation for Bundle Block Adjustment. *ISPRS*, 26(3):374-378.

Jahn, J., 1975. Beitrag zur analytischen Nahbildmessung. *Oesterreichische Zeitschrift fuer Vermessungswesen und Photogrammetrie*, 62(4).

Jodoin, S.J., 1987. *The Calibration of a Parabolic Antenna with the Aid of Close-range Photogrammetry and Surveying*. TR-130, Surveying Engineering Department, University of New Brunswick, Fredericton, N.B.

Johnson, G.W., Li, J., Wassyng, A., Leonard, M.S., 1983. Stereophotogrammetric Mapping of the Human Face for Clinical Analysis and Research in Craniofacial Surgery. *Proceedings of ASP-1983 Annual Meeting*, Washington, D.C., 274-283.

Jones, A., 1987. Still Video. *Photovideo Retailer*, 1987(Dec):22-27.

Juhl, J., and Lavridsen, B., 1982. The AUC Self-Calibrating Block Adjustment Method and its Results from Jamijarvi Test Field. *Photogrammetria*, 38(1982):23-34.

Kavouras, M., 1982. *On the Detection of Outliers and the Determination of Reliablity in Geodetic Networks*. TR-87, Surveying Engineering Department, University of New Brunswick, Fredericton, N.B.

Keefe, M. and R. Donald, 1986. Capturing Facial Surface Information. *PE&RS*, 52(9):1539-1548.

Khlebnikova, T.A., 1983. Determining Relative Orientation Angles of Oblique Aerial Photographs. *Mapping Sciences and Remote Sensing*, 21(1):43-48.

Killian, V.K., 1984. Numerische Auswertung zweier nicht orientierter photogrammetrischer Bilder eines ebenen Vierecks. *Oesterreichische Zeitschrift fuer Vermessungswesen und Photogrammetrie*, 72(3):95-100.

Kilpelae, E., 1980a. Compensation of Systematic Errors of Image and Model Coordiantes. *ISP*, 23(B9): 407-427.

Kilpelae, E., 1980b. Compensation of Systematic Errors in Bundle Adjustment. *ISP* 23(B9):428-435.

Kim, B.G., 1987. Surface Water Velocity Measurements on Delavan Lake Using Aerial Photographs. *PE&RS*, 53(6):605-607.

Klein, K., 1987. PC Power in Analytical Photogrammetry. *Proceedings of ASPRS 1987 Fall Convention*, Reno, Nevada, 249-255.

Knight, W., 1987. Notes for Numerical Linear Algebra. University of New Brunswick, N.B. Canada.

Konecny, G., 1965. Interior Orientation and Convergent Photography. *PE*, 31(4):625-634.

Kratky, V., 1979. On-line Analytical Solutions in Close-range Photogrammetry. *The Canadian Surveyor*, 33(2):177-192.

Kraus, K., 1972. Film Deformation Correction with Least Squares Interpolation. *PE*, 1972(May):487-493.

Kraus, K. and Mikhail, E.M., 1972. Linear Least Squares Interpolation. *PE*, 1972(Oct):1016-1029.

Kruck, E., and P. Lohmann, 1986. Aerial Triangulation of CCD Line-scanner Images. Draft paper, obtained from the authors.

Kubik, K., 1987. A Note on Photogrammetric Block Adjustment with Additional Parameters. *PE&RS*, 53(11):1531-1532.

Kubik, K., Lyons, K., Merchant, D., 1988. Photogrammetric Work Without Blunders. *PE&RS*, 54(1):51-54.

Kupfer, G., Mauelshagen, L., 1982. Correlations and Standard Errors in Bundle Block Adjustment with Some Emphasis on Additional Parameters. *Photogrammetria*, 38(1982):57-72.

Lanckton, A., 1970. Hybrid Stereoplotter. *PE*, 1970 : 280-289.

Lin, E.Y.H., 1982. *A Note for Box-Jenkins Model and Wagner- Whitin Algorithm*. Dept. of Industrial and Management Engineering, The University of Iowa.

Lindlohr, W., and Wells, D., 1985. GPS Design using Undifferenced Carrier Beat Phase Observations. *manuscripta geodaetica*(1985), 10:255-295.

Luhmann, T. and Altrogge, G., 1986. Interest-Operator for Image Matching. *ISPRS*, 26(3/2):459-474.

Luhmann, T. and Wester-Ebbinghaus, 1987. Digital Image Processing by Means of Reseau-Scanning. *Proceedings of 41st Photogrammetric Week*, Stuttgart.

Marzan, G.T., and Karara, H.M., 1976. *Rational Design for Close-range Photogrammetry. Civil Engineering Studies*, Photogrammetry Series, No. 43, University of Illinois, Urbana-Champaign.

Masry, S.E., 1979. *Basics of Instrumental and Analytical Photogrammetry*. LN-33, Surveying Engineering Department, University of New Brunswick, Fredericton, N.B.

Masry, S.E., 1981. Digital Mapping Using Entities- A New Concept. *PE&RS*, 48(11):1561-1565.

Masry, S.E., 1984. Class Notes for Digital Mapping (I). Surveying Engineering Department, University of New Brunswick, Fredericton, N.B.

McDonnell, P.W., 1979. *Introduction to Map Projections*. Marcel Dekker, Inc..

Mertikas, S., C. Field, D.E. Wells, 1987. The Estimation of Accuracy in Navigation. *Proceedings of the Canadian Hydrographic Conference*, Burlington.

Mikhail, E.M. and Ackermann, F., 1976. *Observations and Least Squares*. IEP-A Dun-Donnelley Publisher, New York.

Mikhail, E.M., M.L. Akey, and O.R. Mitchell; 1984. Detection and Sub-pixel Location of Photogrammetric Targets in Digital Images. *Photogrammetria*, 39(1984):63-83.

Mikhail, E.M.,and Mitchell, O.R.; 1984. *Metric Aspects of Digital Images and Digital Image Processing*. Technical Report, No. CE-PH-84-9, Purdue University.

Mills, R., 1987. APL: A Better Image Processing Language. *Processings of ASPRS 1987 Annual Convention*, Baltimore, Vol. 6:121-130.

Moffitt F.H., and Mikhail, E.M., 1980. *Photogrammetry*, 3rd Ed. Harper & Row, Inc.

Molenaar, M., 1978a. Essay on Empirical Accuracy Studies in Aerial Triangulation. *ITC Journal*, 1978(1):81-97.

Molenaar, M., 1978b. Preadjustment Error Detection in Independent Model Blocks. *ITC Journal*, 1978(3):514-541.

Moniwa, H., 1977. *Analytical Photogrammetric System with Self-calibration and its Applications*. PhD Thesis, Department of Surveying Engineering, University of New Brunswick, Fredericton, N.B.

Moreland, M.S. and Pope, M.H. and Armstrong, G.W.D. (Editor), 1981. *Moire Fringe Topography and Spinal Deformity, Proceedings of an International Symposium*. Pergamon Press.

Moritz, H., 1972. *Advanced Least-Square Methods*. Geodetic Science Report 175, Ohio State University, Columbus, OH.

Moritz, H., 1980. *Advanced Physical Geodesy*. Sammlung Wichmann Neue Folge, Band 13, Herbert Wichmann Verlag Karlsruhe.

Munjy, R., 1986a. Self-Calibration using the Finite Element Approach. *PE&RS*, 51(3):411-418.

Munjy, R., 1986b. Calibrating Non-metric Cameras using the Finite Element Method. *PE&RS*, 52(8):1201-1205.

Murai, S., Nakamura, H., Suzuki, Y., 1980. Analytical Orientation for Non-metric Camera in the Application to Terrestrial Photogrammetry. *ISP*, 23(B5):516-525.

Murai, S., Matsuoka, R., Okuda, A., 1984a. A Study on Analytical Calibration for Non-metric Camera and Accuracy of Three Dimensional Measurement. *ISPRS*, 25(A5): 570-579.

Murai, S., Matsuoka, R.,Okuda, A., 1984b, Comparison of Accuracy amongst Bundle Adjustment Methods. *Journal of the Japan Society of Photogrammetry and Remote Sensing*, 23(2):4-11.

Novak, K., 1986. *Orientierung von Amateuraufnahmen ohne Passpunkte*. Geowissenschaftliche Mitteilungen Heft 28, Technische Universitaet Wien.

Oimoen, D.C., 1987. Evaluation of a Tablet Digitizer for Analytical Photogrammetry. *PE&RS*, 53(6):601-603.

Okamoto, A., 1981. Orientation and Construction of Models, Part I : The Orientation Problem in Close-Range Photogrammetry. *PE&RS*, 47(10):1437-1454.

Okamoto, A., 1986. Potential Theory in Photogrammetry. *ISPRS*, 26(3):543-563.

Owolabi, K., 1988. Hotelling T^2 statistic and its Applications in Least Squares Adjustment. *Proceedings of ASPRS 1988 Fall Convention*, Virginia Beach, 243-251.

Owolabi, K., 1989. *Simultaneous Distributional and Model Robustness in Photogrammetric Bundle Block Adjustment*. PhD Thesis, University of New Brunswick, Canada. In preparation.

Papo, H.B., Perelmuter, A., 1982. Free Net Analysis in Close Range Photogrammetry. *PE&RS*, 48(4):571-576.

Pedroza, M., 1987. *Geometrical Analysis of A Parabolic Antenna*. Course Report for SE6001, Department of Surveying Engineering, University of New Brunswick.

Pepin, M.J., 1983. *The Digital Mapper Analytical Plotter*. M.Sc.E. Thesis, Department of Surveying Engineering, University of New Brunswick.

Pope, A.J., 1970. *An Advantageous Alternative Parameterixation of Rotations for Analytical Photogrammetry*. National Ocean Survey, Rockville, Md..

Pope, A.J., 1974. Two approaches to Nonlinear Least Squares Adjustments. *The Canadian Surveyor*, 28(5):633-669.

Pope, A.J., 1976. *The Statistics of Residuals and the Detection of Outliers*. U.S. Dept. of Commerce, NOAA Technical Report NOS. 65 NGS 1, Rockville, Md.

Rampal, K.K., 1976. Least Square Collocation in Photogrammetry. *PE&RS*, 42(5):659-669.

Rampal, K.K., 1979. A Closed Solution for Space Resection. *PE&RS*, 45(9):1255-1261.

Rao, C.R., 1971. Estimation of Variance and Covariance Components --- MINQUE Theory. *Journal of Multivariate Analysis* 1, 257-275,1971

Rao, C.R., Mitra, S.K., 1971. *Generalized Inverse of Matrices and its Application*. John Wiley & Sons.

Rapp, R.H., 1966. Comparison of Space Resection Adjustments. Journal of the Surveying and Mapping Division, *Proceedings of the ASCE*, 92(SU1):17-23.

Rawiel, V.R., 1987. Eine Methode zur Bestimmung der Inneren Orientierung von Messbildern in der Nahbildmessung. *Bildmessung und Luftbildwesen*, 48(1980):36-42.

Reutebuch, S., 1987. PC-Based Analytical Stereoplotter for Use in Forest Service Field Offices. *Proceedings of ASPRS 1987 Fall Convention*, Reno, Nevada, 222-232.

Robertson, G., 1986. Panel Discussion, ISPRS Commission V, Ottawa Meeting.

Rollin, J.R., 1986. A Method of Assessing the Accuracy of Cartographic Digitising Tables. *The Cartographic Journal*, 23(Dec):144-146.

Rostom, R.S., 1981. Stability of Relative Orientation. *Photogrammetric Record*, 10(57):343-357.

Ruether, H., and Adams,L.P., 1984. Two Phase Photogrammetry with Displayed Control. *ISPRS* , 25(A5):19-28.

Sarjakoski, T., 1986. Software Engineering in Photogrammetric Systems. *ISPRS*, 26(3/2):588-601.

Schaffrin, B., 1981. Best Invariant Covariance Component Estimators and its Application to the Generalized Multivariate Adjustment of Heterogeneous Deformation Observations. *Bulletin Geodesique*, 55(1981):73-85.

Schaffrin, B. and Grafarend, E., 1986. Generating Classes of Equivalent Linear Models by Nuisance Parameter Elimination, Applications to GPS observations. *Manuscripta geodaetica*, 11:262-271.

Schaub, G., 1988. Video ESP. *VIDEO*, 1988(April):55-58.

Schroth, R., 1984. An Extended Mathematical Model for Aerial Triangulation. *ISPRS*, 24(A3B):962-970.

Schut, G.H., 1959. Construction of Orthogonal Matrices and their Application in Anlytical Photogrammetry. *Photogrammetria*, 15(4):149-162.

Schut, G.H., 1978. *Adjustment of Bundles*. P-PR-47, National Research Council, Canada.

Schut, G.H., 1979. Selection of Additional Parameters for the Bundle Adjustment. *PE&RS*, 45(9): 1243-1252.

Schwartz, P.G., 1984. Testing the Personal Stereoscopic Measuring Precision: Further Results. *ISPRS*, 25(A3b):985-987.

Searle, S.R., 1971. Topics in Variance Component Estimation. *Biometrics*, 27: 1-76.

Shih, T.Y., 1985. MINQUE -- The Method and Examples. Term Report for SE 6122: Approximation and Time Series, University of New Brunswick, Canada.

Shih, T.Y., 1987. The Closed Solution for Space Resection. Graduate Seminar paper, Department of Surveying Engineering, University of New Brunswick.

Shih, T.Y., and Faig, W., 1986. An Economical Approach to Measuring Anthropological Shapes by Photogrammetry. *ISPRS*, 26(5): 341-348.

Shih, T.Y., Faig, W., 1987. Physical Interpretation of the Extended DLT- model. *Proceedings of ASPRS Fall Convention*, Reno, Nevada, 385-394.

Shih, T.Y., Faig, 1988. A Solution for Space Resection in Closed Form. *ISPRS*.

Shmutter, B, and Perelmuter, A., 1979. Block Triangulation by Intersections. *Photogrammetria*, 35(1979):93-99.

Shortis, M. R., 1982. Sequential Adjustments of Close-range Stereopairs. *ISPRS*, 24(5/1):461:470.

Sjoberg, L.E., 1985. Adjustment and Variance-Covariance Component Estimation with a Singular Covariance Matrix, *Zeitschrift fuer Vermessungswesen* , 1985(4):145-151.

Sommerville, I., 1985. *Software Engineering*. Addison-Wesley Publishing Co.

Takasaki, H., 1975. Simultaneous All-Around Measurement of a Living Body by Moire Topography. *PE&RS*, 41(12):1527-1532.

Terada, H., Ikeda, T., 1978. Biostereometrical Application of Moire Fringe Method with Special Reference to our Optical Device and in aid of Parallel Light. *SPIE*, Vol. 166:24-30.

Thorpe, J., 1983. The Analytical Plotter in Commercial Production. *Proceedings of ASP-1983 Annual Meeting*, Washington, D.C., 70-76.

Torlegard, K., 1981. *Accuracy Improvement in Close-range Photogrammetry*. Helft 5 der Schriftenreihe des wissenschaftlichen Studienganges Vermessungswesen an der Hochschule der Bunderswehr Muenchen.

Turner-Smith, A.R., and Harris, J.D., 1986. Measurement and Analysis of Human Back Surface Shape. *ISPRS*, 26(5):355-362.

Utz, P., 1988. Super VHS - A Quantum Leap. *AV Video*, 1987(July):43-73.

van. Wijk, M.C. and Ziemann, H., 1976. The Use of Non-Metric Cameras in Monitoring High Speed Processes. *PE&RS*, 42(1):91-102.

van Wijk, M.C., 1979. Moire Contourgraph -- an Accuracy Aanalysis. *Biomechanics*, 13: 605-613.

Vanicek, P., and Krakiwsky, E.J., 1982. *Geodesy : The Concepts*. North Holland, Amsterdam.

Vanicek, P., 1983. Diagrammatic Approach to Adjustment Calculus. *Proceedings of Development of Theory and Techniques of Astronomical and Geodetic Calculations*. University Jagiellonskim, Krakow, Poland, May, 1983.

Vlcek, J., 1988. Nature of Video Images. Workshop Notes for First Special Workshop on Videography, Terre Haute, IN.

Voon, A., 1986. *Differential Distortions in Photogrammetric Block Adjustment*. TR-123, Department of Surveying Engineering, University of New Brunswick, Fredericton, N.B.

Vozikis, E., Baumann, J.U., Koenig, A., 1984. Use of Photogrammetry in Orthopedics and Surgery. *ISPRS*, 25(A5):700-715.

Wang, Zhi-zhuo, 1979. *Principles of Photogrammetry*. Surveying and Mapping Publishing Co., China(in Chinese).

Welch, R. and Dikkers, K., 1978. Educational and Research Aspects of Non-Metric Close-Range Analogue Photogrammetry. *Photogrammetric Record*, 9(52):537-547.

Welch, R., and Jordan, T.R., 1983a. Microcomputer-Based Photogrammetry. *Proceedings of ASP 49th Annual Meeting*, 233-235.

Welch, R., and Jordan, T.R., 1983b. Analytical Non-metric Close-Range Photogrammetry for Monitoring Stream Channel Erosion. *PE&RS*, 49(3):367-374.

Welsch, W. 1981. Estimation of Variances and Covariances of Geodetic Observations, *Australian Journal of Geodesy, Photogrammetry and Surveying*, 34:1-14.

Wells, D., 1985. Lecture notes for Functional Analysis Applied to Surveying, SE6101. Department of Surveying Engineering, University of New Brunswick, Fredericton, N.B.

Wester-Ebbinghaus, W., 1980. Aerial Photography by Radio Controlled Helicopter. *Photogrammetric Record* 10(55):85-92.

Williamson J.R. and Brill M.H., 1987. Three-Dimensional Reconstruction from Two-Point Perspective Imagery. *PE&RS*, 53(3):331-335.

Wong, K.W., 1972. Photogrammetric Calibration of Television Systems. *ISP*,19(5).

Wong, K.W., 1976. Mathematical Formulation and Digital Analysis in Close-range Photogrammetry. *PE*, 41(11):1355-1373.

Wong, K.W., 1986. Stereo Solid State Camera Systems. *ISPRS*, 26(5):454-458.

Wong, K.W., Ho, W.H., 1986. Close-range Mapping with a Solid State Camera. *PE&RS*, 52(1):67-74.

World Book, 1979. *The World Book Encyclopedia*. World Book- Childcraft International Inc.

Wunderlich, W., 1982. Rechnerishe Rekonstruktion eines ebenen Objekts aus zwei Photographien. *Mitteilungen, der geodaetischen Institute der Technischen Universitaet Graz*, Folge 40, 365-377.

Yzerman, H., 1988. The A.P.Y. System for Interpretation, Compilation and Revision of Geographic Data. Photogrammetric Systems Brochure.

Ziemann, H. and El-Hakim, S.F., 1983. On the Definition of Lens Distortion Reference Data with Odd-Power Polynomials. *The Canadian Surveyor*, 37(3): 135-143.

Ziemann, H. and El-Hakim, S.F., 1986. System Calibration and Self Calibration. Part I: Rotationally Symmetrical Lens Distortion and Image Deformation, *PE&RS*, 52(10):1617-1625. Part II and III were obtained from the authors in draft form.